NEVADA BUREAU OF MINES AND GEOLOGY 1996

NBMG OPEN-FILE REPORT 96-3

VOLCANIC ROCK-HOSTED URANIUM DEPOSITS IN NORTHWESTERN NEVADA AND SOUTHEASTERN OREGON — POSSIBLE SITES FOR STUDIES OF NATURAL ANALOGUES FOR THE POTENTIAL HIGH-LEVEL NUCLEAR WASTE REPOSITORY AT YUCCA MOUNTAIN, NEVADA

Stephen B. Castor

Christopher D. Henry

Lisa A. Shevenell

This information should be considered preliminary.
It has not been edited or checked for completeness
or accuracy.

VOLCANIC ROCK-HOSTED URANIUM DEPOSITS IN NORTHWESTERN NEVADA AND SOUTHEASTERN OREGON – POSSIBLE SITES FOR STUDIES OF NATURAL ANALOGUES FOR THE POTENTIAL HIGH-LEVEL NUCLEAR WASTE REPOSITORY AT YUCCA MOUNTAIN, NEVADA

Stephen B. Castor, Christopher D. Henry, and Lisa A. Shevenell

Nevada Bureau of Mines and Geology
Mackay School of Mines, University of Nevada
Reno, Nevada

April 19, 1996

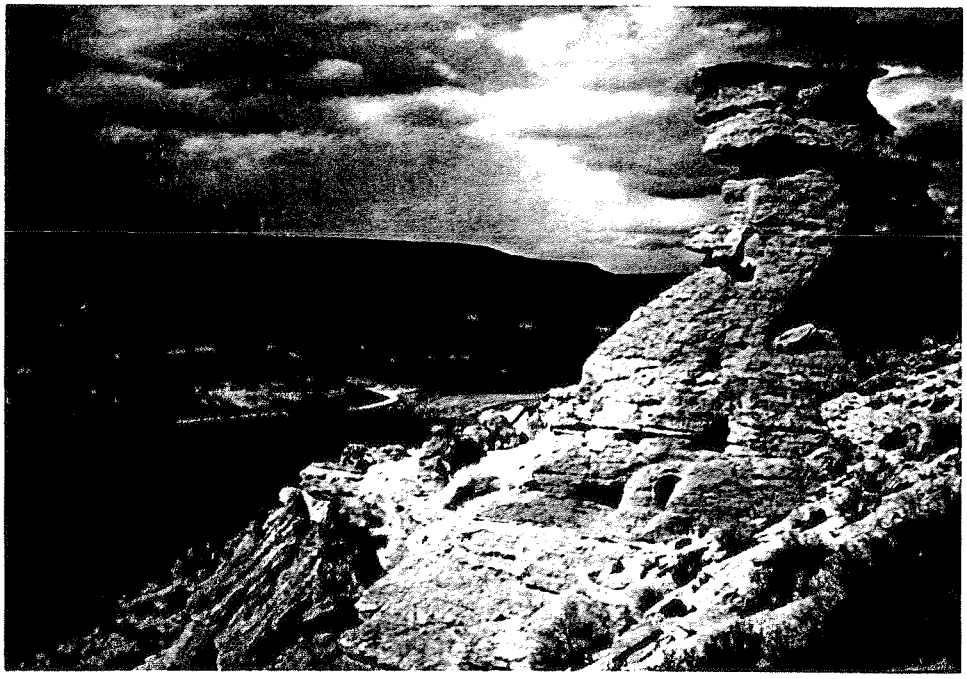

Virgin Valley uranium district from the southeast. View shows air-fall tuff of the Virgin Valley Formation (foreground); nearly flat-lying, uranium-bearing, fluvial and lacustrineVirgin Valley Formation beds across Virgin Creek; Canyon Rhyolite in shadow (background); and Mesa Basalt (on the horizon).

TABLE OF CONTENTS

INTRODUCTION 1
METHODS 1
McDERMITT CALDERA, OREGON AND NEVADA 12
General geologic setting 12
Hydrologic setting 12
Kings River district 15
Geology 15
Rock chemistry 20
Mineral assemblages 23
Bretz-Opalite district 24
Geology 26
Rock chemistry 26
Mineral assemblages 27
VIRGIN VALLEY, NEVADA 27
General geologic setting 27
Idaho Canyon Tuff 28
Rhyolite Lavas of Virgin Valley 28
Virgin Valley Formation 28
Thousand Creek Formation 33
Mesa Basalt 33
The Virgin Valley caldera 33
Geology of uranium mineralization 34
Rock chemistry 36
Mineral assemblages 36
Hydrologic setting 40
LAKEVIEW URANIUM MINING DISTRICT, OREGON 40
Geology 42
Rock chemistry 45
Mineral assemblages 45
Hydrologic setting 47
STEENS MOUNTAIN, OREGON 47
Geology 47
Rock chemistry 48
Mineral assemblages 48
Hydrologic setting 48
BOTTLE CREEK, NEVADA 48
Geology 48
Rock chemistry 50
Mineral assemblages 50
Hydrologic setting 50
PAINTED HILLS AREA, NEVADA 50
Geology 51
Rock chemistry 53
Mineral assemblages 53
Hydrologic setting 53
DOGSKIN MOUNTAIN, NEVADA 53
Geology 55
Rock chemistry 55
Mineral assemblages 56
Hydrologic setting 56
PETERSEN MOUNTAIN, NEVADA AND CALIFORNIA 56
Geology 56
Rock chemistry 57
Mineral assemblages 57
Hydrologic setting 57

ORIGIN OF VOLCANIC ROCK-HOSTED URANIUM DEPOSITS, NORTHWESTERN NEVADA AND SOUTHEASTERN OREGON....57
COMPARISON OF THE SETTING OF NORTHWESTERN NEVADA AND SOUTHEASTERN OREGON URANIUM DEPOSITS WITH THAT AT YUCCA MOUNTAIN....63
General geology....63
Rock chemistry....64
Mineral assemblages....65
Hydrologic setting....66
DISCUSSION OF NATURAL ANALOGUE POTENTIAL AND RECOMMENDATIONS....68
ACKNOWLEDGMENTS....72
REFERENCES....73

TABLES

Table 1. Analyses of NBMG control samples con 1, con 2, Sampson, and Goodspring....4

Table 2. Selected elemental contents of samples from areas in northwestern Nevada and southeastern Oregon that contain volcanic rock-hosted uranium deposits....5

Table 3. Major oxide and trace element contents of non-mineralized samples from the Virgin Valley, Kings River, and Lakeview areas....9

Table 4. SEM/EDX analyses of major chemical components of U minerals....10

Table 5. Hydrologic data sites used for this study....11

Table 6. $^{40}Ar/^{39}Ar$ dates for rocks from the Virgin Valley and Kings River areas....12

Table 7. Summary of trace element concentrations in waters in Virgin Valley, near McDermitt, and at Yucca Mountain....16

Table 8. Summary of NURE trace element concentrations in stream waters in three areas....16

Table 9. Summary of NURE trace element concentrations in well waters in three areas....17

Table 10. Summary of NURE trace element concentrations in spring waters in three areas....17

Table 11. Charactersistics of uranium occurrences and rock types at Virgin Valley, Nevada....35

Table 12. Comparison of the main hydrologic features in the study areas....68

Table 13. Summary of charactersistics of uranium deposits in northwestern Nevada and southeastern Oregon, and comparison with the geologic setting at Yucca Mountain, Nevada....69

FIGURES

Figure 1. Map of northwestern Nevada and southeastern Oregon showing mining districts with uranium production or occurrences....2

Figure 2. Generalized geologic map of the McDermitt caldera as modified from Dayvault and others (1985)....13

Figure 3. Piper diagram for McDermitt caldera area waters....14

Figure 4a. Geologic map of the Kings River district....18

Figure 4b. Geologic cross section of the Moonlight mine....19

Figure 5. Scatter plots of selected elements for samples with more than 20 ppm U....21

Figure 6. Backscattered SEM image of a layer of uraniferous zircon that shows finely crustiform texture in quartz-adularia breccia matrix, Moonlight mine....24

Figure 7. Backscattered SEM image of metazeunerite crystals (bright) with pharmacosiderite lining a cavity in breccia, Moonlight mine 25

Figure 8. Backscattered SEM image of pyrite framboids in silicified rhyolite with sulfide, sample MLT 4S, Horse Creek area....25

Figure 9. Regional geologic map of the Virgin Valley area....29

Figure 10. Detailed geologic map of the Virgin Valley uranium district....30

Figure 11. Volcanic stratigraphy in the Virgin Valley caldera as determined by $^{40}Ar/^{39}Ar$ dates reported in Table 6....31

Figure 12. Backscattered SEM image of acicular radiating weeksite crystals in opal, Virgin Valley 37

Figure 13. Secondary electron image of mata-ankoleite and carnotite in lignite, Virgin Valley 38

Figure 14. Backscattered SEM image of pyrite framboids in uranium-rich petrified wood, Virgin Valley....38

Figure 15a. Photomicrograph, crossed polars, yellow carnotite on fracture plane, Virgin Valley....39

Figure 15a. Photomicrograph, crossed polars, yellow carnotite spheroids in tuff, Virgin Valley....39

Figure 16. Piper diagram showing water chemistry data from the Virgin Valley area....41

Figure 17. Geologic map of the Lakeview uranium district from Castor and Berry (1981) 43

Figure 18. White King mine pit from the east 44

Figure 19. Lucky Lass mine pit from the east 44

Figure 20. Backscattered SEM image of galena (large bright grain), U- P silicate (small bright to light gray grains), arsenopyrite (irregular gray grains associated with galena and U- P silicate), and pyrite (isolated gray grains) in quartz (black). Sample C95-73, White King mine....46

Figure 21. Backscattered SEM image of spheroidal U-P silicate (gray) with tiny cinnabar crystals (bright) in quartz (black), sample C95-72, White King mine 46

Figure 22. Pike Creek Canyon U occurrence, Steens Mountain 49

Figure 23. Backscattered SEM image of autunite in fracture at Pike Creek Canyon (sample C95-85).....50

Figure 24. Geologic map of the Painted Hills uranium district modified from mapping in Cupp and others (1977)....52

Figure 25. Photomicrograph of autunite (bright) in fracture in limonitized tuff, Garrett prospect, Painted Hills (sample C95-132.) 54

Figure 26. Radioactive rock along the footwall of a mafic dike in a prospect (sample sites C95-126-130), Painted Hills district)....54

Figure 27. Piper diagram showing the general chemical nature of Yucca Mountain groundwater....67

INTRODUCTION

Studies of natural analogues constitute a necessary and respected approach to understanding problems in the physical sciences and are particularly critical to evaluating the effectiveness of potential nuclear waste isolation sites and strategies (e.g., Brookins, 1984; Krauskopf, 1988; Pearcy and Murphy, 1991). Several uranium deposits, for example, at Oklo (Gabon), Poços de Caldas (Brazil), and Cigar Lake (Canada), are being studied as analogues for waste isolation sites (Cramer, 1986; Curtis and others, 1989; Chapman and others, 1992).

The geologic, hydrologic, and climatic setting of the potential nuclear repository site at Yucca Mountain, Nevada, differs substantially from that of other potential repositories and natural analogues that are currently being studied. The Yucca Mountain site is in tuffaceous volcanic rocks containing assemblages of devitrification products and diagenetically formed zeolites and clay minerals, is in an oxidizing environment above the water table, and is in the tectonically active Basin and Range province in an arid climate. Processes of alteration of the repository and migration of radionuclides are likely to be markedly different from those in other settings, such as the three areas cited above. Although no single uranium deposit can exactly match the characteristics of Yucca Mountain, uranium deposits hosted by similar rocks in similar geologic-hydrologic-climatic settings would be among the best geologic natural analogues. The complete range of lithologic, mineralogic, geochemical, structural, and hydrologic characteristics of potential analogues needs to be considered because it is the interplay of these features with the technological system of a nuclear repository that will govern processes such as radionuclide migration. Therefore, studies at a number of sites will be necessary to provide a comprehensive natural analogue for Yucca Mountain.

Uranium deposits at two locations, Peña Blanca in Chihuahua, Mexico, and the McDermitt caldera area of Nevada and Oregon, are most commonly cited as appropriate analogues to Yucca Mountain (Murphy and others, 1990; Alexander and Van Luik, 1991; Pearcy and Murphy, 1991). It is important to recognize that the McDermitt caldera, which is within the area addressed by our study (Fig. 1), contains several uranium deposits with distinct characteristics. Additionally, uranium deposits occur in volcanic rocks in other areas within the Nevada-Oregon region studied.

Available data suggest that the uranium deposits in the Nevada-Oregon region could serve as good analogues for the interplay of the natural environment with nuclear waste storage at Yucca Mountain. All of these deposits are in volcanic rocks within the Basin and Range province, in geologic-hydrologic-climatic settings that are grossly similar to those at Yucca Mountain. However, additional data are necessary to characterize them more thoroughly, to determine whether processes active at these deposits would be similar to processes at Yucca Mountain, and to evaluate their potential as analogues. This report addresses those needs.

METHODS

The literature was searched for information on uranium deposits and occurrences in volcanic rocks in northwestern Nevada and southeastern Oregon. Selected deposits were examined and sampled during the Spring and Summer of 1995. During field work, γ radiation was measured using a Mount Sopris model 132-SC scintillometer. Radioactivity measurements are reported in the following text as "x background," the ratio of site radioactivity against that measured on unmineralized rock in the surrounding area.

Samples were collected in the field for chemical analysis, petrographic study, and $^{40}Ar/^{39}Ar$ dating. Sample preparation was done by the Nevada Bureau of Mines and Geology (NBMG). Chemical analyses were performed using instrumental neutron activation analysis (INAA) by the U.S. Geological Survey, Denver, Colorado, and inductively-coupled plasma atomic-emission spectrometry (ICP-AES) by USML Laboratories, North Highlands, California. Blind submittals of NBMG control samples along with project

Figure 1. Map of northwestern Nevada and southeastern Oregon showing mining districts with uranium production or occurrences.

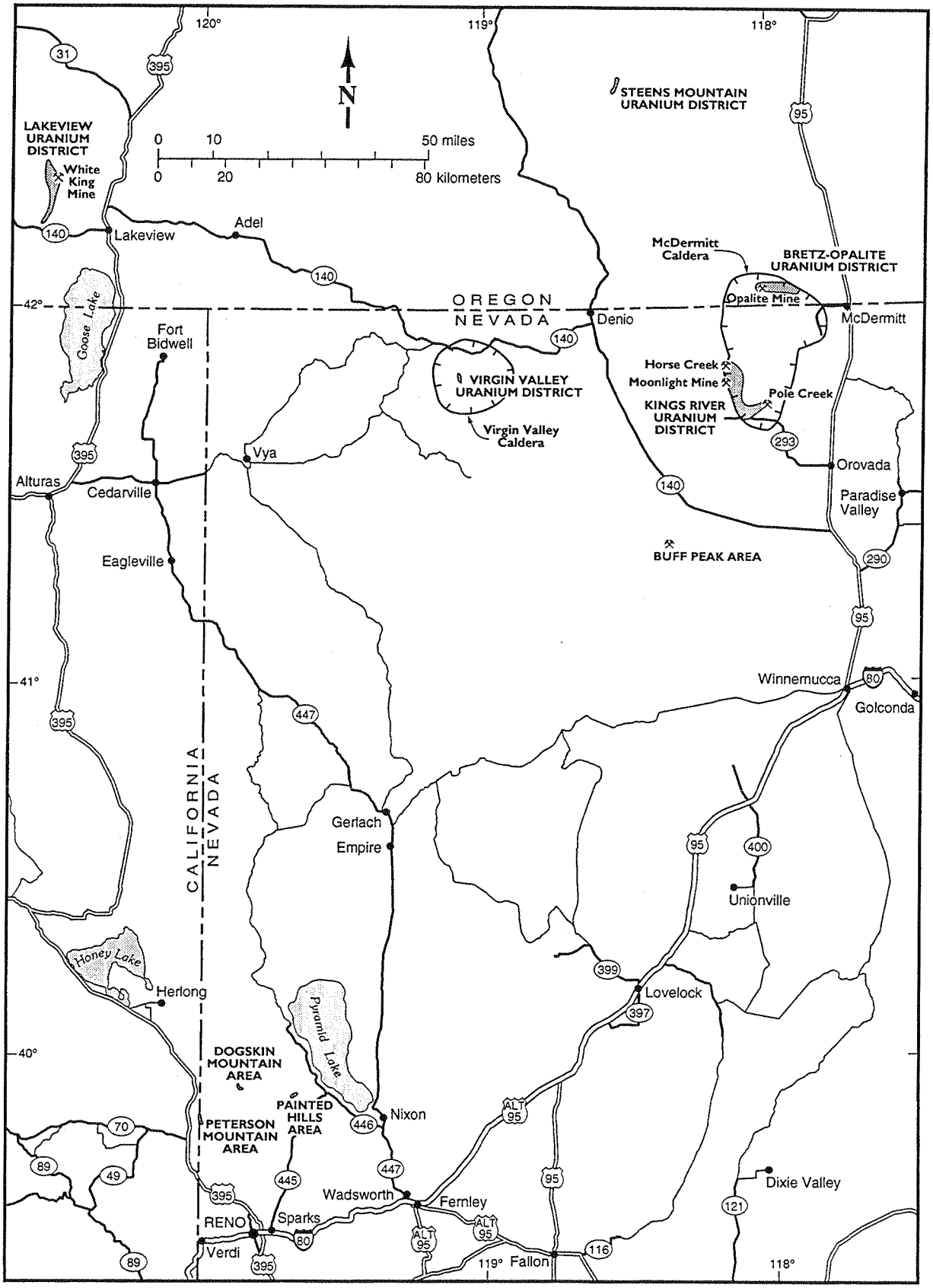

samples were used to determine accuracy and reproducibility of analyses by contracted laboratories (Table 1). Analytical data for project samples are reported in Table 2.

INAA is a relatively low cost method used to provide accurate analyses of many elements , including U and Th. However, because preanalytical irradiation of U produces elements such as Mo and Zr, analyses for these elements in samples that contain large amounts of U must be interpreted with care (Hoffman, 1992). Mo analyses by ICP-AES are available from USML and were used instead of INAA Mo analyses. Despite corrections for Zr measured in samples with high U, some samples were judged to have erroneously high Zr contents. Selected samples were analyzed for Zr by XRF at NBMG; these analyses are reported in lieu of INAA values and are so noted in Table 2.

USML Laboratories uses organic extraction techniques to avoid interference problems in ICP-AES analyses between some common elements, such as Fe and Te. The company reports precise analyses of 15 elements that are particularly applicable to epithermal mineral deposits. In addition to data from the USGS, INAA data for samples that were collected from the McDermitt caldera prior to this study were obtained from Bondar-Clegg, Inc., Denver, Colorado.

Major oxide and trace element analyses of 15 samples of rhyolitic rock from the Virgin Valley, Moonlight mine, and Lakeview areas were done using XRF techniques by Washington State University. Results of these analyses are reported in Table 3. Approximately 30 samples were analyzed by powder X-ray diffraction (XRD) methods using a Philips XRD system at 30Kv and 20mA at NBMG. Mineral phases were identified on XRD scan charts using JCPDS files and standard search methods.

Petrographic work was done on selected samples using a combination of optical petrography and microbeam analysis. The latter work was performed using a JEOL JSM-840M scanning electron microscope (SEM) with a KEVEX Quantex 6 EDX microanalysis system. All SEM work was performed at 15 kv on polished thin sections or rock chips following gold coating. Metal and mineral standards were used for SEM/EDX mineral analyses performed during this study, which are reported as oxide contents of major components in Table 4. In most cases, SEM/EDX analyses are reported with raw totals; however, in some cases it was necessary to report normalized values. Because SEM/EDX does not yield information on hydroxyl ion content, all analyses are reported as if they are for anhydrous minerals. The analyses reported in Table 4 are meant to be used as comparative data rather than as full mineral analyses.

Water chemistry and water level data from the study sites were sought through a search of the University of Nevada NEON on-line library search catalog. The federal and state government catalogs were searched, as well as the northern and southern Nevada libraries located at the University of Nevada, Reno and Las Vegas. Each search was conducted using the site name (e.g., Petersen Mountain) as part of a title or subject. Although numerous references to the geology of the mineralized areas within some of the study areas were located, very little relevant information on hydrogeology or hydrogeochemistry appears in published reports. The only site for which any hydrologic data reports were available was the McDermitt area. Data were also requested from Washoe County (Mike Widmer, Department of Public Works) for the area denoted as the Pyramid area below. Although considerable data have been collected and archived by the Washoe County office, none of the data within Washoe County were collected from the areas of Petersen Mountain, Dogskin Mountain or Painted Hills. Data on surface waters and groundwaters were also obtained from NURE files. Radon data from NBMG files and reports were also compiled. It was found that the majority of water data for the study sites were located in the EPA STORET database, which incorporates data archived in the USGS WATSTORE database. Hence, geochemical data for the areas of latitude and longitude noted below were obtained from the EPA STORET database, retrieved using the commercial software produced by EarthInfo (1993), and exported to a dBase file format which was later manipulated and viewed using Excel 4.0.

The number of analyses of water samples and the degree to which they are complete varies widely within and among the areas searched. This information is summarized for major element data in Table 3 below where # Records indicates the total number of analyses available for all sites and all dates of sample

Table 1. Analyses of NBMG control samples con 1, con 2, Sampson, and Goodspring. Recommended values determined by averaging commercial round robin analyses. * standard analysis by Bondar-Clegg. √ element analyzed by USML. Analyses in ppm except as noted.

Standard	U	Fe %	Ca %	Na %	K %	Rb	Sr	Cs	Ba	Th	La	Ce	Sm	Eu
con 1	4	1.40	13.10	0.78	1.60	60	397	2	1200	6.4	31.1	49	5.5	0.86
con 1	4	1.57	12.70	0.78	1.42	69	436	2	1310	6.2	31.2	51	5.4	0.97
con 1	4	1.39	12.90	0.82	1.93	73	515	2	1410	6.5	29.6	50	5.4	0.98
con 1*	4	1.60		0.48		57		2	1100	5.0	17.0	31	3.6	<1.00
recom. values	3	0.90	13.00	0.57	1.47	42	460	2	1100	3.9	18.0	32	3.1	0.70
con 2	1	3.92	4.06	2.74	1.18	25	725	1	813	2.5	17.6	31	3.9	1.04
con 2	2	4.46	3.53	3.12	1.66	30	744	1	931	2.6	20.5	35	4.4	1.10
con 2	1	4.32	3.59	2.97	0.71	30	859	1	939	3.0	17.7	38	4.0	1.05
con 2*	1	4.30		2.58		31		1	1100	2.9	15.0	31	3.7	<1.00
recom. values	1	4.10	4.00	2.95	1.45	39	780	1	990	2.7	18.0	34	3.1	1.20
Goodspring	7	4.77	18.6	0.02	0.68	1	<50	0	206	0.3	4.1	1	0.3	0.19
Goodspring	7	5.46	19.0	0.07	NA	3	<50	0	83	0.4	4.3	4	0.7	0.13
recom. values	6	4.70	18.0	0.00	NA	NA	61	NA	79	NA	4.0	NA	0.3	0.50
Sampson	137	6.13	10.10	0.01	0.95	1	<50	0	125	0.1	3.8	4	0.9	0.31
Sampson	123	5.96	9.64	0.03	NA	3	<50	0	121	0.1	4.0	3	0.6	0.36
recom. values	112	5.80	9.00	0.00	NA	NA	38	NA	75	0.4	6.0	9	2.3	0.40

Standard	Tb	Yb	Lu	Zr	Hf	Ta	W	Sc	Cr	Co	Ni	Zn	As	Se
con 1	0.82	2.28	0.37	143	3.4	0.61	2.0	9.2	72	4.7	23	125	8	<1.0
con 1	0.75	2.55	0.41	161	3.4	0.62	1.7	9.8	79	5.3	27	146	8	<1.0
con 1	0.79	2.73	0.41	144	3.6	0.71	3.7	10.0	88	4.2	30	119	4	0.5
con 1*	0.70	<2.00	0.40	<200	2.0	<0.50	1.0	6.1	41	6.0	33	<100	3	<5.0
recom. values	0.60	1.90	0.30		2.0	0.41		7.0	73	4.5	42	81	4	0.6
con 2	0.41	1.06	0.17	122	3.0	0.35	1.5	11.5	153	16.2	64	93	2	<1.0
con 2	0.44	1.17	0.22	122	3.0	0.40	1.6	13.1	168	18.0	68	108	3	<1.0
con 2	0.45	1.11	0.17	137	3.2	0.41	1.1	12.9	154	17.4	67	43	2	0.1
con 2*	<0.50	<2.00	<0.20	<200	3.0	<0.50	<1.0	12.0	130	19.0	66	<100	4	<5.0
recom. values	0.40	0.90	0.14		3.0	0.44		12.6	170	20.0	59	70	2	0.1
Goodspring	0.13	0.19	0.03	43	0.3	0.25	10.3	0.4	22	32.1	140	100k	1390	110.0
Goodspring	0.18	0.17	0.03	134	0.6	0.17	12.6	0.5	24	36.6	159	113k	1720	158.0
recom. values	NA	0.30	NA	<200	1.0	NA	8.0	NA	13	37.0	116	118k	1329	NA
Sampson	0.13	0.27	0.02	164	0.1	0.04	15.1	0.1	24	113	998	9,590	433	6.9
Sampson	0.16	0.44	0.05	69	0.1	0.05	24.4	0.1	23	108	1,070	7,860	486	9.7
recom. values	NA	0.40	1.00	<200	NA	NA	19.0	NA	26	123	1,151	9,151	387	NA

Standard	Bi√	Cd√	Cu√	Ga√	Hg√	Mo√	Pb√	Sb√	Sn√	Te√	Tl√	Ag√	Au√ ppb
con 1	0.56	0.59	22.2	3.63	0.11	9.8	5.8	1.2	1.39	<0.50	1.04	0.19	2.0
con 1	0.52	0.59	21.6	3.47	0.11	6.2	5.4	1.1	<0.50	<0.50	0.87	0.20	1.3
con 1	0.38	0.49	19.3	3.15	<0.10	4.9	4.5	0.7	<0.50	<0.50	0.67	0.12	6.9
recom. values	0.35	0.40	21.0		0.10	9.0	4.8	0.9	1.00	0.19		0.11	0.7
con 2	0.43	<0.10	23.9	2.48	<0.10	1.2	2.9	0.5	<1.00	<0.50	1.07	0.08	4.2
con 2	0.41	<0.10	22.1	2.25	<0.10	1.2	2.6	0.4	0.51	<0.50	0.88	0.07	2.2
con 2	0.27	<0.10	24.3	2.60	<0.10	1.3	1.9	0.3	0.54	<0.50	0.59	0.05	1.3
recom. values	0.29	0.04	24.0		0.02	3.0	2.1	0.3	1.00	0.15		0.04	0.9
Goodspring	1.01	2523	1212	4.90	10.20	42.6	>9780	244	<0.50	<0.50	<0.50	24.8	146
Goodspring	0.82	2486	1183	4.56	10.20	42.5	>9350	244	<0.50	<0.50	<0.50	26.8	165
recom. values	3.50	2615	1230	NA	NA	53.0	21083	253		NA	NA	27.0	155
Sampson	13.0	190	7888	62.2	7.04	151	3256	54.4	<0.50	<0.50	0.66	109.0	4.7
Sampson	12.4	85	7531	58.7	6.85	147	3183	52.0	2.01	<0.50	<0.50	111.0	8.7
recom. values	17.0	221	7314	NA	NA	146	2963	66.0	2.00	NA	NA	115.3	NA

Table 2. Selected elemental contents of samples from areas in northwestern Nevada and southeastern Oregon that contain volcanic rock-hosted U deposits.

Sample	Latitude (d:m:s)	Longitude (d:m:s)	Description	U	Fe %	Ca %	Na %	K %	Rb	Sr	Cs	Ba	Th	La	Ce	Sm	Eu	Tb	Yb	Lu
Kings River district																				
Pole Creek																				
C95-96	41:43:51	118:01:16	Limonitic flow-banded rhyolite	345	1.07	1.60	1.53	3.10	141	<20	4	148	11.0	16.5	37	7.5	0.85	3.01	28.60	4.79
C95-97	41:43:51	118:01:16	Flow-banded rhyolite	18	1.81	0.25	1.39	2.97	115	23	4	219	12.1	40.3	83	11.7	0.71	1.55	5.25	0.90
C95-98	41:43:51	118:01:16	Ash-flow tuff (?)	32	1.36	0.52	2.66	4.59	185	37	5	511	14.3	26.7	51	10.6	1.41	1.52	8.28	1.30
C95-99	41:43:03	118:00:44	Limonitic non-welded ash-flow tuff (?)	162	2.28	5.39	1.13	4.37	148	76	2	595	17.3	27.6	62	11.0	2.00	2.96	24.30	4.15
Moonlight mine																				
C95-102	41:47:21	118:08:44	Intermediate volcanic rock	4	3.69	3.01	2.73	2.70	111	237	5	990	9.8	34.9	67	7.4	1.57	1.13	3.08	0.49
C95-104	41:47:19	118:09:28	Altered rhyolite	12	0.46	0.58	1.73	5.90	283	79	5	1260	14.6	50.8	135	9.9	1.51	1.11	3.77	0.59
C95-105	41:47:17	118:09:31	Limonitic altered rhyolite	25	1.14	0.34	0.41	9.16	320	95	2	1210	13.6	35.8	69	6.4	0.96	0.67	3.52	0.51
C95-107	41:47:20	118:09:11	Peralkaline flow-banded rhyolite, devitrified	7	1.77	0.14	1.17	6.16	321	35	5	115	18.8	51.5	112	13.2	0.49	2.26	8.67	1.36
C95-118A	41:47:16	118:09:33	Unoxidized to partly oxidized breccia vein	1,200	2.29	37.40	0.05	3.97	228	358	35	371	11.5	31.5	74	7.8	1.16	1.90	8.84	1.21
C95-118B	41:47:16	118:09:33	Unoxidized to partly oxidized breccia vein	988	2.23	20.60	0.09	3.23	126	290	1	408	6.6	4.6	16	4.1	1.38	1.36	13.90	2.24
C95-120	41:47:16	118:09:33	Oxidized breccia	1,940	2.11	8.42	0.13	5.24	230	273	1	895	10.7	5.9	31	6.3	1.50	1.26	8.65	1.42
C95-121	41:47:31	118:09:37	Limonitic breccia	1,030	11.10	3.12	0.79	9.59	182	365	3	1030	7.6	9.9	36	5.7	2.07	1.32	6.73	1.28
H95-82	41:43:30	118:07:42	Ash-flow tuff, hydrated vitrophyre	9	2.16	0.30	2.00	3.46	282	105	76	143	17.7	50.4	111	13.5	0.71	1.97	7.94	1.23
MLT 8*	41:47:16	118:09:33	Oxidized breccia from portal of incline	4,420	2.90		1.30		160		<1		10.0					1.30	20.00	
AAI 484*	41:47:16	118:09:33	Oxidized breccia	2,830	7.00		0.17		200		<1		8.8					<0.50	19.00	
Horse Creek																				
C95-122	41:48:00	118:09:45	Flow-banded rhyolite	25	1.57	0.08	0.77	6.04	279	31	2	244	16.8	47.2	107	11.9	1.06	2.24	8.13	1.33
C95-123	41:50:29	118:09:14	Rhyolite with sulfide	200	1.63	0.80	1.20	8.09	193	<20	6	84	15.8	40.5	111	11.5	0.53	2.21	12.70	1.82
MLT 4*	41:50:17	118:09:30	Breccia with silica and sulfide(?) in matrix	193	2.90		1.70		160		2		15.0	18.0		4.3			24.00	
MLT 4S*	41:50:17	118:09:30	Rhyolite with sulfide	997	3.00		0.19		<20		<1		45.5					2.30	52.00	
MLT 6A*	41:59:21	118:09:13	Breccia with limonite and hematite	351	6.40		0.75		220		6		10.0	16.0		8.3	2.00	1.80	14.00	
MLT 16*	41:48:23	118:09:47	Drill core, breccia with sulfide	171	4.30		0.16		370		2		10.0	19.0	33	5.7		1.20	10.00	
MLT 17*	41:48:23	118:09:47	Drill core, quartz - sulfide vein	219	4.00		0.14		270		3		12.0	17.0	23	5.8		1.20	12.00	
MLT 18*	41:48:23	118:09:47	Drill core, sulfide veins in brecciated rhyolite	488	4.20		0.14		300		3		16.0	25.0		3.5	2.00	1.60	14.00	
MLT 19*	41:48:23	118:09:47	Drill core, breccia with sulfide	291	4.40		0.14		330		14		6.2	22.0	50	5.3	1.00	0.70	3.00	
MLT 21*	41:48:23	118:09:47	Drill core, sulfide - fluorite veins	127	6.20		1.50		300		48	1200	4.9	40.0	83	8.1	2.00	0.90	2.00	
MLT 22*	41:48:31	118:09:50	Brecciated rhyolite with hematite	131	2.10		0.43		280		4		18.0	36.0	82	11.5		2.10	13.00	
MLT 23*	41:48:32	118:09:50	Brecciated rhyolite with limonite	68	5.60		0.74		260		3		17.0	40.0	80	10.4		1.70	16.00	
Bretz-Opalite district																				
Aurora deposit																				
C95-89	42:01:59	117:54:23	Argillized and oxidized scoria	331	3.44	0.84	0.62	2.11	76	32	11	1330	7.0	11.6	23	4.9	2.61	0.84	5.01	0.78
C95-90	42:01:59	117:54:23	Argillized scoria	139	0.51	0.39	2.05	3.62	107	106	8	2300	6.8	43.6	80	6.2	3.09	0.58	2.37	0.41
Bretz mine																				
C95-91	42:02:46	117:53:56	Silicified rhyolite	34	0.17	0.34	0.02	0.31	2	<20	1	28	2.8	1.5	6	1.3	0.13	0.67	5.26	0.94
C95-92	42:02:50	117:54:07	Limonitic scoria	192	9.67	0.33	0.06	1.12	10	103	5	596	4.4	2.4	7	1.6	0.24	0.79	3.14	0.52
C95-93	42:02:53	117:54:11	Silicified rock with sulfide	103	0.92	0.43	0.15	0.77	18	39	1	428	20.9	31.4	37	2.8	0.14	0.74	4.18	0.73
Cottonwood Creek																				
C95-94	42:02:59	117:55:16	Silicified shale with petrified wood fragments	193	1.25	0.84	0.48	0.70	46	103	27	200	2.3	6.7	14	2.7	0.49	0.47	4.51	0.82
Opalite mine																				
C95-95	42:03:09	118:02:02	Silicified breccia	175	0.24	0.48	0.02	0.46	1	23	0	217	14.0	0.5	5	3.4	0.67	2.09	18.30	3.36
Virgin Valley																				
C95-110	41:47:52	119:06:17	Canyon Rhyolite, highly radioactive	2,690	2.21	5.68	1.99	3.37	156	118	7	243	20.0	17.9	37	10.1	0.37	1.84	11.50	1.87
C95-111	41:47:45	119:06:33	Canyon Rhyolite	10	0.33	0.10	2.51	3.20	170	<20	5	33	20.0	33.3	111	6.4	0.25	0.90	4.03	0.60
C95-112	41:47:37	119:06:24	Bedded tuff with U mineral on fracture	189	0.73	1.38	0.88	1.27	113	92	12	140	11.5	41.2	96	9.3	0.78	1.76	8.41	1.26
C95-113	41:47:53	119:06:03	Lignite	2,250	0.81	2.86	0.60	2.10	111	40	12	154	14.7	15.8	47	20.4	2.00	5.61	33.60	5.11
C95-114	41:47:53	119:06:04	Air-fall tuff with opal ± zeolite	426	1.16	1.13	0.76	3.69	262	33	20	203	24.2	29.5	71	9.0	0.70	1.73	8.11	1.22
C95-115	41:47:00	119:05:45	Opalized air-fall tuff	20	1.15	0.13	1.16	3.50	166	45	11	100	17.3	48.4	108	11.4	0.66	1.62	7.18	1.13
C95-115	41:47:00	119:05:45	Opalized air-fall tuff	37	1.09	0.08	1.01	2.35	144	28	12	58	15.8	41.4	90	9.6	0.57	1.44	6.59	1.06
C95-116	41:44:18	119:08:30	Peralkaline rhyolite, flow-banded, devitrified	14	1.39	0.25	3.01	3.34	249	20	9	97	27.9	36.9	78	13.8	0.94	2.53	12.10	1.89
C95-116a	41:44:18	119:08:30	Peralkaline rhyolite, non-hydrated glass	12	1.28	0.48	3.19	4.09	236	37	9	35	26.1	33.9	85	13.6	0.85	1.99	10.00	1.60
C95-124	41:47:48	119:06:05	Opalized wood ± sulfide	755	0.77	2.88	0.18	0.38	46	21	10	71	7.0	0.4	2	1.1	0.11	0.18	0.72	0.15
VV-2	41:47:46	119:06:06	Brown opal	1,380	0.31	4.43	0.21	0.29	31	24	8	86	2.1	1.7	4	3.0	0.27	0.83	4.81	0.64
VV-5	41:47:50	119:06:05	Argillized tuff	645	1.21	3.72	1.23	2.86	85	109	6	216	8.0	14.9	22	6.6	0.66	1.58	6.86	0.97
VV-6	41:47:56	119:06:12	Zeolitized tuff	96	2.40	0.83	0.99	4.03	147	159	11	240	15.5	28.6	65	6.6	0.76	0.75	1.80	0.32
VV-7	41:47:58	119:06:16	Highly radioactive breccia in rhyolite	9,740	1.41	18.00	1.74	2.97	150	<20	4	274	12.1	14.1	45	5.9	0.37	1.08	7.65	1.18
VV-9	41:47:01	119:05:47	Fluorescent opal replacing diatomite	657	0.55	1.82	0.08	0.21	3	40	3	179	0.5	1.9	6	1.6	0.13	0.25	1.44	0.25
VV-11	41:47:00	119:05:45	Fluorescent opal with Mn oxide	1,190	0.30	3.96	0.05	0.19	1	23	1	266	0.1	1.1	4	1.6	0.14	0.23	1.69	0.26
H95-57	41:31:18	119:07:36	Late porphyritic rhyolite, hydrated glass	14	1.35	0.20	3.05	3.91	256	24	9	39	25.9	51.7	111	15.7	0.21	2.63	13.50	2.10
H95-68	41:51:54	118:58:12	Canyon Rhyolite, hydrated vitrophyre	9	0.91	0.20	1.79	5.09	224	<20	6	48	19.6	49.5	96	10.0	0.29	1.21	6.16	1.02
H95-75	41:49:24	119:03:18	Virgin Valley Fm., reworked tuff with clay & zeolite	4	3.12	1.85	1.85	2.38	82	396	4	1050	10.6	45.5	88	10.5	1.62	1.40	5.57	0.91
H95-77	41:50:18	119:04:48	Virgin Valley Fm., reworked tuff with clay	3	4.15	1.78	1.24	1.08	65	251	5	323	10.3	38.1	74	8.6	1.56	1.02	3.98	0.63
H95-78	41:50:18	119:04:48	Virgin Valley Fm, hydrated glassy reworked tuff	6	2.33	0.75	1.11	3.20	178	90	5	647	17.6	67.1	136	12.6	1.02	1.26	5.70	0.90

Unmarked = INAA (USGS), † = GFAA (USML), √ = ICP ES (USML), * INAA by Bondar Clegg

Table 2 (continued)

Sample	Latitude (d:m:s)	Longitude (d:m:s)	Description	U	Fe %	Ca %	Na %	K %	Rb	Sr	Cs	Ba	Th	La	Ce	Sm	Eu	Tb	Yb	Lu
Lakeview district																				
White King mine																				
C95-70	42:19:57	120:31:16	Flow-banded rhyolite	13	0.21	0.30	1.55	3.97	174	88	124	236	12.9	8.6	18	3.8	0.11	0.67	4.31	0.68
C95-71	42:19:55	120:30:59	Argillized breccia	108	0.45	1.20	0.37	4.47	148	171	125	1490	6.2	12.6	20	1.5	0.37	0.27	1.57	0.22
C95-72	42:19:55	120:30:59	Breccia with argillized matrix, highly radioactive	2,850	0.66	4.87	0.10	29.50	58	118	86	2360	2.3	2.2	10	1.2	0.80	0.92	4.56	0.60
C95-73	42:20:10	120:31:13	Brecciated flow-banded rhyolite	1,460	0.44	2.38	0.37	2.07	92	182	312	2050	7.3	1.6	4	0.8	0.41	0.57	2.53	0.43
C95-74	42:20:10	120:31:13	Brecciated flow-banded rhyolite	197	0.65	1.43	0.41	1.44	145	264	489	520	8.9	6.8	17	3.8	0.25	0.51	1.65	0.32
Lucky Lass mine																				
C95-75	42:20:07	120:32:22	Air-fall tuff	6	2.55	0.62	1.01	3.96	190	<20	6	50	15.5	56.4	115	10.6	0.74	1.53	5.51	0.86
C95-78	42:20:10	120:32:21	Altered basalt	323	2.54	5.90	2.94	1.05	19	638	1	912	1.4	25.3	47	6.3	1.88	0.92	3.30	0.50
C95-80	42:20:10	120:32:21	Altered basalt	693	2.45	6.42	2.79	1.06	13	649	1	670	1.3	17.0	40	4.0	1.54	0.59	1.59	0.22
Thomas Creek																				
C95-81	42:19:55	120:35:13	Flow-banded rhyolite	5	0.22	0.49	2.24	4.04	126	33	3	72	8.3	9.4	18	2.0	0.19	0.39	1.87	0.32
C95-82	42:20:01	120:33:08	Basalt	1	5.50	5.44	2.41	1.80	32	453	1	837	1.9	20.9	40	3.9	1.09	0.57	2.19	0.34
C95-83	42:20:09	120:33:31	Flow-banded rhyolite, non-hydrated glass	9	0.42	0.65	2.65	3.63	181	<20	8	61	14.2	9.9	18	4.1	0.10	0.80	4.39	0.72
C95-83	42:20:09	120:33:31	Flow-banded rhyolite, non-hydrated glass	9	0.44	0.51	3.20	3.64	210	<20	9	21	16.0	10.5	22	4.3	0.13	0.86	4.88	0.76
Bottle Creek																				
C-95-147	41:22:08	118:21:28	Pink flow-banded rhyolite	20	0.71	0.43	2.92	3.53	584	20	17	135	42.3	15.9	32	10.9	0.23	2.75	16.00	2.51
C-95-148	41:22:08	118:21:28	Light gray rhyolite	18	0.69	0.85	2.43	4.16	358	71	18	155	36.1	12.2	30	9.6	0.09	2.11	8.90	1.32
C-95-149	41:22:10	118:21:27	Vitrophyre, hydrated	10	0.51	0.48	2.73	2.17	223	189	27	560	14.3	15.1	27	2.6	0.47	0.43	1.55	0.24
C-95-150	41:22:10	118:21:21	Silicified brecciated rhyolite	1,150	1.07	1.95	0.08	7.82	190	46	2	350	10.6	11.0	21	2.2	0.46	0.43	2.03	0.32
C-95-151	41:22:10	118:21:21	Argillized rhyolite	16	0.66	0.71	0.98	1.71	73	174	71	509	13.0	14.5	24	4.0	0.44	0.42	1.65	0.25
C-95-152	41:21:17	118:22:10	Altered rhyolite with quartz veins	11	0.40	0.28	0.12	5.65	275	36	6	486	26.1	16.9	34	6.0	0.10	0.80	4.15	0.67
C-95-153	41:21:13	118:22:13	Quartz veins in rhyolite	0	0.17	0.42	0.01	<0.45	22	38	1	165	0.2	0.4	1	0.1	0.02	0.01	0.07	0.01
C-95-154	41:20:50	118:22:18	Quartz veins in pre-Tertiary metamorphic rock	0	0.54	2.89	0.03	1.48	20	285	2	225	0.2	0.8	1	0.3	0.08	0.05	0.16	0.02
Steens Mountain																				
C95-84	42:34:47	118:32:33	Rhyolite	13	4.76	0.29	0.23	5.20	153	82	3	363	3.8	27.7	54	5.5	1.16	0.67	1.88	0.32
C95-85	42:34:47	118:32:33	Breccia vein; rock flour, quartz, and Fe oxide matrix	2,160	0.55	6.79	1.24	4.43	105	60	4	358	7.8	23.7	36	4.2	0.57	0.94	4.77	0.76
C95-86	42:34:47	118:32:33	Rhyolite with stockwork veins	1,090	1.27	2.17	2.52	4.10	114	56	2	402	9.9	36.9	67	6.8	0.33	1.23	4.21	0.67
C95-87	42:34:48	118:32:34	Flow-banded rhyolite	3	0.62	0.27	1.30	5.11	126	23	2	258	8.9	33.9	63	4.9	0.23	0.67	2.90	0.46
C95-88	42:34:48	118:32:27	Breccia vein	872	0.58	1.81	2.13	3.43	88	<20	1	303	8.2	26.7	41	5.2	0.30	0.92	3.21	0.54
Painted Hills																				
C95-126	39:53:50	119:41:10	Opalized tuff	289	1.11	1.50	1.66	3.20	151	111	7	948	19.1	40.4	86	5.2	0.56	0.57	2.03	0.34
C95-127	39:53:50	119:41:10	Zeolitized (?) tuff	19	1.14	0.11	1.62	3.66	341	176	53	1150	24.1	52.6	98	6.5	0.67	0.62	2.49	0.37
C95-128	39:53:50	119:41:10	Mafic dike rock	28	3.47	4.33	2.68	1.19	30	507	1	572	3.2	14.5	26	3.8	1.00	0.45	1.35	0.18
C95-130	39:53:50	119:41:10	Argillized tuff	7	1.10	1.41	1.37	2.00	122	133	11	504	21.5	37.4	68	5.9	0.56	0.61	2.54	0.44
C95-132	39:54:02	119:41:00	Altered tuff, highly radioactive	12,800	15.80	21.80	0.39	1.04	478	<20	51	225	12.7	8.7	52	12.0	0.03	2.15	9.61	1.41
C95-133	39:54:02	119:41:00	Altered tuff, highly radioactive	8,310	7.08	21.50	0.63	0.98	278	<20	35	219	21.2	3.8	30	19.0	3.31	4.55	20.10	3.61
PH-2	39:53:47	119:41:13	Altered welded ash-flow tuff, limonitic	357	6.16	0.77	2.06	2.99	148	202	3	502	15.4	29.6	36	5.7	0.33	0.76	2.15	0.35
PH-3	39:53:47	119:41:13	Altered welded ash-flow tuff, highly radioactive	4,220	1.39	12.00	1.54	1.84	123	<20	2	400	14.1	6.0	14	7.6	0.47	1.25	5.96	0.76
Petersen Mountain district																				
C-95-134	39:49:00	119:59:55	Limonitic nonwelded ash-flow tuff	280	1.59	0.77	2.67	6.23	308	91	9	746	27.2	64.6	112	8.6	0.48	0.96	3.46	0.54
C-95-135	39:49:00	119:59:55	Hematitic nonwelded ash-flow tuff	2,320	1.85	7.02	2.21	4.54	263	441	25	972	24.1	43.0	94	7.1	0.45	0.80	3.03	0.55
C-95-136	39:49:03	119:59:52	Highly radioactive ash-flow tuff	5,600	1.46	18.10	1.59	5.96	262	120	12	1170	20.0	66.5	60	2.8	1.12	0.67	3.43	0.70
C-95-137	39:49:03	119:59:48	Fresh welded ash-flow tuff	9	1.64	0.88	2.64	4.38	166	324	4	1630	20.5	38.5	75	6.1	1.08	0.62	2.13	0.37
C-95-138	39:49:03	119:59:54	Nonwelded ash-flow tuff	8	1.55	1.45	2.15	2.05	146	222	51	843	22.0	42.9	83	6.9	0.74	0.66	2.17	0.37
Dogskin Mountain district																				
C-95-139	39:54:16	119:52:17	Hematitic altered welded ash-flow tuff	719	1.61	2.21	1.39	3.36	185	86	8	281	27.6	51.0	109	7.6	0.19	0.97	5.61	1.01
C-95-140	39:54:16	119:52:17	Gray altered welded ash-flow tuff	267	1.21	0.52	0.52	3.93	232	127	33	404	40.8	26.8	52	2.8	0.38	0.28	1.38	0.29
C-95-141 *	39:54:16	119:52:17	Altered welded ash-flow tuff with gray silica veins	175	0.45	0.42	0.87	3.19	136	79	4	634	36.9	26.6	44	2.6	0.37	0.43	4.10	0.58
C-95-142	39:54:17	119:52:19	Altered welded ash-flow tuff with gray silica veins	276	0.33	0.66	0.51	2.88	115	36	4	250	22.0	12.6	32	1.8	0.27	0.43	2.67	0.42
C-95-143	39:54:18	119:52:23	Welded ash-flow tuff	9	1.93	0.64	2.24	5.09	166	108	9	1650	21.0	58.0	111	10.2	1.80	1.16	3.33	0.52
C-95-144	39:55:31	119:52:57	Reddish-brown clay gouge	3,580	2.44	8.77	0.15	4.67	48	162	2	1370	6.0	33.3	47	6.3	1.24	0.89	2.60	0.39
C-95-145	39:55:31	119:52:57	Altered ash-flow tuff with Mn and Fe oxides	219	5.31	2.58	1.50	2.91	100	737	5	3230	15.1	48.4	110	6.6	1.34	0.76	3.18	0.53
C-95-146	39:55:31	119:52:57	Sheared and altered ash-flow tuff	282	1.49	1.96	2.35	2.31	83	726	2	2790	12.3	38.3	72	5.3	1.31	0.54	1.98	0.35

Unmarked = INAA (USGS), † = GFAA (USML), √ = ICP ES (USML), * INAA by Bondar Clegg

Table 2 (continued)

Sample	Zr	Hf	Mo√	Ta	W	Sc	Cr	Co	Ni	Zn	As	Se	Ag√	Bi√	Cd√	Cu√	Ga√	Hg√	Pb√	Sb√	Sn√	Te√	Th√	Au† ppb
Kings River district																								
Pole Creek																								
C95-96	3,550*	71.4	4.8	1.24	7.9	12.5	150	0.7	17	63	21	<1.0	0.06	0.41	0.06	4.6	1.12	<0.08	7.7	20.8	1.29	0.17	1.04	0.5
C95-97	280	9.3	84.6	0.96	5.7	1.4	121	0.8	3	66	52	<1.0	0.07	1.60	0.11	3.7	1.09	0.06	16.7	35.2	2.20	0.30	1.02	1.8
C95-98	461	16.8	21.4	1.57	13.3	2.6	96	0.8	9	42	106	<1.0	0.10	0.64	0.13	6.2	1.05	0.67	3.0	14.9	1.91	0.29	1.15	1.2
C95-99	1,270	38.1	52.3	0.98	14.8	16.3	18	0.8	2	112	281	<1.0	0.08	1.14	0.14	6.6	0.52	0.61	18.8	24.1	1.55	0.19	6.53	5.9
Moonlight mine																								
C95-102	298	7.3	1.7	1.22	2.0	14.3	57	16.4	37	101	13	<1.0	0.07	0.50	0.06	58.9	3.00	0.03	3.7	2.2	1.44	0.18	1.10	1.8
C95-104	299	7.9	5.1	1.47	5.6	4.2	71	0.4	6	30	73	<1.0	0.08	0.54	0.06	3.2	0.53	0.01	9.4	2.4	0.37	0.22	1.02	2.7
C95-105	382	8.9	6.6	1.48	8.2	3.8	158	0.8	5	15	657	<1.0	0.23	0.49	0.10	10.4	1.07	1.24	18.2	55.4	0.69	0.22	1.42	40.3
C95-107	621	14.9	0.6	3.82		0.4	1	30.1	4	153	64	<1.0	0.10	0.16	0.34	3.7	1.09	0.79	18.9	7.5	2.17	0.15	0.66	2.0
C95-118A	6,690	42.2	109.0	1.24	32.3	8.9	15	0.8	15	165	12200	6.0	27.9	12.30	1.08	256.0	7.21	1.83	712.0	91.7	2.64	10.30	18.60	504.0
C95-118B	13,500	93.7	97.9	0.29	22.8	16.2	143	3.8	17	77	8600	2.6	12.1	2.71	0.44	86.8	4.40	0.69	72.2	93.8	2.09	4.28	4.05	478.0
C95-120	33,100*	113.0	10.4	0.99	16.9	14.2	51	0.6	16	137	2240	<1.0	2.09	1.14	0.53	110.0	1.88	1.63	39.1	88.1	1.60	0.51	1.84	1,150.0
C95-121	6,960	51.2	34.9	0.83	19.1	15.6	88	3.5	31	397	9930	<1.0	2.70	0.92	0.75	30.3	3.79	1.33	10.6	257.0	0.95	0.19	6.77	149.0
H95-82	406	12.9	1.8	2.57		0.8	<1	17.7	6	130	14	<1.0	0.07	0.33	0.18	2.8	1.35	<0.04	8.4	0.2	0.55	0.08	0.33	1.0
MLT 8*	49,500	203.0	88.3	<0.50	32.0	33.3		50.0	140		3210		4.11	1.21	1.54	160.0	<0.50	0.42	27.5	181.0		1.82	47.20	290.0
AAI 484*	20,000	72.0	34.8	<0.50	12.0	10.0			95		6290		36.0	1.95	0.75	223.0	3.95	1.94	35.5	94.6		7.09	12.30	200.0
Horse Creek																								
C95-122	461	12.0	10.5	1.75	13.0	1.6	232	1.3	14	72	156	<1.0	0.28	0.70	0.37	5.9	1.31	1.90	20.8	21.2	1.32	0.23	3.49	7.5
C95-123	526	14.1	30.3	1.77	13.4	0.9	244	1.2	11	88	10800	<1.0	0.49	0.62	0.30	7.2	0.72	0.24	7.6	136.0	1.22	0.12	3.62	98.3
MLT 4*	3,300	<2.0	354.0	<0.50	13.0	17.0			60		>9000		20.4	2.93	1.88	53.1	<0.50	2.71	4.6	133.0		<0.50	20.30	565.0
MLT 4S*	8,000	9.0	1,925.0	<0.50	<5.0	17.0			79		7830		114.0	15.20	<0.10	67.8	<0.50	4.79	8.9	145.0		1.10	82.60	>9000.0
MLT 6A*	2,200	11.0	280.0	<0.50	32.0	7.3			36		2180		1.43	2.39	2.39	27.9	<0.50	1.07	8.6	84.3		<0.50	5.63	<7.0
MLT 16*	400	4.0	153.0	0.90	43.0	9.2	63	18.0	61		1150		0.75	1.51	0.14	83.5	<0.50	1.02	33.2	82.1		<0.50	8.22	120.0
MLT 17*	490	3.0	910.0	<0.50	64.0	12.0	87	15.0	51		837		10.4	7.62	2.81	94.9	<0.50	0.53	54.6	68.7		1.39	24.40	45.0
MLT 18*	810	9.0	1,097.0	0.80	43.0	9.2	73	10.0	55		784		7.12	9.15	1.07	57.9	<0.50	0.81	34.7	80.9		0.85	27.30	46.0
MLT 19*		4.0	55.4	<0.50	50.0	11.0	100	15.0	67		115		1.27	0.70	0.58	37.7	0.69	0.26	13.3	14.9		<0.50	2.72	17.0
MLT 21*		<1.0	67.3	0.80	32.0	13.0	180	14.0	52		255		1.37	0.89	0.36	29.1	5.80	0.38	24.1	11.9		<0.50	1.81	74.0
MLT 22*	540	12.0	21.3	1.60	12.0	1.3			34		480		0.27	0.25	0.33	25.6	<0.50	0.65	12.3	56.3		<0.50	0.82	56.0
MLT 23*	670	7.0	80.8	1.30	8.0	0.9	65		32		1540		0.16	0.68	0.42	23.1	<0.50	4.43	13.5	227.0		<0.50	1.62	110.0
Bretz-Opalite district																								
Aurora deposit																								
C95-89	159	6.9	38.5	0.98	239.0	27.7	3	0.9	<15	34	490	<1.0	0.08	0.97	0.09	8.6	2.76	0.96	7.3	17.7	1.46	0.23	2.15	1.1
C95-90	106	5.9	11.7	1.02	213.0	21.8	19	1.0	<15	35	95	<1.0	0.10	0.60	0.05	2.0	2.13	0.47	6.6	6.6	1.24	0.23	1.07	2.8
Bretz mine																								
C95-91	350	10.5	1.4	1.49	18.2	1.0	141	0.5	3	8	34	<1.0	0.06	0.39	0.09	5.0	0.24	0.82	8.6	24.8	0.25	0.21	1.01	1.6
C95-92	811	12.6	29.6	1.69	45.8	14.7	86	19.9	13	466	800	11.2	0.07	1.32	0.74	25.0	0.58	989.00	67.5	39.7	2.15	0.21	1.96	3.7
C95-93	609	20.9	23.0	3.20	31.7	1.5	234	1.2	4	62	151	<1.0	0.18	0.83	0.12	8.3	0.56	65.20	40.0	33.8	1.47	0.22	2.69	1.9
Cottonwood Creek																								
C95-94	93	3.0	52.6	0.24	1.5	2.3	37	0.8	3	33	190	<1.0	0.09	1.25	0.58	12.2	2.41	1.78	7.4	12.8	0.62	0.28	1.55	2.0
Opalite mine																								
C95-95	1,620*	35.0	1.8	5.48	44.7	14.0	191	0.5	7	65	25	<1.0	0.07	0.74	0.02	1.9	0.32	141.00	1.8	3.4	1.42	0.18	0.85	8.8
Virgin Valley																								
C95-110	<45	7.0	67.3	1.84	7.7	2.4	99	1.3	42	406	134	<1.0	0.3	1.62	1.10	6.7	1.87	0.13	18.7	20.2	3.41	0.35	2.19	<2.0
C95-111	164	6.8	0.8	1.67	3.6	2.4	95	0.5	7	24	18	<1.0	0.1	0.48	0.07	1.6	0.40	0.01	12.7	1.3	1.79	0.16	1.12	0.6
C95-112	70	8.2	<1.0	1.36	<1.5	6.2	11	0.9	8	75	7	<1.0	0.1	0.58	0.05	8.3	2.92	0.03	17.3	2.0	1.70	0.26	1.43	1.9
C95-113	276	9.4	30.5	1.35	11.2	7.8	7	0.7	25	87	37	3.5	0.3	1.70	0.12	14.6	2.98	0.15	35.6	8.7	4.01	1.14	3.62	<2.0
C95-114	104	13.4	3.8	2.32	2.0	5.5	30	1.1	11	114	13	<1.0	0.1	0.80	0.05	1.7	3.75	0.02	10.9	3.4	2.63	0.20	2.54	2.5
C95-115	354*	12.3	79.7	1.90		5.8	<1	133.0	9	417	38	<1.0	0.1	1.05	3.12	0.4	0.85	0.01	2.5	1.3	<0.27	0.28	0.97	2.0
C95-115	315	10.6	59.5	1.56	1.7	5.1	26	0.4	11	364	117	<1.0	0.1	1.20	1.08	0.4	0.56	0.13	2.5	1.3	0.50	0.21	1.19	1.8
C95-116	565	16.7	1.6	2.72	2.1	6.1	77	0.6	3	144	10	<1.0	0.1	1.98	0.08	1.7	0.40	0.02	12.8	0.7	1.20	0.22	1.20	1.6
C95-116a	492	16.6	0.1	3.29		5.9	1	16.9	1	126	13	<1.0	0.1	0.20	0.04	0.5	0.12	<0.02	0.4	0.2	0.14	0.10	0.48	0.6
C95-124	80	2.3	266.0	0.49	1.6	1.8	39	0.3	16	19	193	2.4	0.4	4.12	0.04	3.7	1.53	0.04	13.6	42.5	1.27	0.64	12.70	<2.0
VV-2	574	1.1	30.5	0.23	9.3	2.9	29	2.4	19	149	23	3.2	0.1	0.94	2.29	4.3	0.91	0.10	7.3	4.5	1.33	0.23	1.95	4.1
VV-5	45	5.2	0.5	0.84	12.8	9.8	14	2.8	8	150	263	2.6	0.1	0.69	0.67	14.4	1.84	0.14	18.9	15.8	2.04	0.22	1.74	1.6
VV-6	121	10.0	0.4	1.49	6.0	7.3	26	0.7	11	104	19	<1.0	0.1	0.57	0.31	6.7	1.47	0.20	15.9	6.6	2.24	0.24	1.36	2.0
VV-7	336*	3.7	0.9	1.13	6.0	2.6	48	1.9	19	578	75	<1.0	0.2	0.75	8.40	9.3	0.78	0.29	19.9	8.4	7.46	0.78	4.61	<2.0
VV-9	45	0.3	1.9	0.07	2.7	0.5	66	0.4	6	65	13	<1.0	0.1	0.44	1.98	1.2	0.42	0.07	0.9	3.7	0.30	0.26	1.23	<2.0
VV-11	84	0.3	1.8	0.11	2.8	1.2	17	0.3	6	67	3	<1.0	0.1	0.48	0.11	2.9	0.36	0.04	0.7	3.7	0.17	0.21	1.05	4.1
H95-57	507	19.4	0.6	3.53		0.5	1	19.2	3	129	13	<1.0	0.0	0.23	0.08	0.8	0.60	<0.01	2.1	0.2	0.45	0.11	0.52	4.0
H95-68	223	9.2	0.5	2.98		4.0	<1	27.0	5	60	6	<1.0	0.0	0.24	0.09	0.6	0.47	0.01	0.7	0.2	0.27	0.15	0.74	0.7
H95-75	300	10.3	0.6	1.83		12.3	11	27.1	12	92	4	<1.0	0.1	0.48	0.09	8.4	4.22	0.00	16.4	0.4	3.40	0.15	0.70	0.8
H95-77	366	8.7	1.3	1.37		17.8	14	13.6	11	57	10	<1.0	0.1	0.57	0.22	20.1	4.20	<0.04	13.2	0.5	1.70	0.19	1.48	0.8
H95-78	406	11.3	1.0	2.43		5.8	1	38.7	6	82	6	<1.0	0.1	0.49	0.21	4.2	1.73	<0.02	5.3	0.4	1.14	0.11	0.59	0.4

Unmarked = INAA (USGS), † = GFAA (USML), √ = ICP ES (USML), * INAA by Bondar Clegg

Table 2 (continued)

Sample	Zr	Hf	Mo√	Ta	W	Sc	Cr	Co	Ni	Zn	As	Se	Ag√	Bi√	Cd√	Cu√	Ga√	Hg√	Pb√	Sb√	Sn√	Te√	Tl√	Au† ppb
Lakeview district																								
White King mine																								
C95-70	76	3.5	1.4	2.77	1.3	3.1	40	0.4	1	25	235	<1.0	0.09	0.73	0.07	1.3	0.53	0.47	7.5	7.6	0.32	0.13	1.13	2.6
C95-71	44	3.8	90.6	1.43	12.7	3.5	38	2.4	4	67	979	<1.0	0.20	3.97	1.00	9.1	1.47	41.50	187.0	175.0	0.78	0.31	5.83	6.3
C95-72	700*	11.9	173.0	1.00	47.6	10.4	17	1.0	27	120	1380	<1.0	15.4	3.98	2.40	63.0	1.38	3,817.00	17660.0	853.0	0.99	0.52	21.20	18.6
C95-73	449	2.7	9.6	1.55	8.5	3.6	34	0.5	21	26	10500	<1.0	0.33	0.88	0.17	3.1	1.15	103.00	122.0	226.0	1.23	0.21	2.03	<2.0
C95-74	171	3.0	12.2	1.96	10.4	3.3	24	2.3	1	54	7070	<1.0	0.48	1.21	0.13	7.2	1.51	69.20	339.0	81.0	0.75	0.27	1.19	<2.0
Lucky Lass mine																								
C95-75	470	11.7	0.3	2.71	2.4	2.5	25	2.6	<1	107	8	<1.0	0.95	0.36	0.04	4.0	0.96	<0.49	1.7	0.7	0.38	0.25	1.11	0.1
C95-78	213	4.8	5.8	0.68	2.0	22.8	223	14.3	41	68	77	<1.0	0.12	0.47	0.15	33.5	1.81	0.02	20.4	2.0	0.76	0.20	2.96	5.3
C95-80	286	3.8	3.5	0.62	1.6	26.8	224	8.4	44	65	86	<1.0	0.11	0.50	0.07	70.0	1.82	0.33	26.0	2.3	0.75	0.22	2.36	3.3
Thomas Creek																								
C95-81	49	3.1	0.1	1.37	1.0	2.9	20	0.2	7	17	3	<1.0	0.12	0.37	0.03	0.4	0.66	0.11	1.9	0.3	<0.01	0.17	0.99	<2.0
C95-82	163	3.3	0.4	0.50	1.5	22.8	59	29.3	62	106	1	<1.0	0.07	0.34	0.03	61.9	2.26	0.01	1.2	0.3	0.22	0.19	0.91	1.6
C95-83	85	3.9	0.2	3.05	1.0	4.4	28	0.2	2	44	5	<1.0	0.13	0.29	0.02	0.6	0.34	0.00	1.0	0.3	<0.03	0.19	0.84	1.8
C95-83	105	4.2	0.1	3.84		5.1	<1	28.7	7	41	5	<1.0	0.03	0.19	0.05	0.2	0.24	<0.02	0.7	0.1	0.35	0.18	0.55	0.8
Bottle Creek																								
C-95-147	209	9.4	1.5	6.54	5.6	2.8	56	0.5	5	65	122	<1.0	0.0	0.32	0.04	2.2	2.17	0.05	1.5	1.4	3.36	0.17	1.28	4.3
C-95-148	183	4.9	1.9	4.00	3.8	3.8	52	0.5	6	44	4	<1.0	0.0	0.31	0.39	2.2	1.48	0.06	4.2	0.5	2.61	0.18	1.05	1.1
C-95-149	55	2.7	0.5	2.64	3.6	2.2	21	0.4	4	32	5	<1.0	0.0	0.36	0.06	0.5	0.24	0.09	5.7	0.2	0.46	0.19	0.71	1.7
C-95-150	133	3.1	744.0	2.03	12.6	1.7	140	9.2	23	16	95	<1.0	0.2	9.98	0.22	1.7	0.52	0.51	80.4	5.7	3.09	0.85	14.30	<2.0
C-95-151	54	2.4	<1.2	2.34	1.5	2.3	14	0.4	6	35	3	<1.0	0.1	0.65	0.05	2.7	0.96	0.13	13.7	0.3	0.85	0.23	0.87	3.7
C-95-152	63	2.9	1.3	1.84	5.2	1.8	128	0.6	7	24	2	<1.0	0.4	0.45	0.05	1.5	0.45	0.08	18.3	0.6	0.28	0.20	0.68	6.1
C-95-153	2	0.0	9.7	0.04	0.9	0.1	149	0.8	6	2	10	<1.0	1.1	0.43	0.05	1.9	0.02	0.02	5.0	0.5	0.37	0.15	0.88	72.1
C-95-154	14	0.2	0.9	0.07	1.5	1.5	188	1.0	5	6	64	<1.0	4.6	0.31	0.01	1.9	0.44	0.11	0.3	1.2	0.21	0.14	0.87	308.0
Steens Mountain																								
C95-84	305	6.9	4.6	0.80	3.0	14.1	58	7.0	23	122	19	<1.0	0.12	0.51	0.33	75.1	1.89	0.05	31.5	2.7	0.69	0.25	0.91	1.5
C95-85	501*	10.4	10.6	2.12	9.1	3.4	56	2.0	35	22	106	<1.0	0.21	0.70	0.06	3.9	0.61	0.74	15.1	1.6	1.25	0.22	1.37	<2.0
C95-86	475	10.6	9.0	2.52	4.9	2.4	102	3.8	26	29	37	<1.0	0.11	0.59	0.11	3.9	0.65	6.20	25.4	1.2	1.19	0.27	1.23	-4.4
C95-87	234*	6.7	0.7	2.19	3.2	1.4	77	0.4	3	14	8	<1.0	0.08	0.42	0.04	1.1	0.84	9.68	2.6	4.7	1.88	0.26	1.22	3.7
C95-88	619	7.4	4.3	2.15	4.2	1.9	135	0.7	16	14	37	<1.0	0.13	0.59	0.08	2.2	0.44	0.30	14.8	0.7	1.20	0.21	1.31	<2.0
Painted Hills																								
C95-126	65	4.7	4.1	1.50	3.6	2.0	76	1.1	8	35	198	<1.0	0.1	0.62	0.08	1.0	1.52	0.01	9.4	5.2	1.49	0.26	1.35	<2.0
C95-127	155	5.9	0.4	1.93	2.4	2.7	22	1.3	2	63	52	<1.0	0.2	0.52	0.23	0.5	1.32	0.00	17.1	1.1	0.44	0.14	0.71	0.7
C95-128	37	2.3	0.5	0.33	2.9	22.1	163	12.5	14	157	9	<1.0	0.1	0.33	0.05	44.1	4.48	0.03	5.1	0.5	0.76	0.16	0.82	0.3
C95-130	131	5.2	0.1	1.71	2.2	2.5	28	1.1	2	50	3	<1.0	0.0	0.57	0.04	0.7	1.36	0.02	8.0	0.6	0.66	0.22	0.96	2.0
C95-132	392*	1.6	2.0	1.58	33.1	0.5	8	1.8	12	158	430	<1.0	0.2	0.56	5.29	3.6	2.21	0.34	275.0	89.6	7.47	0.27	4.46	<2.0
C95-133	809	6.0	0.2	2.73	17.8	0.6	12	1.6	5	136	107	<1.0	0.2	0.80	0.56	3.7	2.83	0.19	62.5	7.5	6.52	0.34	3.28	<2.0
PH-2	39	5.0	5.4	1.31	8.0	1.4	173	23.0	27	61	63	<1.0	0.4	0.46	0.74	12.3	0.84	0.86	4.2	1.9	1.17	0.17	3.36	1.7
PH-3	1,060	4.0	0.9	1.44	17.1	3.3	88	1.8	38	52	21	<1.0	0.1	0.62	0.62	5.0	0.73	0.95	29.4	1.2	3.67	0.27	2.65	<2.0
Peterson Mountain district																								
C-95-134	58	7.8	1.4	1.59	0.9	5.3	17	0.5	8	60	44	<1.0	0.0	0.33	0.14	3.2	14.90	0.44	8.9	5.5	0.69	0.19	0.79	7.7
C-95-135	169	7.2	1.7	1.48	8.7	5.2	17	0.9	10	51	33	<1.0	0.2	0.45	0.15	5.5	16.00	0.96	13.2	11.6	1.82	0.17	1.27	7.5
C-95-136	453	7.4	0.4	1.20	116.0	5.9	12	1.3	<15	30	33	<1.0	0.2	0.47	0.04	4.0	2.44	5.53	11.6	12.3	3.26	0.11	2.26	<2.0
C-95-137	274	8.2	3.9	1.20	1.7	6.0	20	3.3	4	71	4	<1.0	0.1	0.34	0.18	5.6	1.64	0.00	4.5	0.6	0.88	0.10	0.87	<2.0
C-95-138	212	6.9	0.2	1.24	3.5	5.7	14	1.6	3	72	11	<1.0	0.0	0.50	0.04	1.5	2.13	<0.02	13.2	0.7	1.17	0.10	1.13	<2.0
Dogskin Mountain district																								
C-95-139	119	11.1	2.5	2.79	4.8	5.1	16	5.7	7	100	17	<1.0	0.0	1.06	0.54	0.7	0.82	0.07	143.0	2.7	0.89	0.18	1.24	5.2
C-95-140	75	4.3	0.2	1.83	5.4	3.7	20	3.3	10	77	8	<1.0	0.0	0.72	0.05	2.8	0.57	0.06	22.1	1.0	0.62	0.17	0.68	<2.0
C-95-141	14	4.5	9.4	1.16	4.8	2.6	36	1.4	2	29	18	<1.0	0.1	1.08	0.07	0.9	0.23	0.03	26.1	0.5	0.30	0.19	0.83	5.0
C-95-142	39	2.8	0.7	0.61	4.8	1.1	87	0.7	8	11	25	<1.0	0.0	0.97	0.04	0.9	0.11	0.01	12.4	1.2	0.41	0.18	0.79	2.3
C-95-143	301	8.7	1.8	2.11	3.6	6.9	34	1.2	5	117	14	<1.0	0.0	0.29	0.32	1.1	0.47	0.04	10.4	2.7	1.32	0.15	0.52	3.2
C-95-144	256	1.9	53.3	0.27	12.3	5.4	18	12.7	51	151	105	<1.0	0.4	1.25	0.67	9.5	2.12	3.20	18.3	6.7	2.04	0.27	1.71	24.9
C-95-145	110	6.3	35.0	0.98	0.7	4.4	13	175.0	2	213	234	<1.0	0.1	0.94	3.83	25.1	1.39	1.35	51.9	7.7	0.59	0.24	2.82	6.2
C-95-146	42	6.2	11.2	0.82	1.1	4.3	16	69.2	7	103	49	<1.0	0.1	0.62	2.92	4.4	1.13	1.07	22.0	1.7	0.59	0.19	2.09	2.2

Unmarked = INAA (USGS), † = GFAA (USML), √ = ICP ES (USML), * INAA by Bondar Clegg

Table 3. Major oxide and trace element contents of non-mineralized samples from the Virgin Valley, Kings River, and Lakeview areas.

	Virgin Valley area											Kings River district			Lakeview
Sample	H95-68	H95-110	C95116A	H95-112	H95-57	C95-115	H95-108	H95-106	H95-75	H95-77	H95-78	H95-82	C95-107	H95-103	C95-83
Map unit	Tcr	Tcr	Tpr	Tpr	Trp	Tva	Tva	Trv	Tvv	Tvv	Tvv	Td	Tp	Td	
Longitude	118 58.2	119 06.3	119 08.5	119 25.3	119 07.6	119 05.8	119 06.4	118 59.2	119 03.3	119 04.8	119 04.8	118 07.7	118 09.2	118 08.6	120 33.4
Latitude	41 51.9	41 48.9	41 44.3	41 55.4	41 31.3	41 47.1	41 45.6	41 47.6	41 49.4	41 50.3	41 50.3	41 43.5	41 47.3	41 47.3	42 20.2
Major oxides (wt. %)															
SiO2	76.87	77.20	77.01	76.21	77.30	82.46	76.21	71.54	65.95	65.22	73.86	76.16	76.16	72.77	76.80
TiO2	0.15	0.13	0.24	0.26	0.11	0.21	0.28	0.31	0.99	1.08	0.46	0.27	0.20	0.39	0.05
Al2O3	12.23	11.95	11.54	11.70	11.40	9.22	11.83	14.85	19.80	20.65	13.94	11.40	11.53	12.55	13.16
FeO*	1.11	0.93	1.51	1.83	1.78	1.51	1.90	2.07	3.94	5.70	3.35	2.88	2.11	4.03	0.49
MnO	0.06	0.06	0.11	0.12	0.04	0.10	0.12	0.05	0.02	0.05	0.05	0.06	0.02	0.13	0.11
MgO	0.07	0.17	0.00	0.10	0.00	0.03	0.24	0.72	0.43	0.90	0.39	0.00	0.06	1.14	0.00
CaO	0.28	0.28	0.14	0.16	0.17	0.15	0.21	1.92	2.22	2.84	1.36	0.98	0.20	0.14	0.53
Na2O	2.63	2.79	4.67	4.75	4.39	1.69	2.44	3.56	2.79	1.89	1.72	3.10	1.74	4.09	4.47
K2O	6.57	6.48	4.77	4.86	4.80	4.61	6.73	4.87	3.79	1.58	4.83	5.13	7.95	4.71	4.40
P2O5	0.01	0.01	0.01	0.01	0.00	0.01	0.03	0.11	0.08	0.09	0.03	0.02	0.03	0.05	0.00
Total**	98.68	99.01	100.66	100.83	99.30	97.30	98.34	99.29	94.69	94.28	95.40	96.89	99.89	98.33	100.71
Na+K/Al	0.94	0.97	1.11	1.12	1.09	0.84	0.96	0.75	0.44	0.23	0.58	0.93	0.99	0.94	0.92
Trace Elements (ppm):															
Sc	2	2	2	1	0	9	3	5	18	14	4	1	2	3	2
V	1	0	16	6	0	10	4	27	84	99	26	2	4	9	4
Cr	0	0	0	0	0	0	0	4	5	14	2	0	0	1	0
Ni	13	8	14	10	14	11	7	10	11	9	11	9	11	3	13
Cu	12	0	4	0	9	6	0	7	14	28	11	3	4	0	7
Zn	62	50	†128	†123	†163	†515	†126	42	†146	111	77	†158	†166	128	30
Ga	22	18	22	24	†30	18	21	16	†30	†28	20	†29	23	26	19
Rb	225	221	238	213	269	179	218	146	88	71	206	294	†315	†281	206
Sr	4	3	2	2	3	4	6	351	443	265	85	116	12	37.0	4
Y	†65	†57	†97	†93	†131	†70	†91	19	†62	42	†67	†87	†85	69	43
Zr	232	184	482	519	542	397	511	209	355	302	389	431	466	315	70
Nb	23.8	21.9	34.3	31.3	†46	26.0	31.5	11.2	28.1	19.6	†41	28.5	29.0	†20	27.9
Ba	0	0	0	0	0	0	0	1205	1092	335	611	88	18	609	0
La	39	34	49	46	41	47	44	18	53	12	58	34	44	48	4
Ce	107	65	100	142	151	141	144	48	87	88	138	142	165	77	43
Pb	19	14	24	24	41	20	23	17	18	19	26	28	23	20	32
Th	21	21	27	25	27	18	25	11	12	14	21	19	19	14	18
U	9		12		14	20			4	3	6	9	7		9

All analyses by XRF at Washington State University, except U by INAA at U.S. Geological Survey. Major oxides normalized on a volatile-free basis.
*Total Fe expressed as FeO; **Total non-normalized major oxides; Na+K/Al = mol. (Na2O+K2O)/Al2O3; † denotes values >120% of highest standard.

H95-68	Canyon Rhyolite, hydrated vitrophyre	C95-115	Air-fall tuff, opalized	H95-78	Virgin Valley Fm, hydrated glassy reworked tuff
H95-110	Canyon Rhyolite, hydrated vitrophyre	H95-108	Air-fall tuff, hydrated glassy pumice	H95-82	Ash-flow tuff, hydrated vitrophyre
C95-116A	Peralkaline rhyolite, non-hydrated glass	H95-106	Rhyolite vent, hydrated vitrophyre	C95-107	Peralkaline flow-banded rhyolite, devitrified
H95-112	Peralkaline rhyolite, non-hydrated glass	H95-75	Virgin Valley Fm., reworked tuff with clay & zeolite	H95-103	Ash-flow tuff dike, vitrophyre
H95-57	Late porphyritic rhyolite, hydrated glass	H95-77	Virgin Valley Fm., reworked tuff with clay	C95-83	Flow-banded rhyolite, non-hydrated glass

Table 4. SEM/EDX analyses of major chemical components of U minerals. Minerals with analyses normalized to 100% denoted by *. ND = not detected.

Sample	MLT 4S-1	MLT 8-1	MLT 8-2	C95118A-1	C95118A-5	C95118B-1	C95118B-2
ZrO2	55.72	51.23	51.33	60.79	60.68	60.84	60.59
SiO2	28.5	36.65	29.44	35.98	30.42	36.18	36.86
UO2	1.78	2.09	4.54	0.79	5.67	1.77	2.42
TiO2	1.97	0.00	0.00	0.00	0.00	0.00	0.00
Al2O3	2.31	4.44	6.17	0.00	0.00	0.00	0.00
CaO	8.82	0.64	1.23	1.10	1.66	0.62	0.50
FeO	1.01	5.00	4.87	0.58	1.63	2.12	0.83
MgO	0.95	0.00	2.30	1.89	0.00	0.00	0.00
TOTAL	101.06	100.05	99.88	101.13	100.06	101.53	101.20
Mineral	Zircon	Zircon	Zircon	Zircon	Zircon	Zircon	Zircon
Area	Horse Creek	Horse Creek	Horse Creek	Moonlight mine	Moonlight mine	Moonlight mine	Moonlight mine

Sample	C9572-1	C9572-2	C9572-C	C95150-1	C95150-2	VV5-1	VV5-2
SiO2	9.55	8.98	11.06	18.76	13.66	ND	ND
UO2	69.17	68.84	71.79	66.21	69.25	81.07	81.99
P2O5	11.69	12.36	10.13	13.31	15.71	7.23	5.69
CaO	1.34	1.26	0.57	ND	ND	ND	ND
PbO	5.97	5.77	3.51	ND	ND	ND	ND
Al2O3	ND	ND	ND	1.71	1.37	ND	ND
As2O3	2.28	2.79	2.95	ND	ND	8.88	9.36
TOTAL	99.99	100.00	100.01	100.00	100.01	97.82	97.04
Mineral	Unknown*	Unknown*	Unknown*	Unknown*	Unknown*	Unknown	Unknown
Area	Lakeview	Lakeview	Lakeview	Bottle Creek	Bottle Creek	Virgin Valley	Virgin Valley

Sample	C95112-1	VV7-1	C95132-2	C95132-1	C95-136	C95-139
SiO2	3.06	33.43	31.83	ND	1.92	4.76
UO2	67.39	61.58	60.80	84.93	73.56	71.66
P2O5	ND	ND	ND	15.35	17.84	17.18
V2O5	19.10	ND	ND	ND	ND	ND
CaO	ND	0.37	0.94	4.39	4.35	3.81
FeO	ND	ND	ND	ND	1.83	0.69
K2O	9.68	4.62	2.96	ND	ND	ND
Al2O3	0.77	ND	1.23	ND	0.50	2.50
TOTAL	100.00	100.00	97.77	104.67	100.00	100.61
Mineral	Carnotite*	Weeksite*	Weeksite?	Meta-autunite	Meta-autunite*	Meta-autunite
Area	Virgin Valley	Virgin Valley	Painted Hills	Painted Hills	Petersen Mtn.	Dogskin Mtn.

collection. The # Sites column refers to the total number of discrete sampling locations. The # Complete Analyses column lists the number of analyses which were sufficiently complete to allow determination of water type (i.e., Na-K-HCO_3 water). The # Sites Complete column shows the total number of sites, removing entries for multiple sampling dates, which are represented in the # Complete Analyses column.

Table 5. Hydrologic data sites used for this study.

Area	# Records	# Sites	# Complete Analyses	# Sites Complete
McDermitt	280	54	38	17
Virgin Valley	24	17	24	17
Bottle Creek	1	1	0	0
Petersen Mountain	0	0	0	0
Dogskin Mountain	4	3	3	3
Painted Hills	9	2	0	0

$^{40}Ar/^{39}Ar$ analyses were done on high purity separates of sanidine or biotite phenocrysts or adularia. Samples were crushed, ground, sieved to various size fractions, and concentrated with standard magnetic and density techniques. Sanidine was leached with dilute HF. Final cleanup to >99 percent purity involved additional magnetic and density separation, HF leach, and, rarely, hand picking. Samples were irradiated at the University of Michigan for 10 hours and analyzed at the New Mexico Bureau of Mines and Mineral Resources. Fish Canyon sanidine (27.84 Ma, relative to an age of 520.4 Ma on hornblende MMhb-1; Cebula and others, 1986; Samson and Alexander, 1987) was used as a neutron fluence monitor. Individual sanidine grains were completely melted using a CO_2 laser operating at 1.6 watts for 5 seconds; biotite was heated incrementally in a resistance furnace. Age results are summarized in Table 6.

Table 6. $^{40}Ar/^{39}Ar$ dates for rocks from the Virgin Valley and Kings River areas.

Sample	Rock type	Quadrangle	Mineral	Age Method	n	Mean	±1s
		Virgin Valley Caldera					
H95-57	Porphyritic rhyolite (Trp)	Alkali Peak	sanidine	single crystal	7	15.69	0.02
H95-106	Rhyolite vent (Trv)	McGee Mountain	biotite	plateau		15.72	0.07
H95-59	Peralkaline rhyolite (Tpr)	Alkali Peak	alkali feldspar				
	coarse fraction			plateau		15.95	0.07
	fine fraction			plateau		16.02	0.04
	Canyon Rhyolite (Tcr)						
H95-71	Uppermost flow	McGee Mountain	sanidine	single crystal	6	16.11	0.03
H95-72	Tuff of Big Mountain (Ttb)	McGee Mountain	sanidine	single crystal	9	16.13	0.06
H95-63	Lower flow	McGee Mountain	sanidine	single crystal	8	16.15	0.07
H95-74	Idaho Canyon Tuff (Tic)	McGee Mountain	sanidine	single crystal	8	16.30	0.06
		Kings River district					
C95-105	Altered rhyolite (Tb)	Calavera Canyon	adularia	plateau		16.13	0.06
H95-103	Vitrophyric tuff dike (Td)	Calavera Canyon	sanidine	single crystal	30	16.15	0.16
C95-107	Peralkaline rhyolite (Tp)	Calavera Canyon	sanidine	single crystal	14	16.33	0.22
C95-103A	Biotite-bearing rhyolite (Tb)	Calavera Canyon	sanidine	single crystal	15	16.45	0.11

McDERMITT CALDERA, OREGON AND NEVADA

General geologic setting

Significant amounts of uranium occur in several areas in the McDermitt caldera, a well-preserved volcanogenic subsidence feature about 30 x 40 km in area that straddles the Nevada Oregon border (Figs. 1 and 2). The presence of this caldera was first noted by Walker and Repenning (1965), who mapped its northwestern wall in Oregon. The structure was apparently given its name by Greene (1975), who mapped part of its geology. The caldera was subsequently proposed to be a cluster of four overlapping smaller calderas that, along with three satellitic calderas, formed the 20,000 km^2 McDermitt volcanic field in Oregon and Nevada (Rytuba and McKee, 1984). However, detailed mapping supporting this proposal has not been published and the configuration of component calderas is a matter of debate (Dayvault and others, 1985; this study). Whatever its configuration, the McDermitt caldera was the source of regional peralkaline to metaluminous ash-flow sheets extruded about 16 Ma that are described by Rytuba and McKee (1984) and Conrad (1983; 1984). These ash-flow sheets overlie mafic volcanic rocks of the Orevada View volcanic series, which has been correlated with the Steens Basalt in Oregon (Conrad, 1983). Intra-caldera ash-flow and flow rocks in an area along the west side of the caldera were described and mapped in detail by Hargrove (1982). Rhyolite flows and possible rhyolitic intrusive rocks occur in several places around the margins of the caldera (Conrad, 1983). Rytuba (1995) mentioned a peralkaline ring dike along the western Caldera margin that hosts uranium deposits; this may be the large dike of "porcelain rhyolite" described by Backer and others (1995). Flows of iron-rich andesite, or icelandite, accompany the rhyolitic rocks of the caldera (Wallace and others, 1980). Volcaniclastic sedimentary rocks are exposed in a nearly continuous peripheral "moat" in the caldera, and the central part of the caldera is occupied by exposures of pre-moat rhyolites and icelandites that probably represent resurgent doming (Fig. 2).

Uranium mineralization differs in mode of occurrence from area to area in the McDermitt caldera, although mineral assemblages and trace element contents are generally similar. Secondary zeolite, smectite, and potash feldspar are commonly associated with the mineralization (Glanzman and Rytuba, 1979). The timing of uranium mineralization may be the same in all of the areas, postdating deposition of peralkaline ash flows and icelandite lava flows that ended about 15.7 Ma (Rytuba and McKee, 1984; Noble and others, 1988), although icelandite deposition may have extended to 6 Ma (Wallace and others, 1980). Noble and others (1988) report a K/Ar date of 15.7 ± 0.4 Ma for adularia from the McDermitt mercury mine in the northeast part of the caldera. The uranium mineralization may be partly coeval with deposition of volcanogenic sediments in the caldera moat. We focus on uranium mineralization in two large areas in the caldera: the Kings River district, which lies along the southwestern caldera margin; and the Bretz-Opalite district, which lies along the northern margin of the caldera.

Hydrologic setting

Hydrologic setting for the McDermitt caldera area is considered in a single section here; most data are from the vicinity of the town of McDermitt which is northeast of the caldera (Fig. 1). McDermitt caldera area waters are near neutral Ca-Na-HCO_3 ±SO_4 waters (Fig. 3) with pH ranging from 6.8 to 9.4. The Na and Ca concentrations of the waters are often nearly equal in terms of mg/L. Of the waters for which a reasonably complete analysis is available, data indicate that TDS of the waters ranges from 66 to 724 mg/L, however these values represent only three sampling sites, McDermitt Creek and Quinn River near McDermitt northeast of the caldera and Thacker Well No 2 in Kings River Valley about 20 km SSW of the Moonlight mine. Temperatures of all waters reported vary between 0.0°C (for river waters collected in winter months) and 28°C.

No wells are reported in STORET in the McDermitt caldera area which have data on depth to water below land surface. However, published depths for two wells in the area (Vic Albisu well, and Fort McDermitt Well) have total completion depths of 183 and 218 m (Welch and Williams, 1987). Presumably these wells were drilled to these depths in order to intercept water, which suggests the water table may be relatively deep. Temperatures of these well waters range from 11.5 to 22.5°C. Data from the Moonlight uranium mine on the west margin of the caldera indicates that the water table is at moderate depths; according to

Figure 2. Generalized geologic map of the McDermitt caldera.

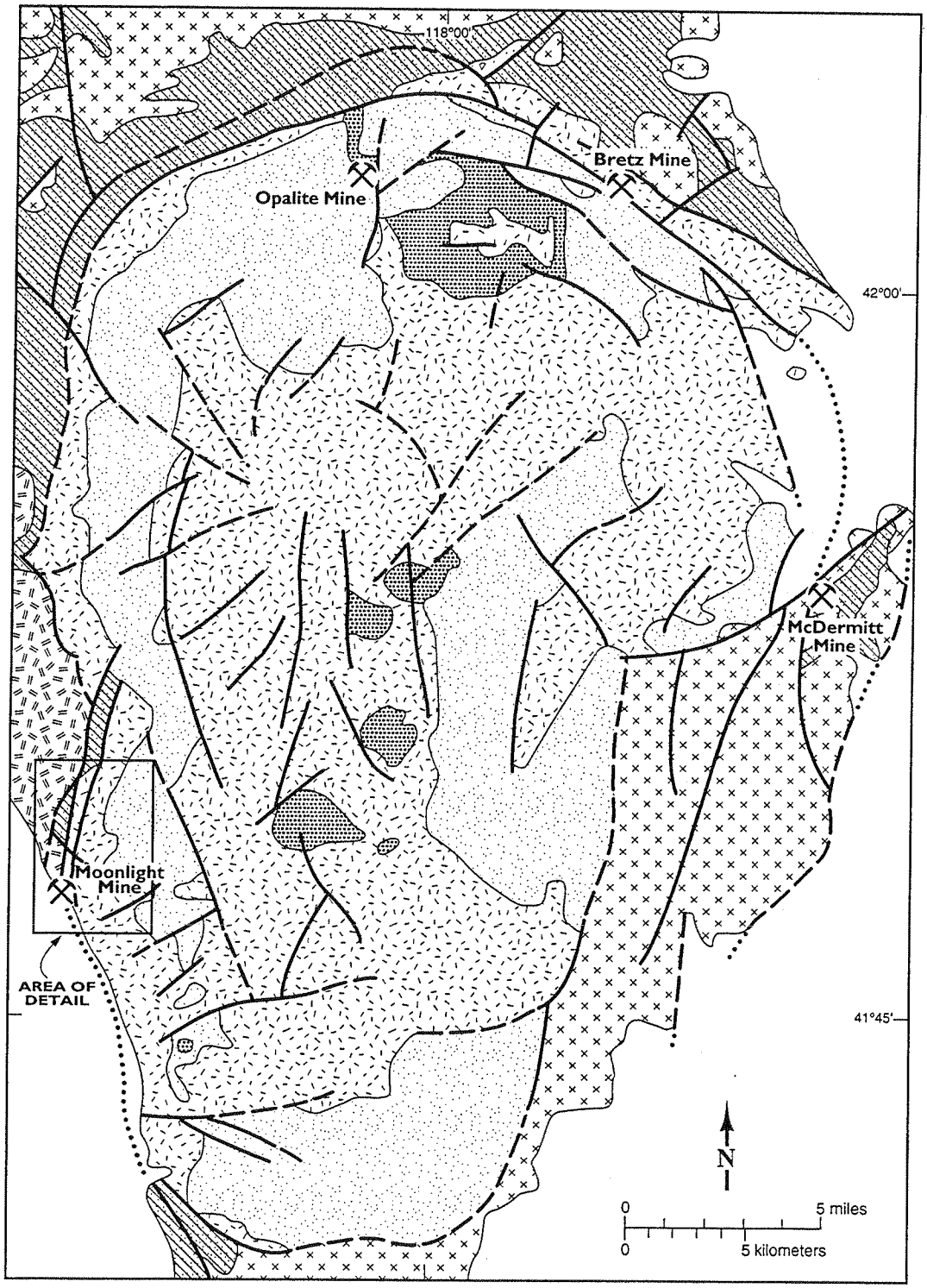

Quaternary deposits

Caldera moat sedimentary rock

Aurora lava, mainly iron-rich andesite (icelandite)

Caldera outflow, mainly peralkaline ash-flow tuff

Intracaldera ash-flow tuff and flow rock, mainly peralkaline and sub-alkaline rhyolite and trachite

Precaldera Tertiary volcanic and sedimentary rocks

Cretaceous granitic rock

Lithologic contact

Fault, dashed where approximately located, dotted where concealed

Geology modified from Dayvault and others (1985).

Figure 3. Piper diagram for McDermitt caldera area waters.

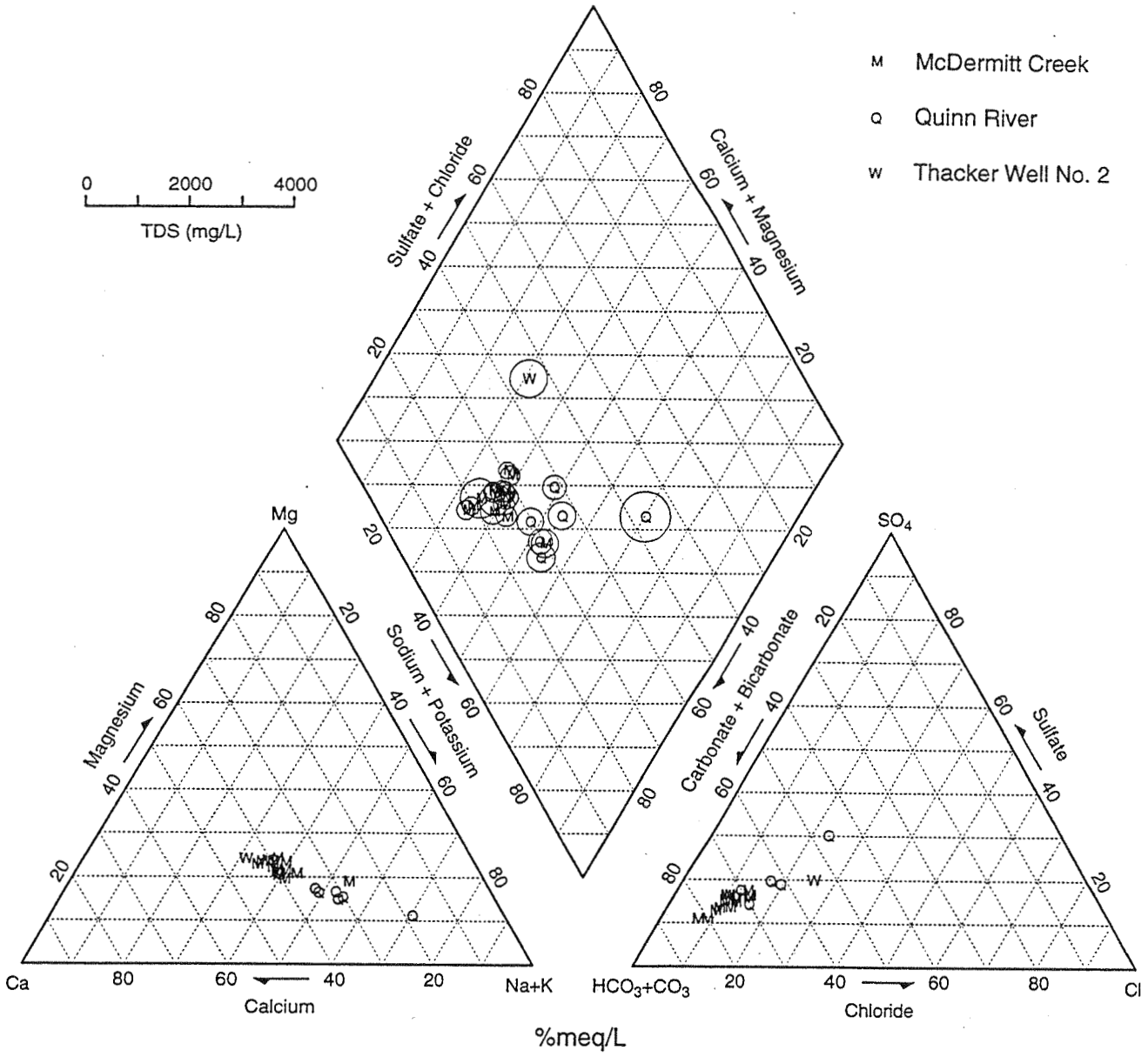

Sharp (1955), pumping stations at depths of 38 and 55 m were used to de-water the main shaft. Sharp also indicated that the water table in the mine was 44 m down the shaft, which is inclined at 60°, making the vertical depth of the water table 38 m.

No information was available on the depth to the water table in the Bretz mine area. However, one of the open pits was filled with water to an elevation of about 1800 m in May, 1996, indicating that the unsaturated zone in mineralized rock is thin because pit walls that contain radioactive rock are only about 10 m above that elevation. In addition, most of the Aurora deposit lies beneath the water table (A. Wallace, personal communication, 1995). At the Opalite mine, underground workings about 10 m beneath the bottom of the open pit are dry.

Water data from three additional sites (Cordero mercury mine, Mentaberrys Well 2, and Noque's Nevada Well) in the McDermitt study area are reported in Welch and Williams (1987). The waters are Na-HCO_3-SO_4 waters with Cl ranging from 14 to 26 mg/L, and TDS of 280 to 400 mg/L. The water temperature at the mine is 56°C, whereas the temperatures at the Mentaberrys and Noque's wells are 26 and 34°C. Hence, all three of these waters are at least slightly thermal, dilute groundwaters sampled from depths between 82 and 214 m. No depths to water level are reported for these sites. Note that all available data for the McDermitt caldera area were collected in the mid-1970s to early 1980s.

Trace element data for water samples from STORET and NURE for the McDermitt caldera area are shown in Tables 7-10. The maximum U content, 19.02 ppb, was in well water from the Quinn River Valley about 7 km SE of the caldera and 12 km from the nearest known U occurrence. Available data on U content for spring and stream waters has much lower maximum values than this, but average values are roughly comparable for all three water types. Other chemical contents are normal, except for Br, which is locally elevated in well water (Table 9) from the Kings River Valley. Castor and others (1982b) report U_3O_8 contents for groundwater samples from the southwest part of the McDermitt caldera, all are 7 ppb or less, except for well water from near the Moonlight mine at 21 ppb.

Kings River Valley district

The Kings River Valley district contains the Moonlight mine (Fig. 1, Fig. 4a), the only location in the McDermitt caldera with reported uranium production. Several carloads of rock containing 0.07-0.22% U_3O_8 were shipped from the mine between 1953 and 1955 (Sharp, 1955), and Garside (1973) estimated total production at about 500 tons of ore. The Kings River district also contains uranium occurrences in the Horse Creek area, 2-6 km north of the Moonlight mine, and in the Thacker Pass-Rock Creek area, 9-18 km southeast of the Moonlight mine (Fig. 1). The Horse Creek area was the site of extensive exploration by Chevron Resources Company in the late 1970s; on the basis of drill data, the company estimated a geologic reserve of 2.4 million tons with an average grade of 0.09 percent U_3O_8 (Vera, 1980). In the early 1980s, the Thacker Pass-Rock creek area was the site of exploration work by Conoco, and the company identified a drill-indicated resource of several million tons of low-grade uranium ore between Pole and Rock Creeks in the eastern part of the area (Castor and others, 1981). Small amounts of uranium mineralization occur at several places in the Montana Mountains - Bull Basin area, which lies east and north of the Moonlight mine - Horse Creek area.

Geology

On the basis of our reconnaissance, uranium mineralization in the Kings River Valley district is mainly along faults. At the Moonlight mine, uranium was mined from breccia along a north-striking fault that dips about 60° to the east (Fig. 4b). Volcanic rocks are commonly enriched in uranium along and near this fault for at least 6 km north of the Moonlight mine. Mineralized zones between 2 and 6 km north of the mine (Fig. 2) have been referred to as the Horse Creek occurrences (Castor and others, 1982b) because they occur along the east side of the Horse Creek drainage.

Table 7. Summary of trace element concentrations in waters in Virgin Valley, near McDermitt, and at Yucca Mountain. Data from STORET database in ppb.

	McDermitt Area					Virgin Valley Area					Yucca Mountain*				
	#	Min	Max	Mean	Stdev	#	Min	Max	Mean	Stdev	#	Min	Max	Mean	Stdev
Ag	26	0	1	0.5	0.5	3	20	60	43	21	7	1	20	3.9	7.1
Al	9	10	40	15.6	11.3	6	16	600	165	240					
As	35	0	27	13	5	18	1	180	31	42	14	0	30	10.0	9.1
B											25	70	900	360	206
Ba	26	33	100	61	24	3	40	100	80	35	17	2.75	79	20.99	22.21
Be	9	0.5	1	0.6	0.2	3	5	15	11.7	5.8	7	0.5	5	1.1	1.7
Br											21	10	320	114	112
Cd	28	0	3	1	0.7	3	3	20	8.7	9.8	7	1	5	1.6	1.5
Co	32	0	3	2.2	1.2						6	3	3	3	0
Cr	32	0	10	1.8	3.6	3	20	30	26.7	5.8	7	5	20	7.3	5.6
Cu	32	0	7	2.4	1.5	6	20	160	58.3	61.4	23	0	20	6.4	5.8
Fe											45	0	520	75	115
Hg	33	0	1.8	0.3	0.4	16	0.5	4	1	1.2	1	0.5	0.5	0.5	0
Li											35	40	950	181	158
Mn											22	0	330	24	69
Mo	9	10	10	10	0	2	100	100	100	0	6	10	10	10	0
Ni	20	0	4	1.5	1.3	3	15	20	16.7	2.9	7	10	120	30	40
Pb	29	0	9	2	2.0	3	30	60	40	17	8	10	300	48	102
Sb						14	1	100	11.8	26.5					
Se	33	0	1	0.8	0.4	3	1	50	34	28	7	0	20	7.3	7.4
Sn						3	50	1000	683	549					
Tl						2	500	500	500	0					
U											2	8	10	9	1.4
Zn	30	0	39	9.0	9.7	3	15	602	212	338	13	0	1200	128	328

* Data include information from sites off of Yucca Mountain proper.

Table 8. Summary of NURE trace element concentrations in stream waters in three areas. Values reported in ppb.

	Bottle Creek					Virgin Valley Area					McDermitt Area				
	#	Min	Max	Mean	Stdev	#	Min	Max	Mean	Stdev	#	Min	Max	Mean	Stdev
Al	6	148	316	216	74	21	112	1307	411	375	21	101	1597	285	321
As	1	1													
B	2	81	142	112	43										
Ba	2	27	54	40	19										
Br		1	116.1			9	1.4	58	22	26.9	8	11.7	1002	155	342
Cu	2	3	12	7.5	6.4										
Fe	2	122	138	130	11.3										
F	4	67	193	102	61	22	3	1178	149	255	22	66	775	274	204
Li	2	2	2	2	0										
Mn	6	4	89	51	34	20	3	111	45	28	7	62	232	99	60
Mo	1	9													
Sr	2	92	142	117	35										
U	1	2.53				9	1.29	17.37	6.3	5.6	9	1.22	5.53	3.0	1.8
V	4	1.3	9	4.5	3.2	17	1	14.4	3.9	3.7	21	1	24.2	8.3	6.1
Y	1	1													
Zn	2	8	30	19	16										
Zr	1	3													

Table 9. Summary of NURE trace element concentrations in well waters in three areas. Values reported in ppb.

	Bottle Creek					Virgin Valley Area					McDermitt Area				
	#	Min	Max	Mean	Stdev	#	Min	Max	Mean	Stdev	#	Min	Max	Mean	Stdev
Ag	3	2	5	3.7	1.5										
Al	12	128	2267	567	600						1	95			
As	6	1	5	2.0	1.5										
B	7	54	585	148	194										
Ba	7	19	62	34	14.9										
Br	5	21.8	126.3	63	46	3	38.6	92.2	68.1	27.2	18	19.8	8998	578	2102
Co	3	2	4	3	1										
Cr	1	6													
Cu	7	4	34	12.7	11.6										
Fe	7	82	1412	546	464										
F	9	44	375	134	106	4	53	176	86	60	22	18	3579	457	853
Li	7	2	23	7.0	7.3										
Mn	17	7	174	72	50	3	65	94	79	16	11	18	203	58	50
Mo	2	4	139	22.2	32.9										
Nb	3	7	9	8.3	1.2										
Ni	4	5	10	6.8	2.2										
Sr	7	51	177	97	52										
Th	3	6	10	8.0	2.0										
U	1	1.42				1	2.5				22	1.15	19.0	3.4	3.9
V	14	1.3	28	11.3	8.6	4	3.3	8.2	5.8	2.7	26	1.2	32.1	9.8	7
Y	6	1	3	1.7	0.8										
Zn	7	39	314	105	97										
Zr	4	2	8	3.8	2.9										

Table 10. Summary of NURE trace element concentrations in spring waters in three areas. Values reported in ppb.

	Bottle Creek					Virgin Valley Area					McDermitt Area				
	#	Min	Max	Mean	Stdev	#	Min	Max	Mean	Stdev	#	Min	Max	Mean	Stdev
Ag	14	2	6	2.9	1.2										
Al	87	33	6093	594	840	3	224	484	342	132					
As	24	1	184	27.5	44.2										
B	39	32	6137	556	1372										
Ba	39	2	216	31.7	33.7										
Br	8	16.1	63.2	34.3	18.7	23	9.9	1474	132	326	10	16	339	109	100
Co	9	2	8	4.2	1.9										
Cr	7	5	9	6.4	1.6										
Cu	37	2	71	10.2	11.7										
Fe	38	14	2312	363	500										
F	46	29	13805	1470	3287	45	26	6038	308	927	19	57	1417	331	334
Li	34	2	509	60	126										
Mn	89	2	749	93	116	40	30	127	55.8	19.4	10	23	249	73.7	70.7
Mo	17	4	139	22.2	32.9										
Nb	16	4	20	9	4.5										
Ni	20	4	22	9.2	4.5										
Sr	39	18	467	102	72										
Th	9	5	14	9.7	2.9										
U	13	1.15	15.6	5.3	5	9	1.1	41.8	7.8	13.2	8	1.92	6.76	4.2	1.7
V	72	1	108	9.9	16.1	43	1	34.7	5.2	6.2	18	2.3	30.3	10.1	8.6
Y	18	1	9	1.6	2										
Zn	39	4	173	34.8	34.7										
Zr	13	2	8	3.8	2.1										

Figure 4a. Geologic map of the Kings River district.

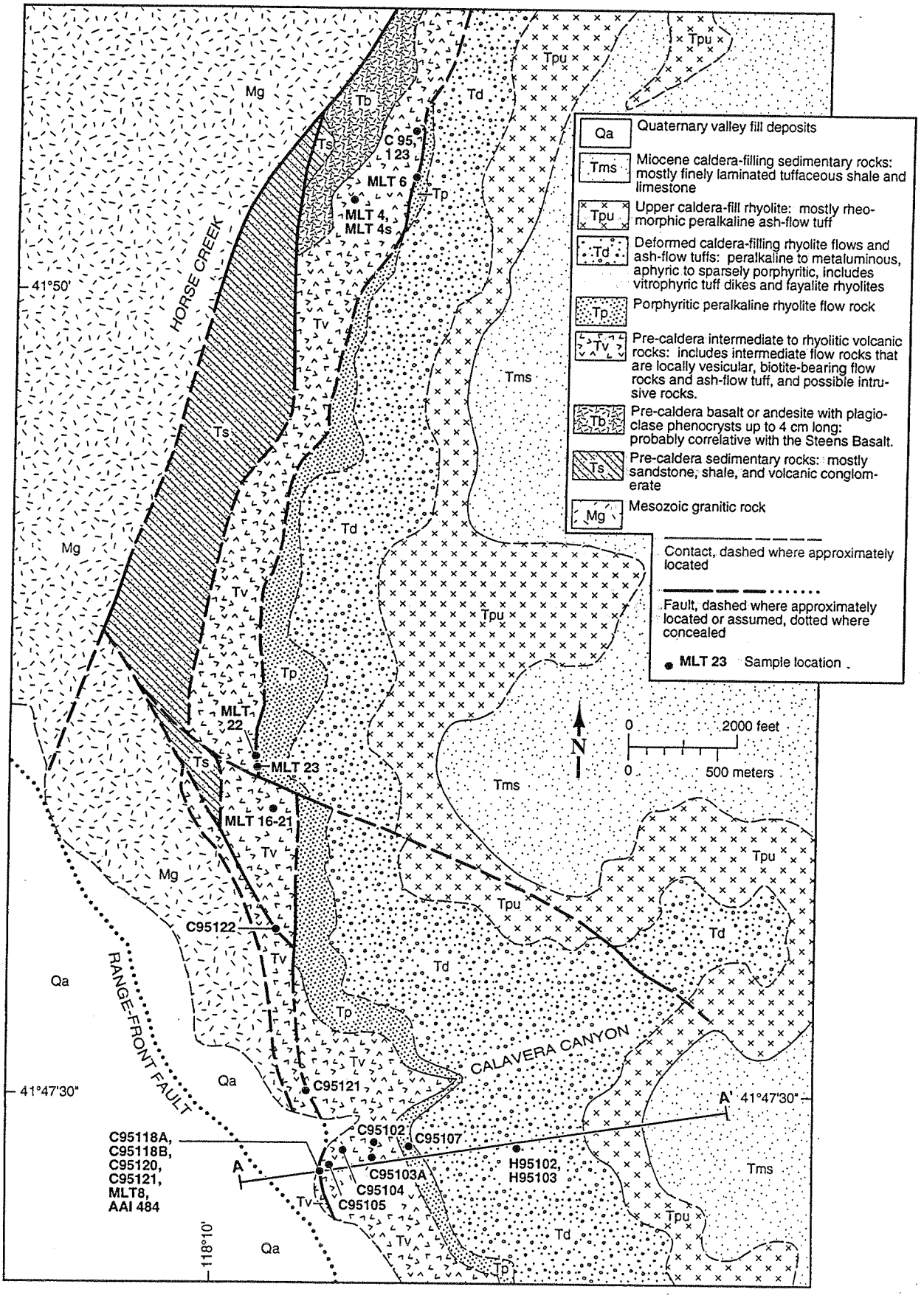

Figure 4b. Geologic cross section of the Moonlight mine. Location on Figure 4a (previous page).

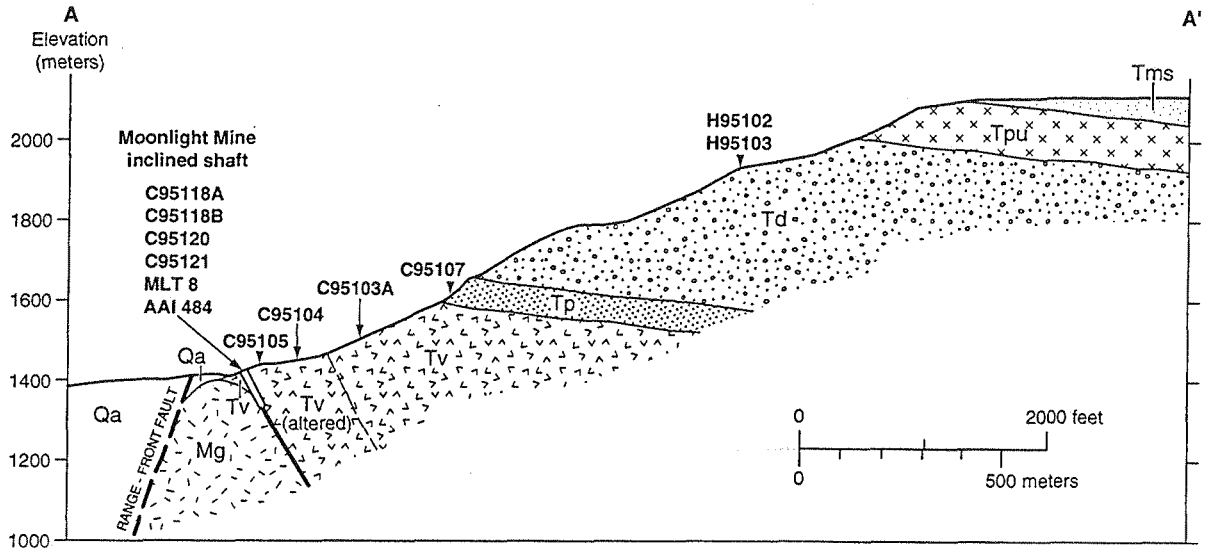

At the main Moonlight adit, radioactive rock occurs in a limonitized and bleached breccia zone as much as 3 m thick along the fault described above. Radioactivity in this zone is generally 25 x background, and locally exceeds 100 x background. Radioactivity drops rapidly away from this zone; the footwall is generally buried by nonradioactive debris and rock 2 m above the breccia zone only measures about 3 x background. Hanging wall rock 30 m above the breccia zone, which is hydrothermally altered and bleached, has radioactivity at about 2 x background. Radioactivity at occurrences in the Horse Creek area ranges up to about 50 x background.

Chevron Resource Company geologists, who investigated uranium mineralization in the Horse Creek area using drilling and detailed mapping, proposed that the mineralization was related to a 6-km-long dike of aphyric rhyolite informally named "porcelain rhyolite" (Bagby, 1980). According to Backer and others (1995), the dike strikes north from the Moonlight mine for about 6 km, dips 55-60° eastward, and reaches a maximum thickness of 150 m. This may be the same dike that is reported by Rytuba (1995) to be 3 km long.

We interpret uranium mineralization in the Moonlight Mine - Horse Creek area to be along the western margin of the McDermitt caldera or caldera complex, possibly along the margin of the Calavera caldera of Rytuba and Glanzman (1979) and Rytuba and McKee (1984). However, our reconnaissance does not support several aspects of caldera relations described by those authors, a point also made by Hargrove and Sheridan (1984). The caldera ring fracture zone in this area consists of north- to northwest-striking faults that separate Cretaceous granitic rock on the west from caldera-filling volcanic rocks on the east. Caldera-fill rocks are predominantly peralkaline rhyolites and related intermediate rocks such as icelandites. Pre-caldera rocks also include Tertiary sedimentary rocks and mafic to biotite-bearing rhyolitic volcanic rocks that underlie caldera fill within the ring fracture zone (Fig. 4a).

The caldera margin is exposed in, and in the vicinity of, the Moonlight mine (Fig. 4a). There, the fault that hosts mineralization dips eastward, into the presumed caldera, and may be part of the ring fracture. Biotite-bearing rhyolite and intermediate volcanic rocks occur in the immediate hanging wall; similar rock and Mesozoic granitic rock are in the footwall (Fig. 4b). Sanidine from the biotite-bearing rhyolite gives an $^{40}Ar/^{39}Ar$ age of 16.45±0.11 Ma (sample C95-103A; Table 6). This rhyolite may represent the exhumed floor of the caldera because ring-fracture faults do not appear to be present east of the mineralized fault. Rytuba and Glanzman (1979) show the ring fracture of the Calavera caldera turning northeast up Calavera Canyon, immediately north of the Moonlight mine. However, the biotite rhyolite and overlying units are not interrupted or displaced across Calavera Canyon (Fig. 4a). We would continue the caldera margin northward along the steep eastern wall of Kings River and probably northeast up Horse Creek where it also seems to be the locus for uranium mineralization.

The steep eastern wall of Kings River above the Moonlight mine consists of a complex sequence of probable caldera fill. A peralkaline rhyolite flow (Tp, Fig. 4b) up to 180 m thick overlies the biotite rhyolite. Sanidine from it gives an $^{40}Ar/^{39}Ar$ age of 16.33±0.22 Ma (sample C95-107; Table 6), similar to or slightly younger than the biotite rhyolite. The peralkaline rhyolite appears to be cut off by the Moonlight mine fault about 6 km to the north of the Moonlight mine and to pinch out about 2 km south of the mine (Fig. 4a). Possible intracaldera tuff and megabreccia that overlie the peralkaline rhyolite consist of chaotically deformed peralkaline to metaluminous rhyolite ash-flow tuff and lava (Td, Fig. 4b). These rocks are cut by vitrophyric dikes of ash-flow tuff (sample H95-103). The tuff and vitrophyric dikes probably constitute the caldera-forming unit, which would be tuff of Double H according to Rytuba and McKee (1984). However, our samples show a sparsely porphyritic, probably peralkaline rhyolite similar to but not identical to the aphyric tuff described by Rytuba and McKee (1984). Sanidine from a vitrophyric dike gives an $^{40}Ar/^{39}Ar$ age of 16.15±0.16 (sample H95-103; Table 6). Aphyric, peralkaline rhyolite lava or highly rheomorphic tuff overlies the deformed rocks. Fine-grained volcaniclastic rocks that cap the plateau about 2 km east of and about 600 m above the mine were probably deposited in an intracaldera lake (Fig. 4b). The plateau, which comprises the Montana Mountains - Bull Basin area, was formed by uplift along a basin-range fault that is covered by alluvium west of the Moonlight mine.

Our interpretation of the geology at the Moonlight mine is similar to that of Hargrove (1982) and Hargrove and Sheridan (1984), who mapped an area approximately 4 km southeast of the mine. Biotite-bearing rhyolite occurs at the foot of the Kings River escarpment and is overlain by a sequence of deformed tuffaceous and flow rocks . Hargrove (1982) and Hargrove and Sheridan (1984) interpreted the deformed rocks to be caldera-fill ash-flow tuff that was rheomorphically folded during caldera collapse. Coarse debris-flow deposits containing clasts of biotite-rich rhyolite that overlie the deformed rocks probably were shed from the caldera wall.

The uranium resource identified by Conoco Minerals in the Pole Creek-Rock Creek area appears to be concentrated in porous parts of an aphyric rhyolite flow and ash-flow sequence that is overlain by caldera moat sedimentary rocks. Uranium is concentrated along steeply dipping faults elsewhere in the Thacker Pass area. The uranium mineralization that occurs at places in the Montana Mountains - Bull Basin area is about 600 m higher in elevation. The mineralization occurs in caldera moat sedimentary or caldera filling tuffs that directly underlie them and may represent surface or near surface extensions of more deep-seated Moonlight mine-Horse Creek mineralization.

Rock chemistry

Samples of rhyolitic flow rock from the Kings River uranium district and elsewhere in the McDermitt caldera are metaluminous to peralkaline. As shown by data in Rytuba and Glanzman (1979) and Dayvault and others (1985), and verified by work done for this study, the peralkaline rocks have relatively high U and Th contents (7-9 ppm and 18-19 ppm, respectively, Table 2, Table 3) and have relatively high contents of other trace elements such as Zr, REE, and Ta, which is also typical for rocks of this type.

At the Moonlight mine, uraniferous breccia along the Moonlight mine fault is about 3 m thick and contains about 0.05% U_3O_8 (Castor and others, 1982b). However, select samples of breccia contain as much as

Figure 5. Scatter plots of selected elements for samples with more than 20 ppm U.

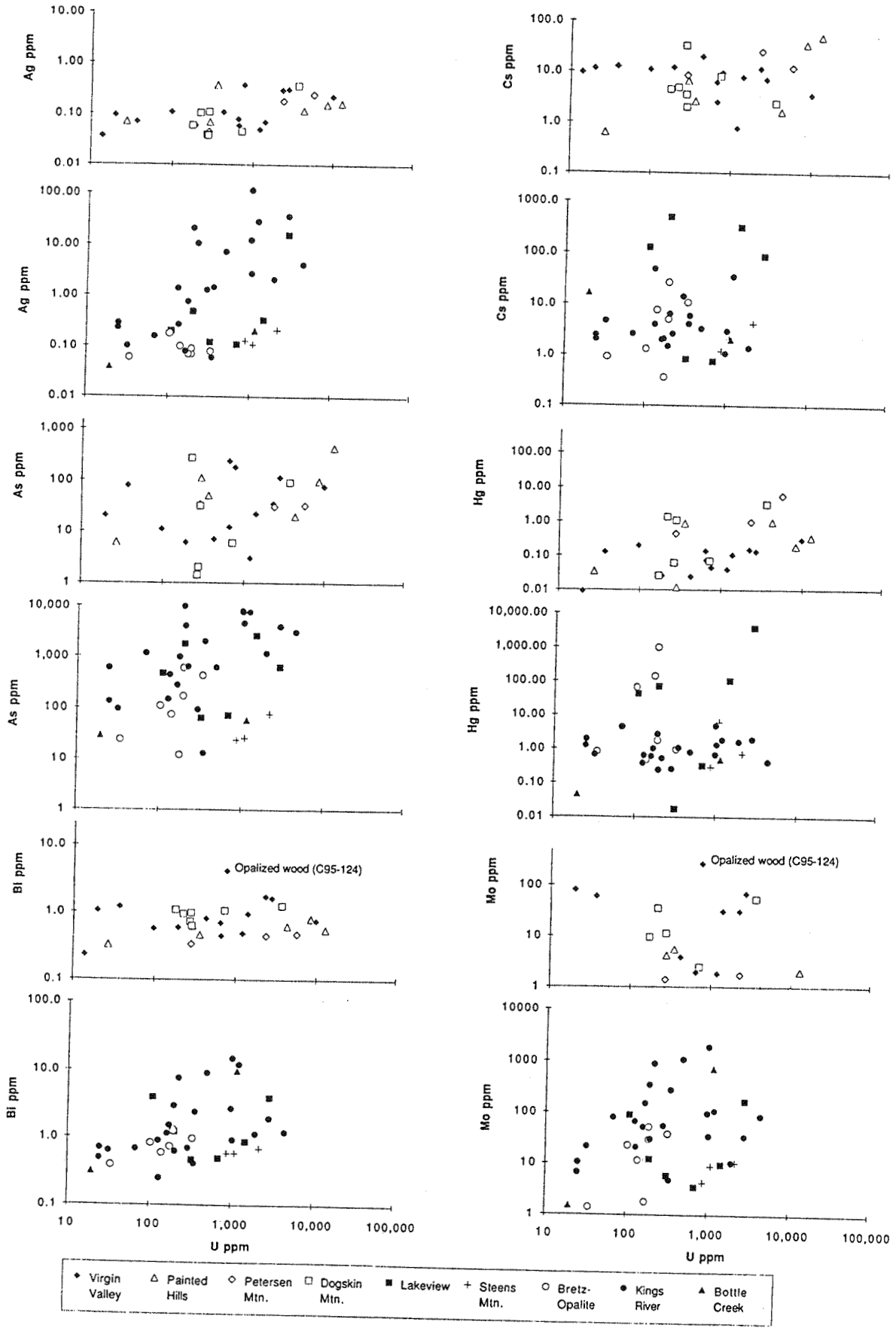

Figure 5 (continued).

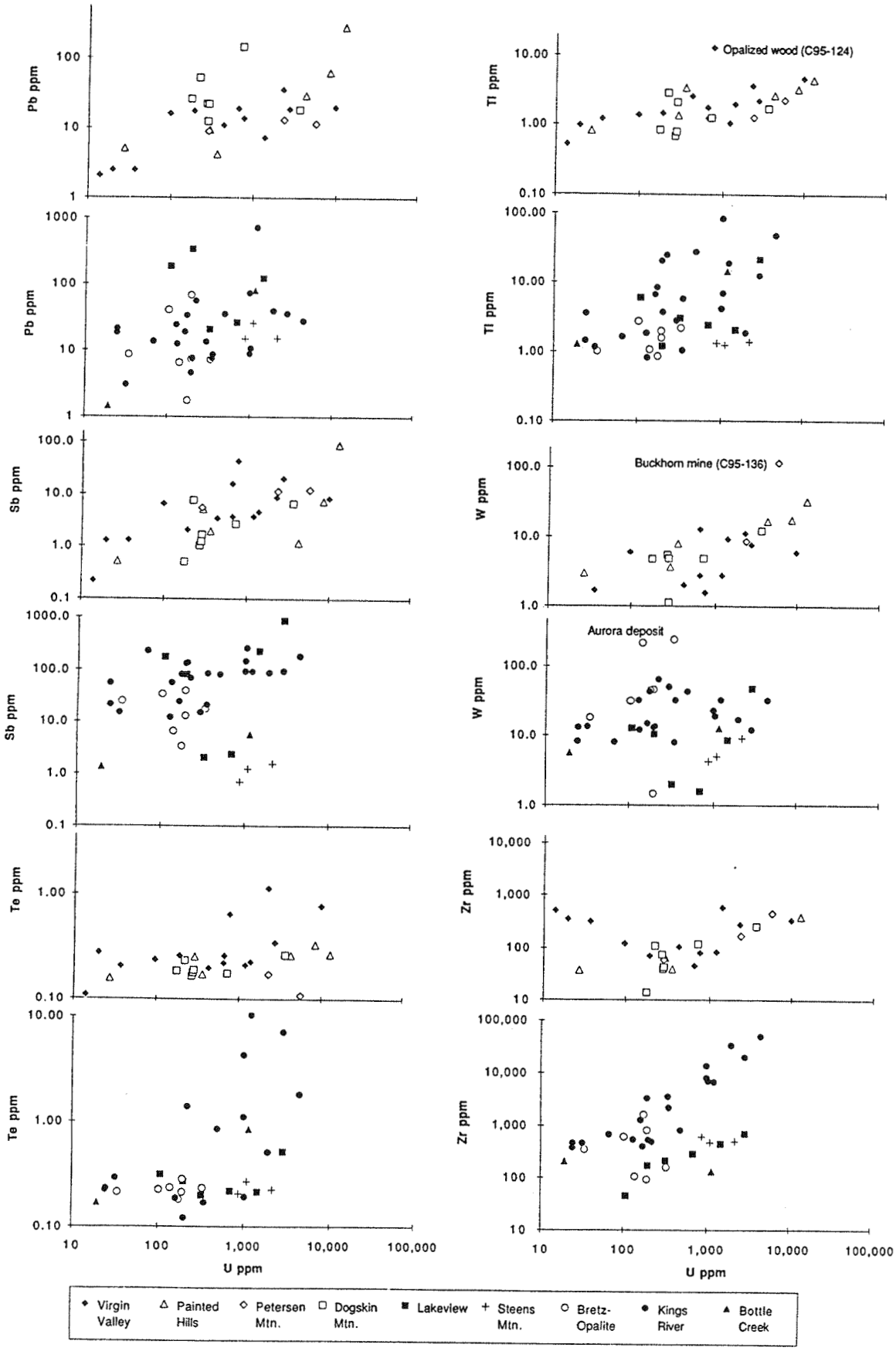

0.4% uranium (Table 2). Uranium-rich rock from the Kings River district contains extremely high Zr and As contents (as much as 5% and 1%, respectively, (Fig. 5). In addition, uraniferous samples have the highest Ag, Bi, Mo, Te, and Tl of any area studied (Fig. 5), along with elevated Cu, Hg, Pb, Sb, W, and Zn (Table 2, Fig. 5). Samples from the Kings River district have the highest Au contents of any area studied; one sample contains > 9 ppm (MLT 4S, Table 2). Rytuba and Glanzman (1979) reported anomalous concentrations of Be at the Moonlight mine but did not report Be analyses. Dayvault and others (1985) reported Be at background levels (2-5 ppm).

Surface samples in the Pole Creek-Rock Creek area contain up to 0.04 % U_3O_8, along with elevated contents of some of the minor elements that are associated with uranium in the Moonlight mine - Horse Creek area northwest (Castor and others, 1982b). Radioactive rock collected from the Pole Creek area for this study contain elevated As, Mo, Sb, Tl, W, and Zr (Table 2). Samples from radioactive occurrences in Thacker Pass to the west of the Pole Creek-Rock Creek area, which have relatively low U contents (maximum of 40 ppm U_3O_8), contain high As, Mo, Sb, and W, and moderately elevated Hg (Castor and others, 1982b).

No samples were collected during this study from the Montana Mountains - Bull Basin occurrences, but they are known to contain elevated amounts of some of the trace elements that occur in the Moonlight mine - Horse Creek deposits (Castor and others, 1982b). In addition, these high-level occurrences have high REE contents.

Mineral assemblages

Although uraninite and coffinite have been reported (Sharp, 1955; Williams, 1980), the only primary uranium-bearing mineral that we have identified in radioactive rock from the Moonlight - Horse Creek area is fine-grained zirconium silicate that contains 1-6 wt% uranium oxide (Table 4). However, in sample MLT 18, a small mass of U+Zr silicate was found to contain 21 wt% uranium oxide suggesting that it is a mixture of phases, possibly zircon and coffinite, that cannot be resolved even at high magnification by SEM. On the basis of information reported by Speer (1982), the highest value of uranium in zircon by microprobe analysis is 5.06 wt% UO_2. The uraniferous zircon from the Moonlight mine and Horse Creek occurrences is clearly a hydrothermal phase, occurring as finely granular breccia matrix (Davault and others, 1985) and as crustiform layers in quartz-adularia-calcite veins (Fig. 6). Uranium at Thacker Pass also seems to occur mainly in hydrothermally introduced zirconium silicate, and uraniferous zirconium silicate was also reported in the Old Man Spring uranium occurrence in Bull Basin (Castor and others 1982b).

Green tetragonal dipyramids of the secondary mineral metazeunerite, $Cu(UO_2)_2(AsO_4)_2 \cdot 8H_2O$, occur in cavities (Fig. 7) in partially to wholly oxidized breccia from the Moonlight mine. Torbernite has also been reported at the Moonlight mine (Sharp, 1955; Taylor and Powers, 1955; Dayvault and others, 1985), but it is possible that this is misidentified metazeunerite because the minerals are difficult to distinguish in hand specimen. Autunite has also been reported at the Moonlight mine (Sharp, 1955; Dayvault and others, 1985), and a secondary uranyl silicate mineral was reported from a uranium occurrence about 0.5 km north of the Moonlight mine (Dayvault and others, 1985).

Gangue minerals in uranium-rich samples from the Moonlight mine and Horse Creek occurrences consist mainly of breccia matrices or vein minerals that include clear to nearly black quartz as finely granular to coarse drusy crystals, white to yellow fine-grained adularia, and white to dark purple fluorite. Minor amounts of calcite, apatite, barite, and Ti oxide are also present. Sulfides, mainly arsenopyrite and pyrite, occur in unoxidized breccia. Galena, sphalerite, pyrrhotite, marcasite, mercury sulfide, and acanthite have also been identified (Dayvault and others, 1985). In Horse Creek sample MLT 4S, two generations of pyrite are present, early fine pyrite framboids (Fig. 8) that contain traces of acanthite, and later coarse pyrite grains. In this sample, powellite ($CaMoO_4$) was found to have partially replaced arsenopyrite and to contain tiny grains of electrum. Oxidized breccia contains limonite, jarosite, and the secondary arsenic mineral pharmacosiderite (Fig. 7).

Alteration of breccia fragments and wall rock at the Moonlight mine includes adularia that replaces feldspar phenocrysts and other phases. Adularia that replaces feldspar phenocrysts in altered rock as much as 30 m vertically above the uraniferous breccia (sample C95-105) gives a $^{40}Ar/^{39}Ar$ age of 16.13 ± 0.06 Ma (Table 6). In the vicinity of the Moonlight mine, the host rhyolite is extensively bleached and silica and clay minerals occur locally as alteration products.

The high-level uranium occurrences in the Montana Mountains-Bull Basin area are associated with alteration phases, such as clay and potash feldspar, that are difficult to distinguish from diagenetic alteration phases in the moat sedimentary rocks (Glanzman and Rytuba, 1979). However, hectorite (lithium-bearing smectite) is associated with uranium in some of the Montana Mountains - Bull Basin occurrences in sedimentary rocks, and this mineral is considered to be a hydrothermal alteration phase.

Figure 6. Backscattered SEM image of a layer of uraniferous zircon that shows finely crustiform texture in quartz-adularia breccia matrix, Moonlight mine.

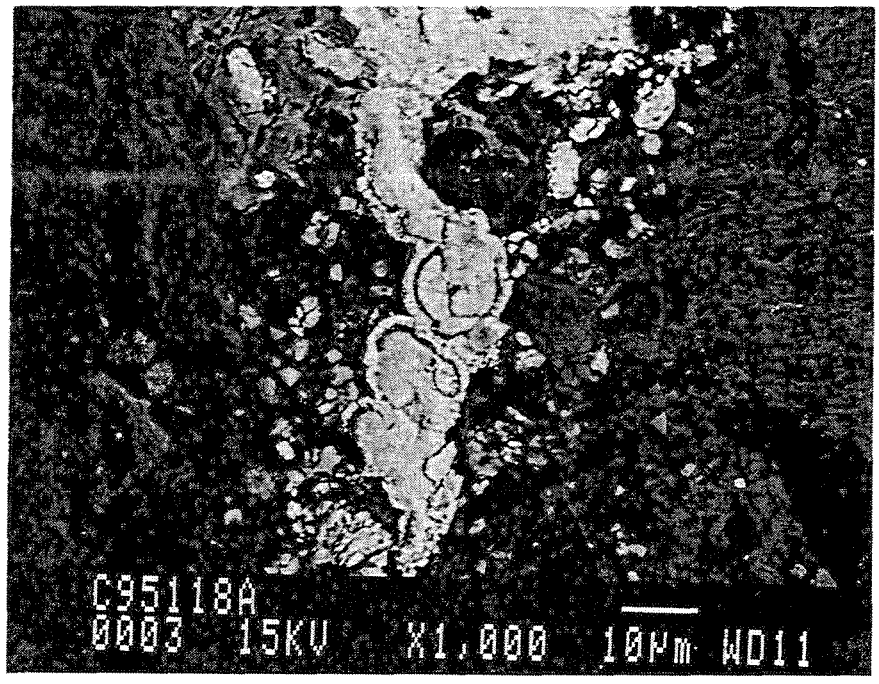

Bretz-Opalite district

Mineral production in the Bretz-Opalite district in the McDermitt caldera (Figs. 1, 2), which is mostly in Oregon, has been restricted to mercury that was produced between 1927 and 1965. No uranium production has been recorded. However, in 1977 the district was the site of the most significant uranium discovery in the study area. About 17 million short tons of rock with an average grade of 0.05 percent U_3O_8 were indicated by drilling in the Aurora deposit which mainly occurs in iron-rich, intermediate (icelandite) flow rocks about 0.8 km south of the Bretz mine (Roper and Wallace, 1981). The Cordero and McDermitt mines, which are in Nevada about 15 km southeast of the Bretz mine, produced more than 400,000 flasks (about 14 million kg) of mercury between 1941 and 1990 from deposits of mercury sulfide and corderoite ($Hg_3S_2Cl_2$) in altered tuffaceous sedimentary rocks. The ore mainly occurs above a brecciated sinter apron in the sedimentary rocks above rhyolitic tuff (Roper, 1976), and while uranium occurs in the ore, it is present in only minor amounts (up to 0.02% U_3O_8, Rytuba and others, 1979).

Figure 7. Backscattered SEM image of metazeunerite crystals (bright) with pharmacosiderite lining a cavity in breccia, Moonlight mine.

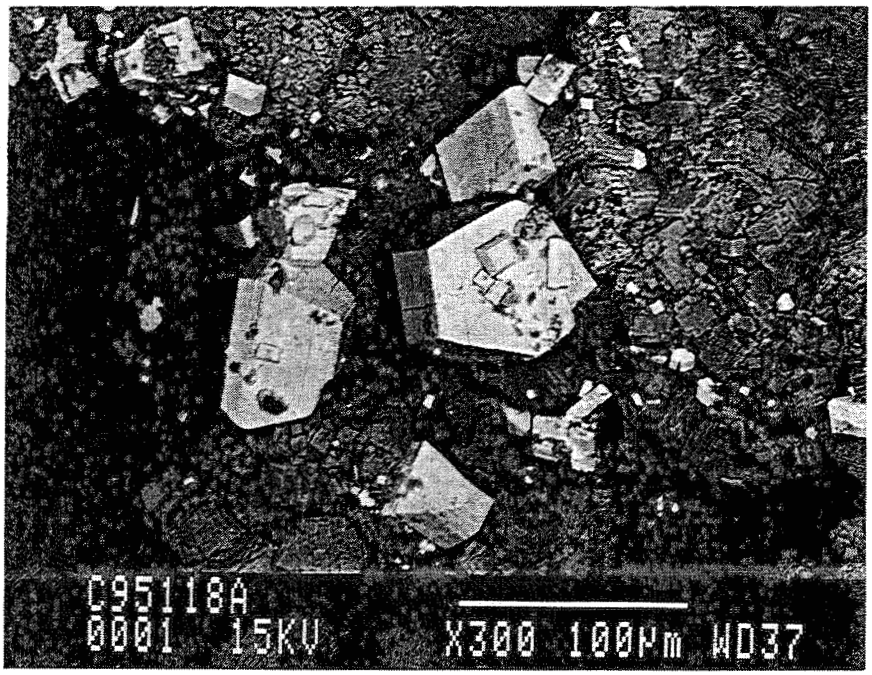

Figure 8. Backscattered SEM image of pyrite frambolds in silicified rhyolite with sulfide, sample MLT 4S, Horse Creek area. For scale, frambolds are 10-20 µ in diameter.

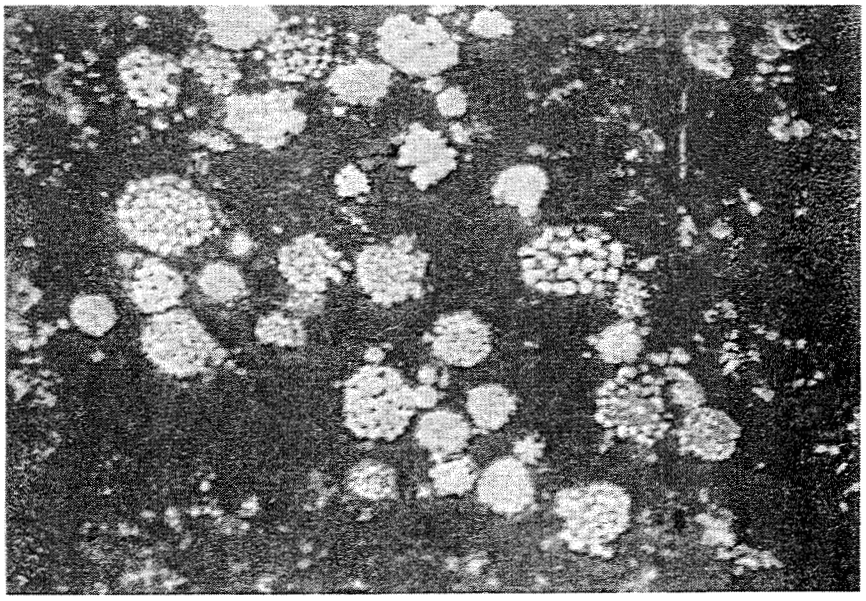

Geology

The Bretz mine is located along the northern McDermitt caldera ring fracture zone (Fig. 2), and consists of a series of open pits that are elongated east-west and that produced about 15,000 flasks of mercury (Fisk, 1968). Berry and others (1982) proposed that the mercury mineralization was concentrated along the ring fractures. Crudely bedded volcaniclastic breccia that is commonly argillized and locally silicified is generally exposed in the south walls of these pits, and rhyolite ash-flow tuff and flow rock is exposed in the north walls. Minor amounts of altered vesicular flow rock is also present. To the south, bedded moat sediments are mostly covered by alluvium. To the north, where ash-flow tuff sheets dip shallowly south into the caldera, are more east-west faults, some of which are marked by workings in mineralized zones controlled by the faulting.

The mineralized flows in the Aurora deposit underlie caldera moat sedimentary rocks that are enriched in uranium, but the sedimentary rocks generally do not contain high U contents. Uranium mineralization in the Aurora deposit occurs in porous flow tops, in breccia layers, and along steeply dipping fractures (Roper and Wallace, 1981). Although the deposit crops out in a small area in a road cut (the discovery outcrop, sample sites C95-89 and C95-90), most of the mineralization is buried under 20-60 m of unmineralized moat sedimentary rocks and younger gravels according to cross sections in Roper and Wallace (1981). The highest radioactivity measured at the surface over the Aurora deposit during this study was about 12 x background in argillized scoriaceous flow rock at the discovery outcrop. Silicified rock at the Bretz mine has radioactivity that ranges from near background to as much as 4 x background. However, limonitized scoriaceous flow rock was the most radioactive rock found during this study at the Bretz mine, at about 5 x background.

A 2-m-thick sequence of moat sedimentary rocks that contains stratabound uranium mineralization is exposed in the Cottonwood Creek area west of the Aurora deposit, and has been shown by drilling to underlie a 3 km^2 area that partially overlies the deposit (Roper and Wallace, 1981). This mineralization, which Roper and Wallace considered to be syngenetic with sediment deposition, is similar in lithology to deposits in the Montana Mountains-Bull Basin area. Stratabound uranium mineralization in the Cottonwood Creek area has surface radioactivity ranging up to about 10 x background.

The Opalite mercury mine is an open pit about 100 m in diameter in a large mound of brecciated and silicified caldera moat volcanogenic sedimentary rocks a few kilometers west of the Aurora-Bretz area. Total production was recorded at about 12,000 flasks (Fisk, 1968). Radioactive areas in the pit range up to about 10 x background, but readings in the pit are generally less than 4 x background.

Rock chemistry

Radioactive rock at the Bretz mine, which includes silicified breccia and argillized and limonitized scoriaceous flow rock, contains up to 0.1 percent U_3O_8 and as much as 1.6% mercury (Berry and others, 1982). Of three samples collected during this study, the most radioactive contains about 0.02% uranium and nearly 1,000 ppm mercury. Other elevated trace elements are As, Mo, Sb, W, and locally Pb (Table 2). Uranium occurs in concentrations as high as 0.33 percent in the Aurora deposit (Berry and others, 1982). During this study, two samples were collected from the discovery outcrop: one of bleached, nearly white, oxidized argillized flow rock, the other of gray argillized flow rock. Elevated trace elements in these samples in addition to U are As, Ba, Hg, Mo, Sb, and W. Samples from the discovery outcrop of the Aurora deposit are particularly enriched in W, and have the highest contents of this metal of any samples collected for this study (Table 2, Fig. 5). Similar data for surface and drill samples from the Bretz mine and the Aurora deposit are reported in Berry and others (1982).

Opalized sedimentary rock from the Cottonwood Creek area, which contains about 0.02% U, also has high Mo, As, Sb, Bi, and Hg (Table 2). A single sample was collected for this study from a radioactive area about 1 m in diameter in silicified breccia at the Opalite mine. It contains 175 ppm U, along with elevated Hg, Sb, W, and Zr (Table 2). Argillized volcaniclastic sedimentary rocks that underlie the sinter contain as much as 0.01 % U_3O_8 (Dayvault and others, 1985).

Mineral assemblages

According to Berry and others (1982), the most radioactive rock found in outcrop at the Bretz mine is silicified breccia with abundant, very fine-grained, sulfide minerals that include pyrite, marcasite, chalcopyrite, galena, and Sb-Fe-Cu sulfide. Uranium minerals were not identified (Berry and others, 1982; this study). On the basis of thin section examination, the silica is mainly chalcedonic to finely granular quartz. In addition to silica, secondary minerals at the Bretz mine include zeolites, smectite clay minerals, and potash feldspar (Glanzman and Rytuba, 1979); however, it is not clear that these minerals were produced by hydrothermal activity. The most radioactive rock found during this study, limonitized scoriaceous flow rock, contains abundant limonite casts after pyrite and some cinnabar. Iron oxide and titanium oxide minerals and barite were reported in uraniferous rock (Berry and others, 1982).

In the Aurora deposit, uranium is reported to occur as uraninite, coffinite, and uranyl phosphates that occur with pyrite framboids and titanium oxide (Roper and Wallace, 1981). Uranyl silicate was reported by Dayvault and others (1985). Alteration minerals that are associated with uranium in the Aurora deposit are montmorillonite, chlorite, clinoptilolite, and opal; other minerals present are marcasite, arsenopyrite, calcite, gypsum, and fluorite (Roper and Wallace, 1981). According to Berry and others (1982), alteration minerals in the discovery outcrop are potassium feldspar, cristobalite, and clay with minor jarosite and siderite. Montmorillonite was found to be the dominant mineral in altered flow rock (sample C95-80) from the Aurora discovery outcrop during this study, with minor chalcedonic silica lining vesicles. XRD analysis confirmed the presence of potash feldspar, probably secondary, and plagioclase, which may be primary.

Radioactive rock from the U occurrence in moat sedimentary rock at Cottonwood Creek contains silicified layers with both chalcedonic quartz and opaline silica, and relatively coarse calcite in layers and cross-cutting veinlets. It also contains chips of fossilized wood. Uranium minerals were sought using SEM techniques, but not found.

Mineralization at the Opalite mine is similar to that at the Bretz mine – silicified breccia with very fine-grained sulfide. Dayvault and others (1985) list pyrite, realgar, native mercury, cinnabar, and an assemblage of mercury oxychloride and oxide minerals at Opalite. Sample C95-93, collected from the most radioactive site found in the Opalite mine during this study, is composed almost entirely of finely granular quartz with fine-grained sulfide. Moat sedimentary rock beneath the silicified rock at Opalite that contains about 0.01% U is highly argillized.

Alteration in the Bretz-Opalite district consists of silicification (both opaline and chalcedonic to fine-grained quartz) and strong argillization in and adjacent to the uranium and mercury deposits. Vertically and laterally zoned diagenetic alteration assemblages in the moat sedimentary rocks that are typical of volcaniclastic rocks, including zeolite minerals, potash feldspar, and smectite clays (Glanzman and Rytuba , 1979), make prospecting by alteration difficult in the Bretz-Opalite district. Nonetheless, mineralized areas in the northern part of the McDermitt caldera are in areas that can be identified by the presence of pertubations of the normal mineral zoning, or more intense alteration (Glanzman and Rytuba, 1979).

VIRGIN VALLEY, NEVADA

General geologic setting

Uranium mineralization in Virgin Valley occurs in air-fall tuff and tuffaceous sedimentary rock of the Virgin Valley Formation and in rhyolite lava of the Canyon Rhyolite (Figs. 9 and 10; Staatz and Bauer, 1951; Henry, 1978; Castor and others, 1982b; Zielinski, 1982; Tuchek and others, 1984). Our interpretation is that the tuffs and lavas that host uranium accumulated within or along the margin of a caldera centered on Virgin Valley and are parts of a genetically related, caldera magma system (Fig. 9). The following interpreted history of the caldera is based on geologic mapping and $^{40}Ar/^{39}Ar$ ages (Table 6; Fig. 11).

Idaho Canyon Tuff

The Virgin Valley caldera formed as a result of eruption of the Idaho Canyon Tuff. Outflow deposits of this peralkaline, probably comenditic, ash-flow tuff crop out just east of the caldera (Fig. 9) and extend symmetrically away from Virgin Valley (Noble and others, 1970; Greene, 1984; this study). Thick, intracaldera tuff presumably underlies Virgin Valley. An $^{40}Ar/^{39}Ar$ age of 16.30 ± 0.06 Ma on the tuff (Table 6; Fig. 11) also dates the time of caldera formation.

Rhyolite Lavas of Virgin Valley

Following caldera formation, rhyolitic lavas and small volume air-fall and ash-flow tuffs erupted along the ring fracture zone. We separate the lavas into three petrographic-age groups (Fig. 11). From oldest to youngest, these are Canyon Rhyolite (Tcr), peralkaline rhyolite (Tpr), and late porphyritic rhyolite (Trpl and Trp). Thick rhyolitic lavas of the Canyon Rhyolite are most voluminous and extensive. These erupted from several known or postulated vents along the ring fracture and form a nearly continuous rim around Virgin Valley (Fig. 9). Well-developed pressure ridges show that the rhyolites flowed generally down and into the paleo-Virgin Valley. Aphyric rhyolite lava in and near the uranium district consists of at least two lobes that flowed down and eastward from a vent around elevation 6657 (Virgin monument) on the Gooch Lake 7.5 minute quadrangle. An ash-flow tuff, the tuff of Big Mountain, is interbedded with Canyon Rhyolite on McGee Mountain and probably erupted from a source near McGee Mountain (Fig. 9). The Canyon Rhyolite lavas and tuff of Big Mountain are petrographically similar, aphyric to sparsely porphyritic rhyolites. Chemical analyses show that the lavas are alkalic but not peralkaline, although alkali mobility resulting from hydration complicates interpretation (Table 3).

The two younger rhyolitic lava groups occur only near the southwestern margin of the caldera, southwest of the uranium area (Figs. 9, 10). A single flow of peralkaline rhyolite lava (Tpr) crops out in the southwestern part of Virgin Valley and overlies air-fall and reworked tuffs (Tct). Greene (1984) correlated the peralkaline rhyolite with similar rhyolite at Catnip Mountain 25 km to the northwest. Chemical analyses of nonhydrated glass from both locations (Table 3) and presence of vapor-phase arfvedsonite confirm peralkalinity. Two flows of porphyritic rhyolite lava are the youngest rhyolitic rocks in the Virgin Valley area (Fig. 9). Greene (1984) designated them rhyolite of Badger Mountain and mapped apparently similar flows as much as 25 km southwest of Virgin Valley. The upper flow (Trp) erupted from the vent just southwest of sample location H95-57 (Fig. 9). Chemical analyses and presence of vapor-phase arfvedsonite indicate the upper flow is peralkaline (Table 3).

$^{40}Ar/^{39}Ar$ ages were determined on sanidine phenocrysts from two sparsely porphyritic Canyon Rhyolites, the tuff of Big Mountain, and the upper porphyritic rhyolite (Trp) and on coarse, vapor-phase alkali feldspar from peralkaline rhyolite (Table 6; Fig. 11). These ages show that the rocks erupted in three distinct episodes 0.15 to 0.20, 0.3, and 0.6 Ma after eruption of the Idaho Canyon Tuff and caldera formation. We infer that undated, aphyric Canyon Rhyolite in the uranium area of Virgin Valley is about 16.15 Ma, the same age as dated, sparsely porphyritic Canyon Rhyolite, on the basis of similarity in stratigraphic position and general occurrence of the lavas.

Virgin Valley Formation (Tvv)

The Virgin Valley Formation is a complex assemblage of air-fall and minor ash-flow tuff, tuffaceous sedimentary rock, lignite, and diatomite that accumulated within the Virgin Valley caldera. Rocks of the formation overlie and were deposited against Canyon Rhyolite lavas but are in part interbedded with the peralkaline rhyolite and late porphyritic rhyolite. We divide the formation into several units whose stratigraphic relations are shown in Figures 9 and 10. Most uranium mineralization occurs within dominantly fluvial deposits of unit Tvf, which have high background uranium concentrations (Castor and others, 1982b). Tuffaceous sedimentary rocks of the Virgin Valley Formation have been extensively altered by diagenesis, producing zeolite and clay.

Air-fall tuff (Tva)

The oldest part of the formation consists of air-fall and minor reworked tuff (Tva) that crops out around the margins of Virgin Valley, mostly close to outcrops of Canyon Rhyolite (Fig. 10). Coarse, massive to finely

Figure 9. Regional geologic map of the Virgin Valley area.

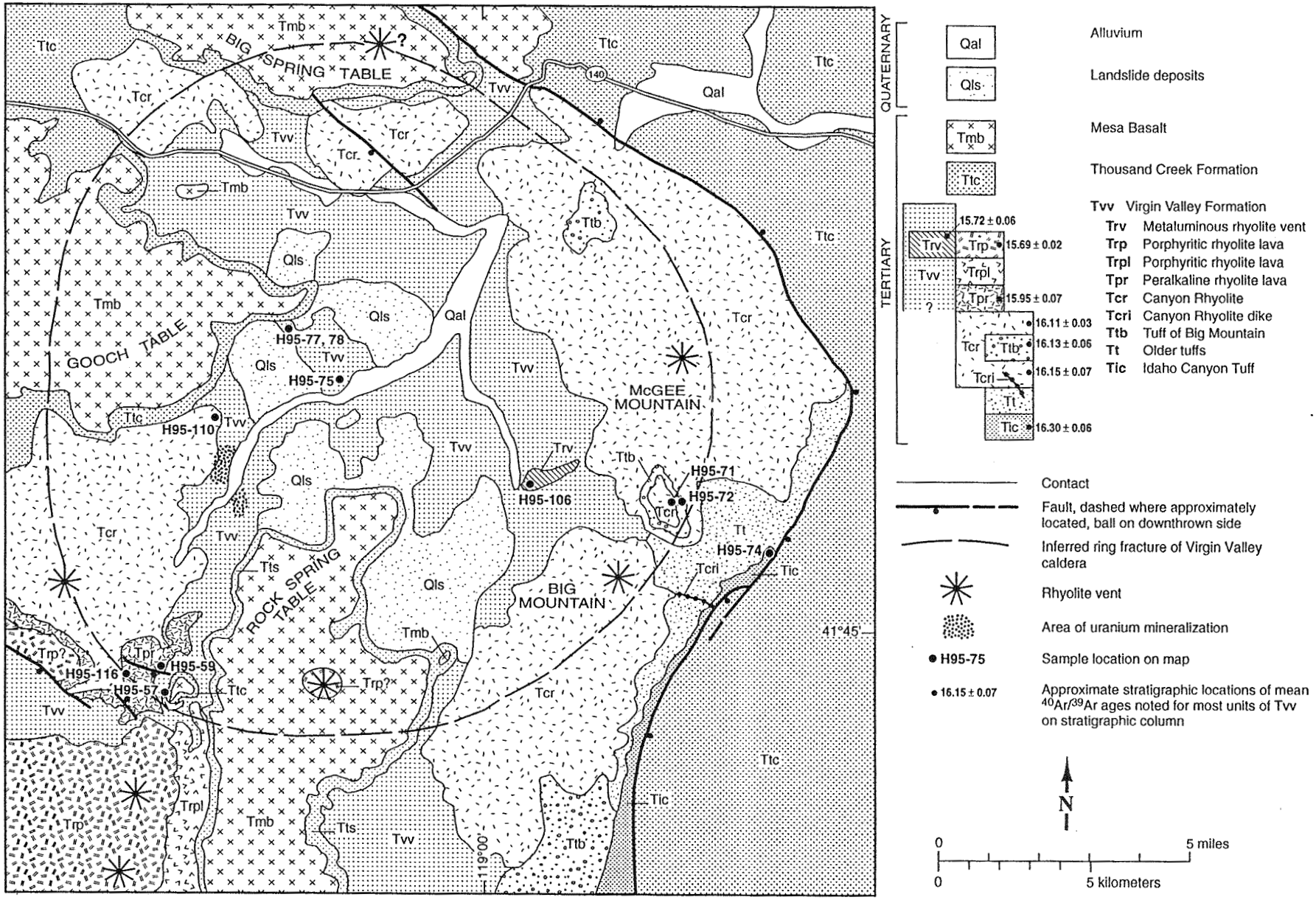

Figure 10. Detailed geologic map of the Virgin Valley uranium district. Explanation on following page.

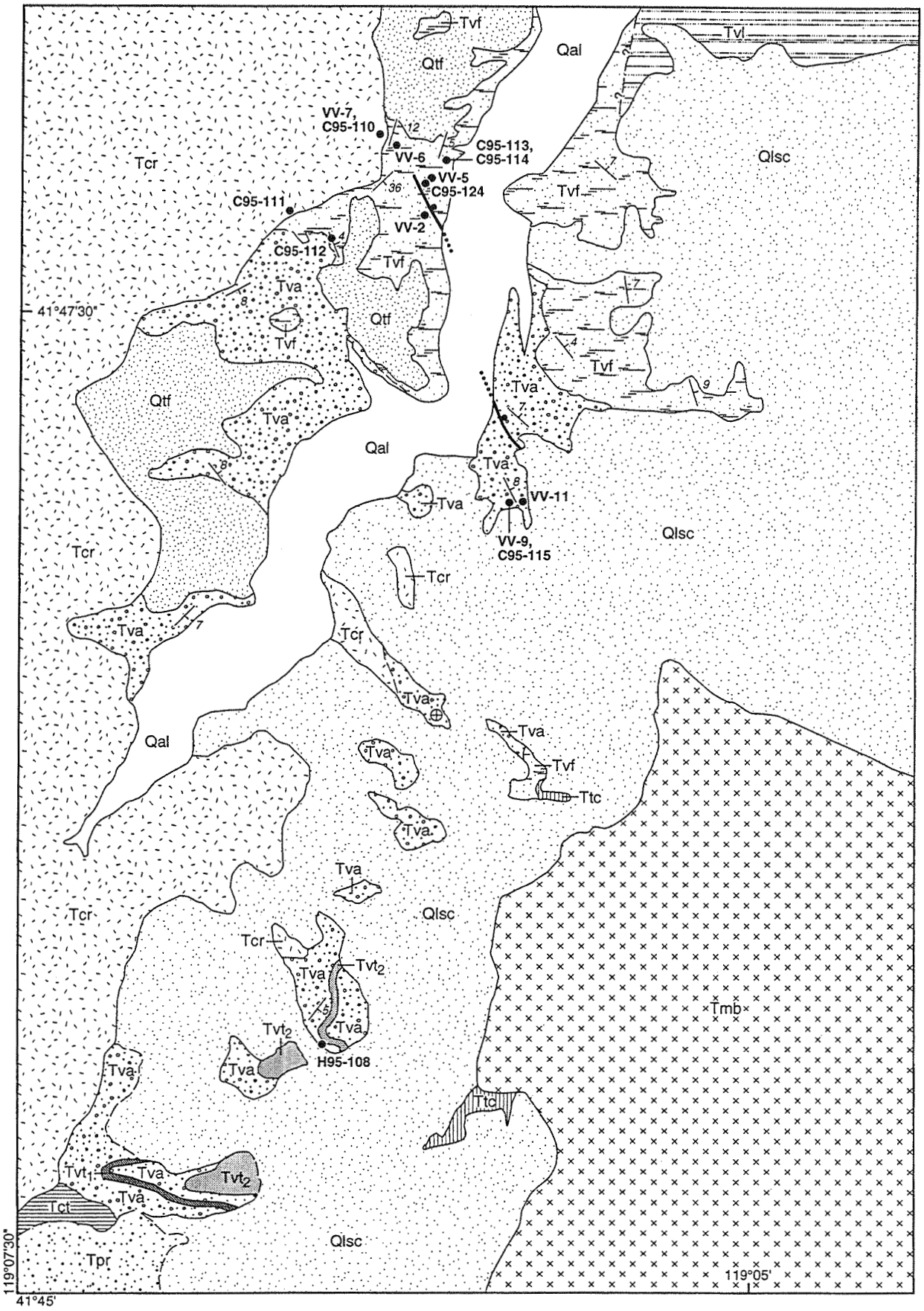

Explanation for Figure 10 (previous page).

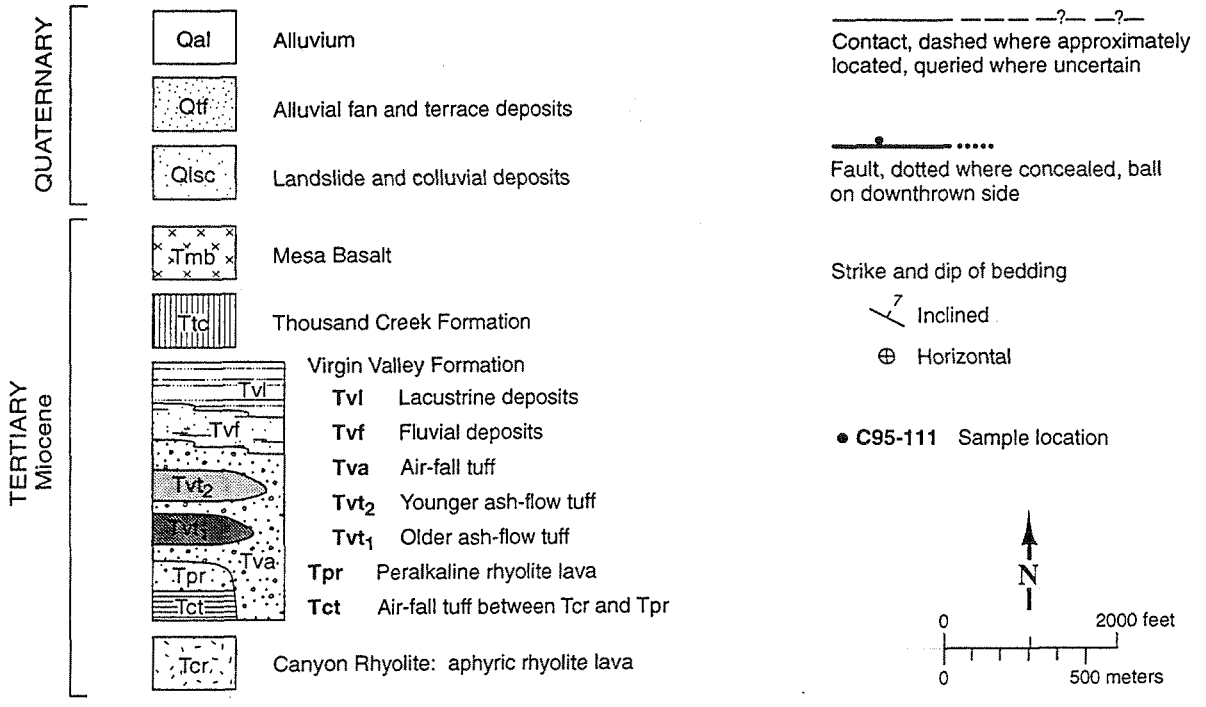

Figure 11. Volcanic stratigraphy in the Virgin Valley caldera as determined by $^{40}Ar/^{39}Ar$ dates reported in Table 6.

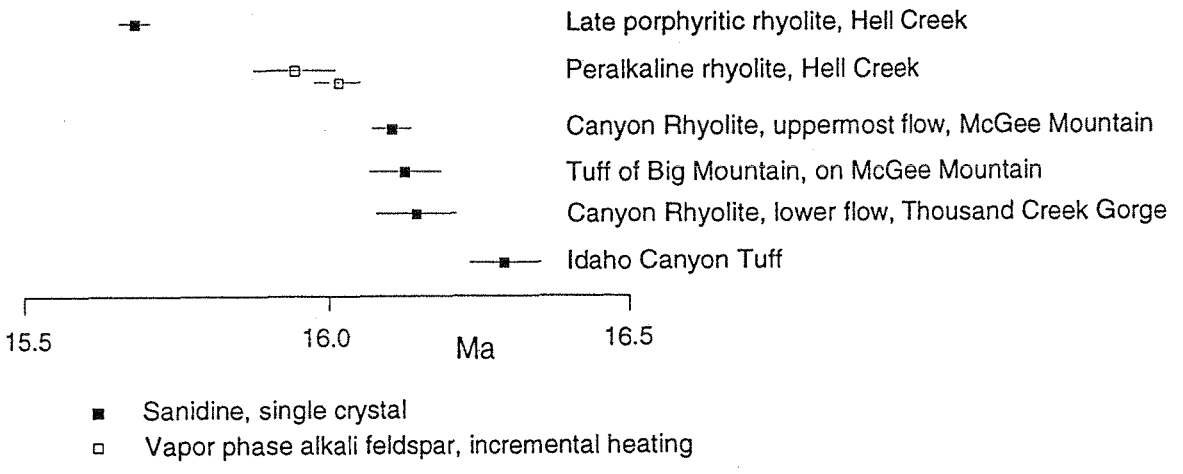

bedded air-fall tuff composed of aphyric to sparsely porphyritic pumice makes up most of the unit. Unit Tct, which also consists of air-fall tuff and is correlative with the lower part of unit Tva, is mapped separately where it underlies peralkaline rhyolite (Tpr) in the southwestern part of Virgin Valley. Unit Tva extends stratigraphically at least to the upper porphyritic rhyolite (Trp). These relations show that air-fall tuffs were deposited over an interval from at least 16.0 to 15.7 Ma. Unit Tva contains two thin, nonwelded ash-flow tuffs (Tvt1 and Tvt2) that are mapped separately in the southwestern part of Virgin Valley and are overlain by and partly interfinger with fluvial tuffaceous sediments (Tvf) toward the middle of Virgin Valley (Fig. 10). Chemical analysis (Table 3) of a single, aphyric, hydrated pumice fragment indicates that the pumice is compositionally similar to the peralkaline rhyolite (Tpr). The distribution, lithologic characteristics, age

relations, and composition of unit Tva indicate it was deposited as coarse, proximal air-fall tuff, pyroclastic equivalents of Canyon Rhyolite and the younger rhyolite lavas. The tuffs probably erupted from vents near the inferred sources for the lavas (Fig. 9).

Rhyolite Vent (Trv)
Low-silica rhyolite that forms a chain of four or five east-northeast-aligned knobs in the eastern part of Virgin Valley is interbedded with tuffaceous sediments of the Virgin Valley Formation. The knobs are small lava flows that apparently erupted from a fissure-dike system that underlies the chain. The rhyolite is petrographically and chemically distinct from the Canyon Rhyolite, peralkaline rhyolite, and late porphyritic rhyolite. The rhyolite vent contains phenocrysts of plagioclase, clinopyroxene, biotite, and hornblende. This assemblage and its chemical analysis shows that it is metaluminous, unlike the other lavas, which are mostly peralkaline (Table 3). Despite the compositional difference, an $^{40}Ar/^{39}Ar$ age of 15.72±0.07 Ma on biotite (Table 6; Fig. 11) shows that it is indistinguishable in age from the upper porphyritic rhyolite (Trp).

Fluvial and Lacustrine Deposits (Tvf and Tvl)
Most of the Virgin Valley Formation consists of fluvial and lacustrine tuffaceous sediments that were apparently deposited within a closed basin centered on present day Virgin Valley. Although lacustrine deposits generally overlie fluvial facies, the two are broadly interbedded and intergradational; probable fluvial deposits occur within mapped lacustrine facies and vice versa. The mapped contact on Figure 9 is a somewhat arbitrary boundary between dominantly fluvial deposits below and lacustrine deposits above.

Fluvial deposits (Tvf) consist of tuffaceous sandstone and siltstone with minor conglomerate. The deposits are lenticular and show abrupt lateral changes. Sandstones are massive to cross-bedded. Massive beds range up to about 1 m thick, are separated by more laminated siltstone, and commonly contain small pumice and rhyolite fragments. Thin (≤ 1 cm) lignite beds are locally present. Most deposits contain little preserved glass. Based on outcrop characteristics, alteration is probably mostly to clinoptilolite.

Lacustrine deposits (Tvl) occupy most of Virgin Valley although they are commonly covered by Quaternary landslide and alluvial deposits. Massive to finely laminated, clay-altered, gypsiferous mudstone containing petrified wood is the most abundant rock type. Slightly silicified siltstone and sandstone in fining-upward sequences 50 cm to 2 m thick form resistant layers within the mudstone. Lignite beds made up of friable plant remains form lenses up to a few centimeters thick and can occur in zones as much as 1.5 m thick. Massive, poorly sorted tuff beds from 2 to 5 m thick are probably debris-flow deposits. These contain abundant wood as twigs and logs up to several meters long; well-rounded, matrix-supported volcanic rock fragments mostly of Idaho Canyon Tuff to 40 cm; and rip-up clasts of tuff to 2 m in a clay-altered tuffaceous matrix. These deposits are the primary host for precious opal in Virgin Valley.

The overall timing of sedimentary deposition of the Virgin Valley Formation is only partly understood, but we infer that tuffaceous sediments began to accumulate soon after eruption of the Idaho Canyon Tuff and caldera collapse (Fig. 11) . The only direct date on the formation is on the 15.7-Ma rhyolite vent (Trv), which is interbedded with tuffaceous sedimentary rock in the eastern part of Virgin Valley (Fig. 9). Lower parts of the fluvial sequence locally interfinger with air-fall tuff that must be at least16.0 Ma (Fig. 11). Stratigraphic relations for the upper parts of the lacustrine deposits are unconstrained. Zielinksi (1982) reported two zircon fission-track ages of 14.4±0.8 and 13.9±2.0 Ma from "rhyolite air-fall ashes of the lacustrine facies." Both are younger than ages that we obtained but partly overlap within their large uncertainties. The sample giving the older age is apparently from our unit Tvf near sample C95-114; based on our ages and stratigraphic relations, this deposit need be no younger than 15.7 Ma. The younger sample is from what we map as Tvf in the uppermost part of the Virgin Valley Formation 1.3 km south of sample C95-115; the fission-track age is possible but cannot be independently evaluated. The tuffaceous sedimentary rocks were probably derived from erosion of the air-fall tuffs, so the zircon ages may indicate the time of eruption of the ash but not reworking into sedimentary deposits. Deposition of the Virgin Valley Formation may have continued well after eruption of any of the tuffs or rhyolite lavas (Fig. 11). Nevertheless, the fission-track ages broadly support the age range we infer for the air-fall tuffs.

Thousand Creek Formation

The Virgin Valley Formation is overlain by the Thousand Creek Formation of friable, coarse to medium sandstone composed mostly of volcanic-rock and mineral fragments. Pumiceous sandstone and a few air-fall tuffs are present, but primary volcanic ash seems to be much less abundant than in the Virgin Valley Formation. Lacustrine deposits of any kind are lacking. The Thousand Creek Formation appears to be a regional fluvial sequence that postdates most local volcanism and whose deposition was not influenced by the former closed basin in Virgin Valley. Nevertheless, the two formations consist of broadly similar tuffaceous sediments, and the contact between the two is difficult to identify and may be gradational. The tuffaceous rocks of the Thousand Creek Formation have undergone much less diagenetic alteration than the Virgin Valley deposits; outcrop examination suggests clinoptilolite is either minor or absent. Based on ages of Virgin Valley rocks and Mesa Basalt, the Thousand Creek Formation accumulated between about 15 and 9 Ma.

Mesa Basalt

Basalt lava of the Mesa Basalt (Merriam, 1910; Wendell, 1970; basalt of Catnip Creek of Greene, 1984) is the youngest volcanic rock of the area. It caps Big Spring, Gooch, and Rock Spring Tables, north, west, and south of Virgin Valley (Fig. 9). Greene reports K-Ar dates of 9.9 ± 1.2 and 8.8 ± 1.1 Ma on samples from the western part of Gooch Table and from 40 km northwest of Virgin Valley, respectively.

The Virgin Valley caldera

The geologic and geochronologic data reveal much about the geometry and evolution of the Virgin Valley caldera, and the caldera setting may have been critical for uranium mineralization. The data indicate that Virgin Valley lies within a caldera that was the probable source of the Idaho Canyon Tuff. However, some aspects of caldera geometry remain uncertain. The symmetrical distribution of Idaho Canyon Tuff around Virgin Valley and its regional thickness variation indicate that the tuff erupted from a source in this area (Noble and others, 1970). Although the total volume of Idaho Canyon Tuff is unknown, its wide distribution suggests a voluminous deposit that should have a caldera source.

The circular arrangement of Canyon Rhyolite, other rhyolite lavas, and their vents are consistent with eruption along or near a caldera ring fracture (Fig. 9). Moreover, the lavas flowed down into what was probably a closed basin.

The Virgin Valley Formation also accumulated within a closed, circular basin. Virgin Valley deposits dip relatively uniformly at 2° to 6° into the basin. Although Wendell (1970) interpreted these dips to result from folding, they are probably a mix of primary dips reflecting the depositional geometry and late subsidence of the caldera. Slump structures produced by soft-sediment deformation trend into the basin and show that the dips existed immediately following deposition. The circular shape of the basin and apparent lack of association with preceding tectonic faulting makes it unlikely that this was a graben. Late subsidence, rather than resurgence, is characteristic of many calderas especially those associated with peralkaline volcanism (Mahood, 1984).

The timing and characteristics of volcanism in the Virgin Valley area are similar to those of calderas worldwide (Lipman, 1984). Major ash-flow eruption was followed by probable ring-fracture rhyolites in three episodes approximately 0.15, 0.3, and 0.6 Ma later (Table 6; Fig. 11). Contemporaneously, large volumes of tuffaceous sediments accumulated within the caldera. Episodic ring-fracture volcanism and tuffaceous sedimentation are characteristic of most other calderas (Smith and Bailey, 1968; Lipman, 1984).

The orientation of the basin-and-range fault that forms the eastern edge of McGee and Big Mountains provides more indirect evidence for a caldera. South of the area depicted in Figure 9, the fault strikes north (Greene, 1984). Near the caldera, the fault forms northeast- and northwest-striking segments that curve around the caldera and parallel and nearly coincide with the inferred ring fracture. The ring fracture or the underlying solidified magma chamber may have influenced the orientation of the fault.

These data indicate an approximately 20- to 25-km-diameter caldera that is now largely buried beneath younger rocks (Fig. 9). Ash-flow tuffs commonly pond within their source calderas, so a thick section of Idaho Canyon Tuff should underlie Virgin Valley. The caldera is not resurgent.

Our interpreted caldera differs significantly from that inferred from gravity data by Plouff (1984). He interpreted a small caldera, approximately 6 x 8 km, defined by a closed gravity low and centered in the northern part of Rock Spring Table. This would correspond only to the southernmost part of the Virgin Valley caldera. Plouff recognized that little geologic evidence existed for a caldera at that location. We suggest that the gravity low might partly coincide with the Virgin Valley caldera, but that the true caldera must have dimensions more like that shown in Figure 9.

The greatest uncertainty regarding the Virgin Valley caldera is in the exact location of the ring fracture, which is nowhere exposed. The most likely possibility is that it approximately underlies the Canyon Rhyolite vents. Occurrence of thin Idaho Canyon Tuff, probably as outflow, southeast of the inferred ring fracture is consistent with this interpretation. However, outflow tuff near its source caldera would have to rest on the caldera rim and therefore should be much higher in elevation than intracaldera deposits. Yet intracaldera Virgin Valley Formation mostly occurs at higher elevation than Idaho Canyon Tuff near McGee Mountain. This requires that the Canyon Rhyolite greatly accentuated caldera topographic relief. Additionally, the inferred ring fracture near McGee Mountain runs either through older tuff (Tt) or along the buried (and inferred) contact between older tuff and Virgin Valley Formation south of McGee Mountain (Fig. 9). We have not examined this area, but detailed mapping of it would be worthwhile.

Geology of uranium mineralization

Uranium mineralization is present over an area of approximately 2 km^2 in the southwestern part of Virgin Valley (Fig. 10). Prospects are spread over a much larger area but contain negligible uranium (Castor and others, 1982b; Tuchek and others, 1984). Castor and others estimated that uraniferous beds contain more than 500 tons U_3O_8 at an average grade of 0.015% U_3O_8. Tuchek and others estimated that the area held 15 to 20 millions tons of low-grade material. Uranium occurrences appear to form distinct groups that reflect either deposit type or geographic relation within this area. For this discussion, we emphasize four uranium mineralization types that are distinguished by geologic setting, mineralogy, and trace element association: (1) in breccia in Canyon Rhyolite, (2) associated with lignite and fossilized wood, (3) in bedded opal, and (4) along fractures in tuff (Table 11).

The most radioactive occurrences in Virgin Valley are in Canyon Rhyolite (sample sites C95-110 and VV-7, Fig. 10). At sample site VV-7, an area of about 1 m^2 has radioactivity in excess of 100 x background and is in an area approximately 50 m in diameter with radioactivity in excess of 2 x background. At this site, an abundant yellow uranium mineral, associated with limonite and white opal, coats fractures or fills space in breccia at the nose of the flow near the contact with tuff of the Virgin Valley Formation.

Deposits in or closely associated with lignite or other carbonaceous material occur along the west side of Virgin Creek just east of the area of mineralization in Canyon Rhyolite. Lignite forms thin lenses or layers (as at sample site C95-113) within the dominantly fluvial part of the Virgin Valley Formation. In addition, carbonized wood is common in some radioactive tuffaceous layers (Castor and others, 1982b), and opalized wood is also present, in one locality (sample site C95-124) as a stump in tuffaceous rock that is apparently in place because its roots extend into underlying strata. Maximum radioactivity in lignite and fossilized wood was measured at about 25 x background.

In addition to its occurrence in fossilized wood, opal is present as thin beds and stratabound lenses that replace fine-grained sedimentary layers and diatomite and as cement in more coarsely tuffaceous sediment. The most notable occurrences of stratiform radioactive opal are in the southernmost part of the

Table 11. Characteristics of uranium occurrence and rock types at Virgin Valley, Nevada. Weak or local trace element enrichment queried.

Sample	U (ppm)	Description	Mineralogy, Remarks	Trace Elements	Th/U
U in fractures or breccia of Canyon Rhyolite (Tcr)				As, Cd, Mo, Sb, Zn, Bi?, Tl?	
C95-110	2,690	Radioactive breccia	Yellow U mineral		0.01
VV-7	9,740	Highly radioactive breccia	Weeksite, carnotite, U silicate, U-As phosphate		0.00
U with lignite or other carbonaceous material				As, Mo, Sb, Se, Bi, Tl, Te?	
C95-113	2,250	Radioactive lignite	Carnotite and metaankoleite in framboid molds(?)		0.01
C95-124	755	Opalized wood	No U minerals found; abundant pyrite framboids		0.01
VV-5	645	Argillized tuff	U-As phosphate		0.01
U in opal				As, Cd, Mo, Sb, Zn, Bi?, Se?	
VV-2	1,380	Radioactive brown opal	U in opal		0.00
VV-9	657	Green fluorescent opal	U in opal replacing diatomite		0.00
VV-11	1,190	Radioactive opal	U in opal with Mn oxide		0.00
C95-115	20	Opalized air-fall tuff	Glass, opal		0.87
C95-115	37	Opalized air-fall tuff	Glass, opal		0.43
Tuff with U along fractures, in cavities, or in unknown sites				Sb, As?, Tl?	
C95-112	189	Bedded tuff	Carnotite, U silicate (soddyite?), pyrite?		0.06
C95-114	426	Air-fall tuff	Carnotite, opal, clinoptilolite		0.06
VV-6	96	Zeolitized tuff	No U minerals found		0.16
Unaltered volcanic rocks					
H95-68	9	Canyon Rhyolite (Tcr)	Hydrated vitrophyre		2.25
C95-111	10	Canyon Rhyolite (Tcr)	Slightly opalized, near C95-110 and VV-07		2.11
C95-116	14	Peralkaline rhyolite (Tpr)	Devitrified		2.05
C95-116a	12	Peralkaline rhyolite (Tpr)	Nonhydrated glass		2.10
H95-57	14	Late porphyritic rhyolite (Trp)	Hydrated vitrophyre		1.86
Altered tuffaceous sedimentary rocks of the Virgin Valley Formation					
H95-75	4	Argillized	Smectite, feldspar, clinoptilolite, glass		2.49
H95-77	3	Argillized	Smectite, feldspar, glass		3.47
H95-78	6	Glassy (hydrated)	Glass, feldspar, smectite		3.08

district on the east side of Virgin Creek (Castor and others, 1982b; this study), where radioactive white to light green opal replaced pure white diatomite. Beds of locally radioactive orange to black opal occur in the same area. Secondary U minerals coat fractures in the opal beds (Castor and others, 1982b), but opal without obvious secondary U minerals locally has radioactivity as high as 13 x background.

On the west side of Virgin Valley, brown opal that appears to have replaced shaly, fine-grained tuffaceous sedimentary rock with local concentrations of wood fragments, is radioactive and contains laterally extensive U-rich rock (Castor and others, 1982b). Sample VV-2, collected from a radioactive site at 20 x background, is an example of this type of opal. Spongy opal replacements of more coarsely tuffaceous rock are also radioactive (sample C95-114, radioactivity 11 x background).

Yellow U minerals occur along fractures in zeolitized tuffaceous sediment in the southwestern part of the district as at sample site C95-112 (Fig. 10). Sample VV-6 may be similar, as may be the fracture fillings in uraniferous opal beds reported by Castor and others (1982b). Although these minerals coat fractures, they do not appear to extend into the host rock and total U concentrations per volume of rock may be low. At sample site C95-112, radioactivity of the host rock was measured at only about 2 x background, whereas the fracture coating was as high as 5 x background.

On the basis of detailed stratigraphic work and sampling, Castor and others (1982b) noted that some stratiform U enrichment in tuffaceous beds in Virgin Valley is correlative with zeolite and clay mineral contents. However, non opalized tuffaceous samples with high U contents were also found to contain carbonaceous material (sample VV-5 is an example of this type of occurrence).

Rock chemistry

Samples of rhyolitic flow rock and tuff from the Virgin Valley caldera in and near the uranium district are mainly peralkaline. As expected for such rocks, they have relatively high U and Th contents (10-14 ppm and 20-28 ppm, respectively) and they also have relatively high contents of other trace elements such as Zr, REE, and Ta (Table 2). Virgin Valley rhyolite samples have overall compositions that are very similar to those of rhyolites from the McDermitt Caldera.

Samples from radioactive occurrences in the Canyon rhyolite have the highest U contents of any samples from the Virgin Valley area, as much as 0.97% U (sample VV-7, Table 2). Associated elevated trace elements include As, Cd, Mo, Sb, and Zn (Table 2, Fig. 5), and Bi and Tl are weakly elevated.

Trace element association in U-rich lignite and fossil wood is somewhat similar to that for Canyon Rhyolite, except that Se is distinctly enriched, whereas Zn and Cd are not. The lignite sample collected for this study (C95-113) has the highest Se and Te contents of any sample from Virgin Valley, and the opalized wood sample (C95-124) has the highest Bi, Mo, Sb, and Tl.

The opal deposits are at most modestly enriched in Mo, Zn, Cd, As, Sb, and possibly Bi (samples C95-114, C95-115, VV-2, VV-9, VV-11, Table 2). A sample of uraniferous brown opal (VV-2) from a stratabound lens west of Virgin Creek is also enriched in Se. The geochemical characteristics of this sample may suggest a closer, geographic association with the lignite-related deposits.

U enrichment along fractures may be unrelated to concentrations of other trace metals. Sample C95-112 is weakly enriched in Sb, which is only slightly above background. Samples VV-6 and C95-114 are geochemically similar, and C95-114 is also slightly enriched in Tl. Sample C95-114 of opalized air-fall tuff is only slightly enriched in Sb and possibly As and Tl, which makes it geochemically most like mineralization along fractures in tuff.

Mineral assemblages

Uranium minerals that we have identified in samples from Virgin Valley are all uranyl (U^{+6}) phases. Uranous (U^{+4}) phases have not been identified; however, a very fine-grained U^{+4} phase may be present in U-rich opal.

Samples from radioactive occurrences in the Canyon Rhyolite contain weeksite, carnotite, a U-silicate (soddyite?), and U-As phosphate. The weeksite (hydrated K-U silicate), which was identified by XRD and SEM/EDX (see Table 3), seems to be the dominant U mineral in these occurrences. It is banded to finely drusy and fibrous to acicular in form. It filled open spaces between breccia clasts and was, in places, subsequently covered with white opal preserving its delicate acicular form (Fig. 12).

Carnotite, meta-ankoleite, and a U-As phosphate occur in radioactive occurrences in lignite or other carbonaceous material. In a sample of radioactive lignite (C95-113), carnotite and meta-ankoleite occur in spherical cavities that may be casts of pollen or of oxidized pyrite framboids (Fig. 13). We could identify no U minerals in sample C95-124, a silicified stump with abundant pyrite framboids (Fig. 14).

Fission-track radiography of U-rich opal indicates that U is disseminated through the opal, and distinct U minerals that occur within opal have not been found (Castor and others, 1982b; Zielinski, 1982). Study of U-rich opal by us also failed to identify U phases. According to Castor and others (1982), U is concentrated in tiny patches of Mn oxide and barite in the opal, and may also occur in minute grains (less than 10 μ) of ilmenite, pyrite and galena. Secondary carnotite, autunite, and uranyl silicate coat fractures in the opal beds (Castor and others, 1982b), but these minerals are generally not present in U-rich opal.

An unidentified U-As phosphate mineral occurs in sample VV-5, which is tuffaceous rock that does not appear to contain opal of abundant carbonaceous material. U-As phosphate, as noted above, occurs in several other types of rock in Virgin Valley. Arsenic phosphate minerals are known, including fermorite ($[Ca,Sr]_5[AsO_4,PO_4]_3[OH]$), but no named mineral has the chemistry of the phase in VV-5 (Table 4).

Identified fracture coating minerals in Virgin Valley are carnotite (Fig. 15a, Table 4) and an unidentified U-silicate mineral (soddyite?). In addition to coating fractures, these minerals also occur in cavities in zeolitized and argillized tuffaceous rocks (Fig 15b).

Figure 12. Backscattered SEM image of acicular radiating weeksite crystals in opal, sample VV-7, radioactive breccia in Canyon Rhyolite, Virgin Valley.

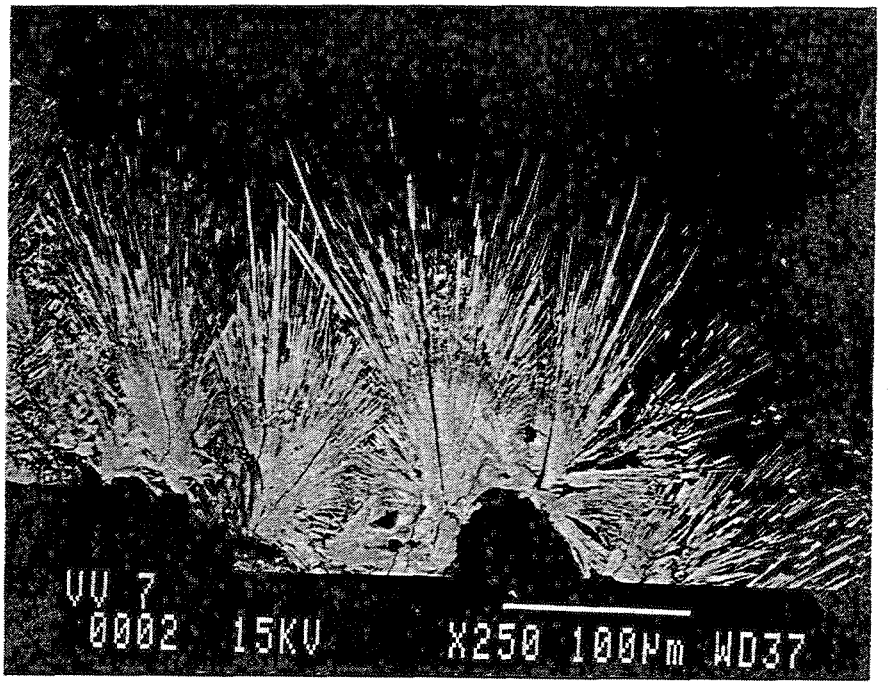

Figure 13. Secondary electron image of meta-ankoleite and carnotite (relatively bright phases) that partially fill spherical cavities (framboid molds?) in lignite, Virgin Valley.

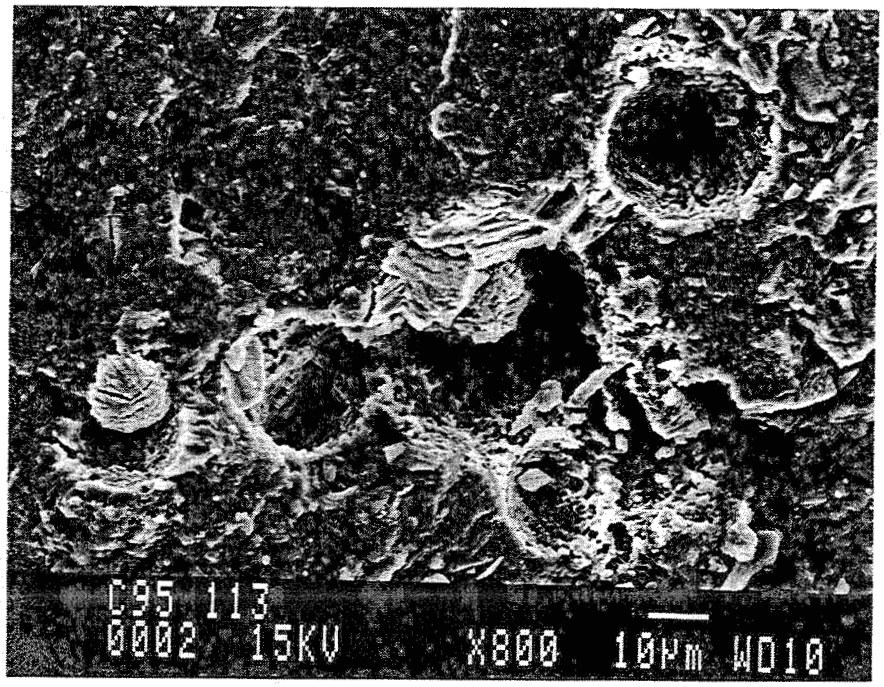

Figure 14. Backscattered SEM image of pyrite framboids in uranium-rich petrified wood, Virgin Valley.

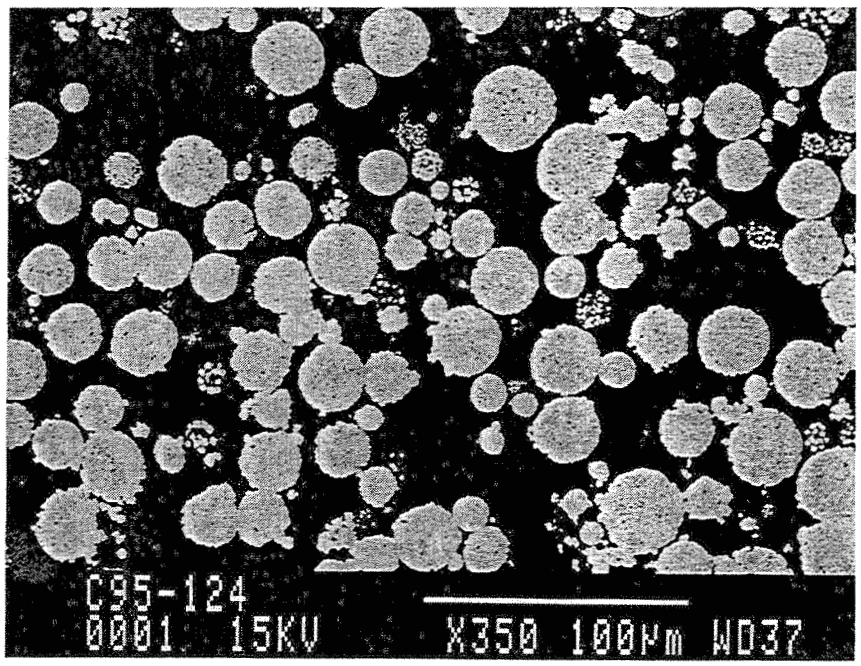

Figure 15a. Photomicrograph, crossed polars, yellow carnotite on fracture plane, sample C95-112, Virgin Valley. Carnotite coating is as much as 30 μ thick.

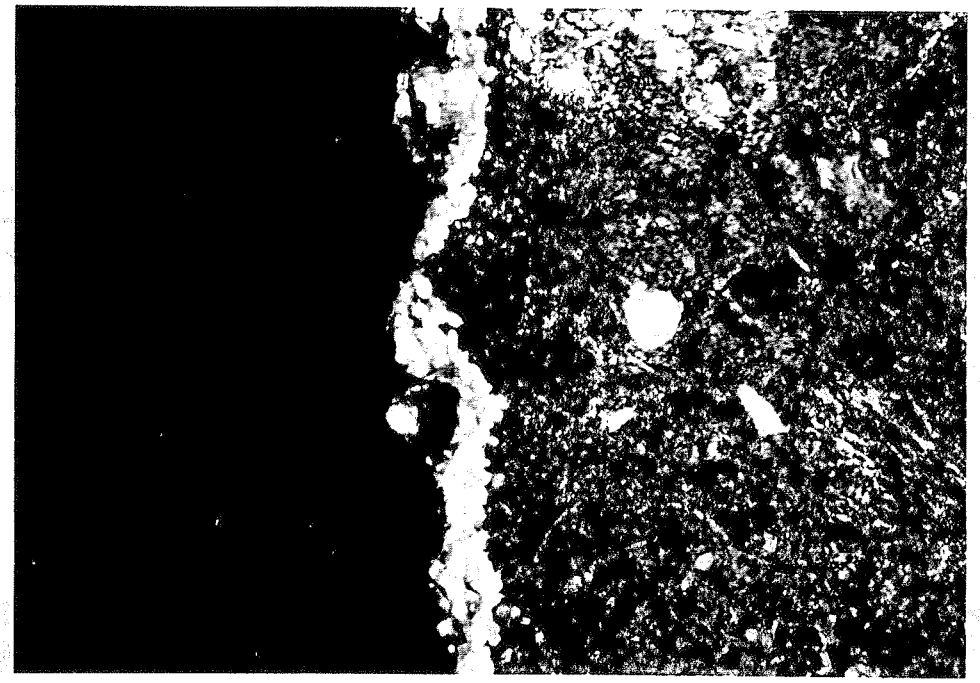

Figure 15b. Photomicrograph, crossed polars, yellow carnotite spheroids partly filling pumice vesicles in tuff, sample C95-114, Virgin Valley. Carnotite spheroids are 10-20 μ in diameter.

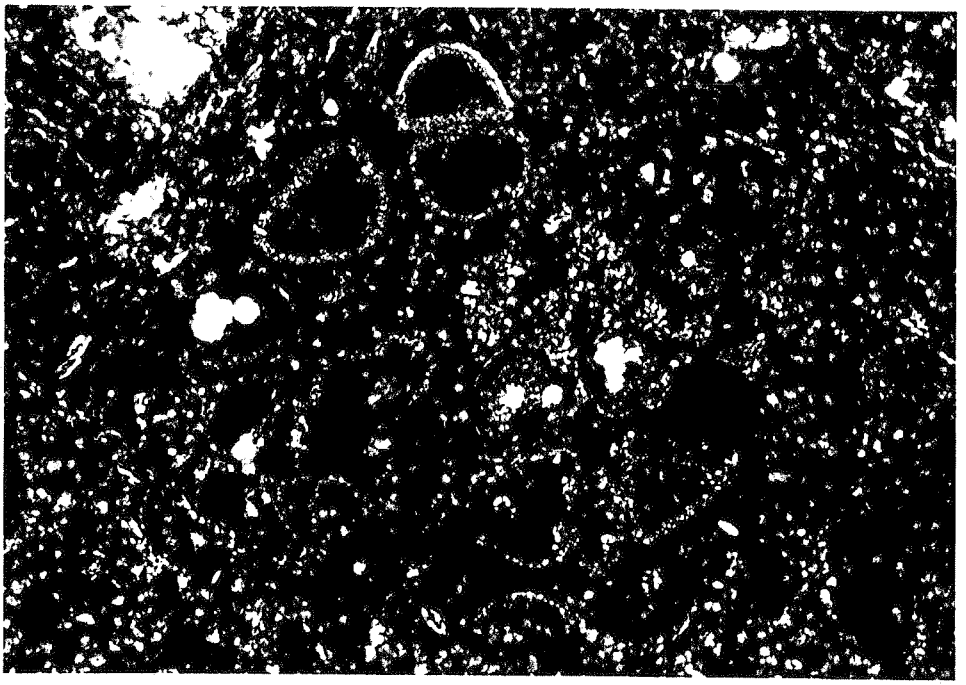

The primary mineral assemblage in the Canyon Rhyolite in the Virgin Valley uranium district is typical for devitrified aphyric rhyolite, and consists mainly of silica and potash feldspar; no glassy rocks were found. However, rocks in the Virgin Valley Formation in the U district consist of tuffs and volcaniclastic sediments that range from glassy rocks to rocks that are nearly completely replaced by diagenetic minerals, mainly clinoptilolite and smectite (montmorillonite). Outcrop characteristics, petrographic analysis, and a few X-ray diffraction analyses indicate that fluvial deposits around the margin of the basin are mostly altered to clinoptilolite and local smectite. Lacustrine deposits within the interior of the basin are dominantly altered to smectite with minor clinoptilolite. Some U enrichment in the Virgin Valley Formation is in the "green beds," a sequence of tuff beds that contain clinoptilolite, cristobalite, potash feldspar, mordenite (?), and some organic carbon; opal beds enriched in U were reported to be interbedded with tuff composed of varying amounts of glass, clinoptilolite, cristobalite, and montmorillonite (Castor and others,1982b).

Hydrologic setting

Nonthermal well and spring waters in Virgin Valley are generally relatively dilute (TDS = 95 to 184 mg/L) Na-HCO_3-SO_4 waters, whereas the hot springs (Bog and Baltazor) have somewhat different chemistries. Figure 16 shows the data from Virgin Valley on a Piper diagram (Piper, 1944). The TDS of Big Spring, located about 15 km north-northwest of the Virgin Valley uranium district, is very low (67 mg/L), and hence, the TDS circle is very small on Figure 16, and located within the symbol plotted for that spring. Water analyses for Baltazor Hot Spring, located about 35 km northeast of the uranium district, have varied somewhat between sampling events, but they are Na-SO_4-HCO_3 waters that contain higher Cl (up to 51 mg/L) than the nonthermal waters, and 600 to 630 mg/L TDS. The Baltazor Hot Spring well is very similar to the spring water indicating they originate from the same reservoir. Bog Hot Spring, which is about 25 km northeast of the uranium district, on the other hand, yields Na-HCO_3-SO_4 water that is slightly more concentrated than the nonthermal waters (TDS = 250 to 276 mg/L). Bog Hot Spring has a temperature of 54 to 57°C, Baltazor Hot spring has had measured temperatures between 90 and 92°C. Only one of the high temperature waters is a well: Baltazor Hot Spring Well (temperature = 92°C). Reported pH of all hot and cold waters ranges from 6.5 to 9.05. Big Spring is somewhat anomalous when compared to the other waters of the area and is a Ca-HCO_3 water. No depths to water level in wells are reported in the available data. However, a perennial creek flows through Virgin Valley within the area of uranium occurrences indicating that the water table in parts of this area is likely to be shallow. Tables 7-9 show trace element analyses contained in STORET and NURE databases. The Virgin Valley area has the highest U contents in stream and spring water in any of the three areas; no well water U contents are available for Virgin Valley from these data sets. Generally higher U and V concentrations are found in spring waters in comparison to stream water samples in the Virgin Valley area. Four springs within 5 km of the uranium area in Virgin Valley contain only background U_3O_8 contents, at 2-5 ppb (Castor and others, 1982b).

LAKEVIEW URANIUM MINING DISTRICT, OREGON

The Lakeview uranium mining district, a 40 km^2 area about 20 km northwest of the town of Lakeview, Oregon (Fig. 1), contains two mines with past uranium production and eight uranium prospects (Fig. 17). Lakeview district mines produced more uranium from volcanic-rock hosted deposits than any other district in North America, and possibly anywhere in the world. Total uranium production at Marysvale, Utah, was greater; but although some uranium ore at Marysvale came from volcanic rock-hosted deposits, it was mostly mined from deposits in plutonic rock (Kerr, 1968). About 350,000 pounds (ca. 77,000 kg) of U_3O_8 were produced from ore from the White King mine in the 1960s (Petersen and McIntyre, 1970). Most of the ore was mined from an open pit about 200 m in diameter, but some early mining was by underground methods. About 30,000 pounds (ca. 14,000 kg) of U_3O_8 were extracted from ore mined from an open pit about 100 m in diameter at the Lucky Lass mine in the 1960s.

Lakeview district uranium ore was processed in a mill at Lakeview during the 1960s, and in the early 1990s mill tailings and other contaminated material from this site were cleaned up in compliance with the Uranium Mill Tailings Radiation Control Act of 1978. The mine sites are presently being studied by the U.S. Forest

Figure 16. Piper diagram showing water chemistry data from the Virgin Valley area.

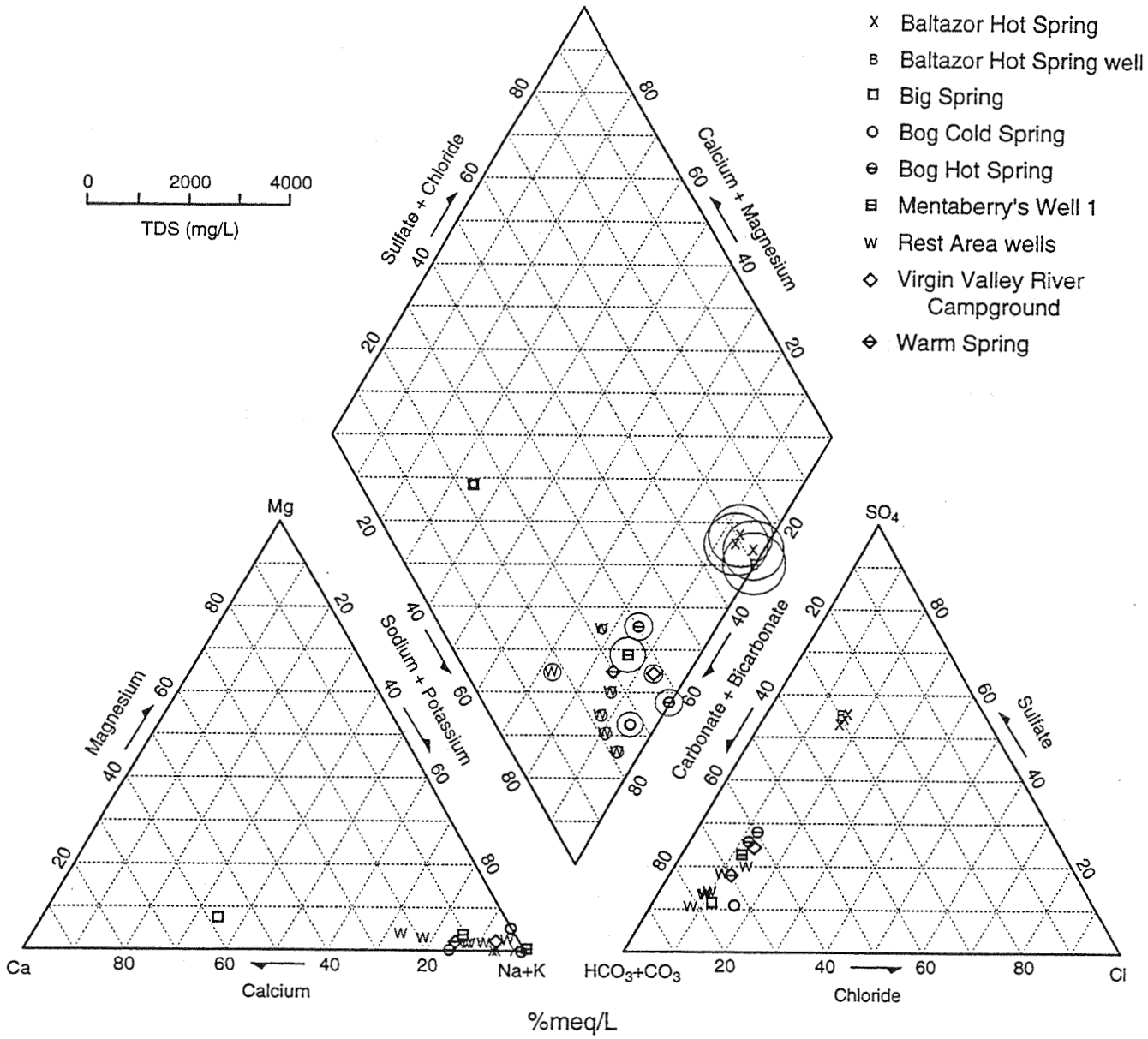

Service and Kerr-McGee Corporation in an attempt to formulate plans for mitigation of environmental damage caused by radioactive elements and heavy metals in surface waters (Fremont National Forest, 1991).

Geology

The Lakeview uranium mining district contains exposures of ash-flow tuff and tuffaceous sedimentary rock that has been correlated with the John Day Formation and with younger rocks such as the Mascall and Virgin Valley Formations (Walker, 1963). These suggested correlative units range in age from 37 to 15 Ma (Fiebelkorn and others, 1983; this report). The tuffaceous rocks are overlain by Upper Miocene basalt flows, and volcanic agglomerate of the Camp Creek Formation (Cohenour, 1960). Correlative basalt from Shoestring Butte just north of the district has been dated at 10.5 ± 0.3 (Fiebelkorn and others, 1983). Silica-rich rhyolite domes that have been dated at 7.0 ± 0.4 to 7.90 ± 0.09 Ma (Fiebelkorn and others, 1983) cut all of the abovementioned rock units. Uranium mineralization occurs in all of the Tertiary rock units in the district and is considered to be related to the rhyolite domes (Castor and Berry, 1981).

At the White King mine, uranium ore occurs in intrusive rhyolite and in volcanogenic sedimentary rocks, tuffs, and Camp Creek Formation breccia. Basalt flow rock, which is exposed along the crest of the northwest pit wall, is not mineralized but is cut by faults with associated argillic alteration that is considered to have been caused by the mineralizing fluids (Castor and others, 1982a). In addition, uranium mineralization is in basalt and in directly underlying sedimentary rocks to the southwest of the White King mine, and the capping basalt may have been important as a trap for hydrothermal fluids in the White King deposit (Castor and Berry, 1981).

During the May 1995 examination for this study, uranium ore in the White King pit was completely covered by water (Fig. 18). However, in 1978 and 1979, a 600 m^2 exposure averaging 0.03% U_3O_8 and locally containing rock with more than 1% U_3O_8 was examined (Castor and others, 1982a). This exposure was reported to be composed entirely of brecciated and silicified, flow-banded rhyolite that contained a 10-cm-wide, near vertical, N80° W, uraniferous chalcedony vein.

Radioactive rock is abundant in mine dumps or stockpiles to the northeast and southeast of the White King mine. In a draft environmental impact statement (Fremont National Forest, 1991) these were referred to as the "low-grade ore stockpile" and the "minespoil pile," respectively. However, it is not clear that these terms are correct, because both piles have surface radioactivity of 2-5 x background, and contain local anomalies as high as 50 x background on the basis of hand-held scintillometer measurements. In addition, rock with the highest U content collected for this study came from the southern pile. Most of the radioactive rock is breccia or flow-banded rhyolite that is dark gray or black due to the presence of fine-grained sulfide. The rock is generally moist below the surface of the piles and appears to be partially disintegrated due to breakdown of the sulfide minerals.

As at the White King mine, uranium ore cannot be examined in situ at the Lucky Lass mine (if any remains) because the pit is partially filled with water (Fig. 19). This was also reported to be the case in 1981 (Castor and others, 1982a). According to Cohenour (1960), the uranium mineralization is in a N35° W-striking, 75° NE-dipping, 3-m-wide fault zone that contains blocks and boulders of altered tuff and basalt in clayey gouge. Petersen and McIntyre (1970) reported that uranium mineralization at the Lucky Lass mine was controlled by several fault zones, the most important being a N75° W, 85° NE structure. Presently exposed pit walls are composed of a 100-m-thick, moderately southwest-dipping section of bedded tuff and nonwelded ash-flow tuff that does not contain radioactive anomalies. However, highly radioactive rock consisting of vesicular mafic volcanic rock and argillized tuff can be found on waste dumps.

Small amounts of uranium mineralization were found at eight other sites in the Lakeview uranium district (Fig. 17). Due to access problems and time constraints, these sites were not examined for the present study. In addition to uranium occurrences in rhyolite, basalt, and tuffaceous sedimentary rock, there are two in welded ash-flow tuff. The ash-flow-hosted occurrences consist of narrow zones of radioactive rock exposed for distances of less than 100 m. The radioactive zones contain silicified rock along northwest-

Figure 17. Geologic map of the Lakeview uranium district (Castor and Berry,1981).

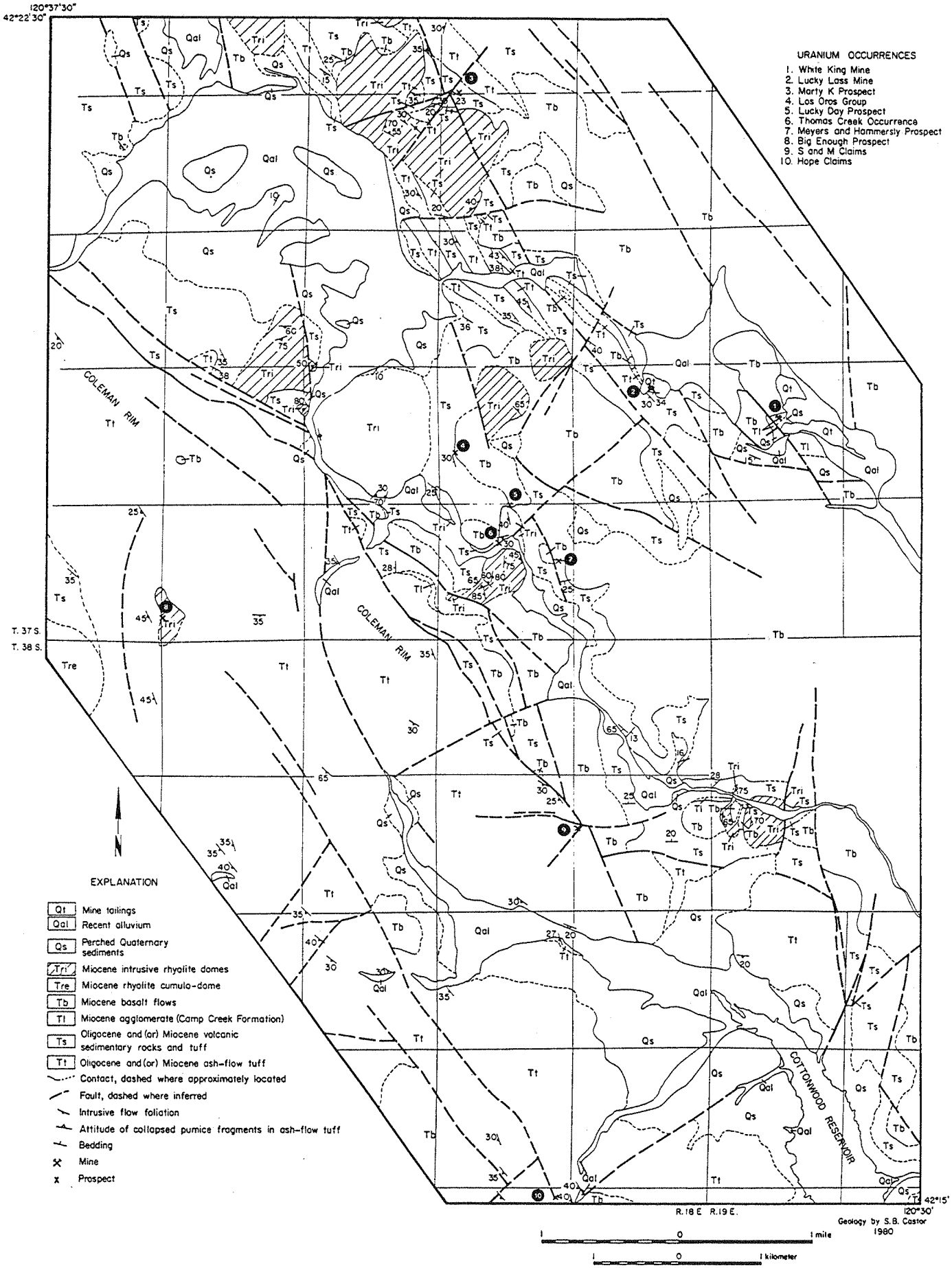

Figure 18. White King mine pit from the east. Photo taken May 23, 1995.

Figure 19. Lucky Lass mine pit from the east. Photo taken May 23, 1995.

striking shear zones (Castor and others, 1982a). These ash-flow tuff-hosted occurrences are not associated with exposed rhyolitic flows or intrusive rock.

Rock chemistry

Five samples were collected at the White King mine during this study: one sample of rhyolite with near background radioactivity from outcrop in the open pit, and four samples of radioactive rock from waste dumps northwest and east of the pit. The rhyolite contains 13 ppm U, while radioactive dump samples contain 0.01-0.28% U (Table 2). Samples with as much as 1.3% U_3O_8 were collected during earlier studies (Castor and others, 1982a). Elevated contents of As, Ba, Bi, Cs, Hg, Mo, Pb, Sb, and Tl are associated with uranium, and the sample that contained the most uranium (C-95-72) also had elevated Ag, Cu, and Zn (Table 2). Similar results were reported for samples collected during an earlier study, along with locally high F (Castor and Berry, 1981).

Samples from the Lucky Lass mine contain up to 0.07% U, along with slightly elevated As, Sb, Ag, and Tl (Table 2). Castor and Berry (1981) reported rock with as much as 1.7% U_3O_8 from the Lucky Lass dump, and high Ag, As, Cr, Cu, Mo, Pb, V, and Zn; however, the Mo and Pb analyses were by emission spectroscopy and are considered suspect, and the Cr, Cu, and V values are at near background levels for the basalt host rock. Uraniferous rock samples from the Lucky Lass mine have considerably lower trace metal contents than samples with similar uranium contents from the White King mine, particularly for As, Sb, Bi, and Pb (Table 2).

Uranium occurrences in ash-flow tuff in the Lakeview district contain as much as 0.03% U_3O_8 and have high As, Cu, Hg, Mo, and Sb contents (Castor and Berry,1981).

Mineral assemblages

Uranium in exposed ore at the White King mine is mainly in secondary minerals, including autunite, abernathyite, uranospinite, torbernite, novacekite, and heinrichite (Castor and others, 1982a). Uraninite and coffinite were reported in unoxidized ore from the White King mine (Walker, 1980). Uraninite was not found in samples of radioactive rock collected for this study, but uranium silicate that contains minor amounts of As, Pb, and Fe, along with variable amounts of P (Table 4) was found during SEM examination (sample C95-73). This mineral, which may be a P-bearing variety of coffinite, occurs as euhedral crystals and rounded grains up to 10 μ in diameter with galena, arsenopyrite, and pyrite in silica (Fig. 20). Sparse, tiny stibnite grains were also noted in this sample. In the most radioactive sample (C95-72), U was found to occur as spheroids and coalesced spheroids of U-Pb-As silicophosphate (Fig. 21) with minor As, Pb, and Ca (Table 3) associated with galena and cinnabar in silica. In thin section, the mineral is brown with low birefringence. It occurs along with minor cinnabar in silica surrounding galena, suggesting that it may have been deposited as a primary phase with the silica and cinnabar; however, the spheroids appear to be connected with tiny veinlets of the same material, which could indicate deposition after silica formation by secondary processes. Although a search of the literature revealed several silicophosphate minerals, including cheralite (Th-Ca-REE silicophosphate), none are known with this composition. Arsenic is also present in late-stage fracture-filling orpiment and realgar. Jordisite (MoS_2) and ilsemannite (hydrated Mo oxide) have also been reported (Castor and Berry, 1981).

Alteration minerals associated with mineralization at the White King mine consist mainly of silica, clay, and potash feldspar. Chalcedonic silica was reported to be present by Castor and Berry (1981), but samples collected for this study contain black, opaline silica that is composed of cristobalite on the basis of XRD analysis. Clay minerals identified by XRD are kaolinite and montmorillonite. An earthy yellow mineral that coats surfaces of dump samples has been identified as plumbojarosite, and limonite is also abundant locally.

Samples of uranium-rich altered basalt from the Lucky Lass mine dump were reported to contain autunite and possible uranophane (Castor and others, 1982a). Pyrite, limonite, and autunite occur in clay that replaces mafic minerals, and yellow uranophane(?) occurs with limonite in vesicles. Other uranium minerals reported are novacekite (Cohenour, 1960) and uraninite (Petersen and McIntyre, 1970). The

Figure 20. Backscattered SEM image of galena (large bright grain), U- P silicate (small bright to light gray grains), arsenopyrite (irregular gray grains associated with galena and U- P silicate), and pyrite (isolated gray grains) in quartz (black). Sample C95-73, White King mine.

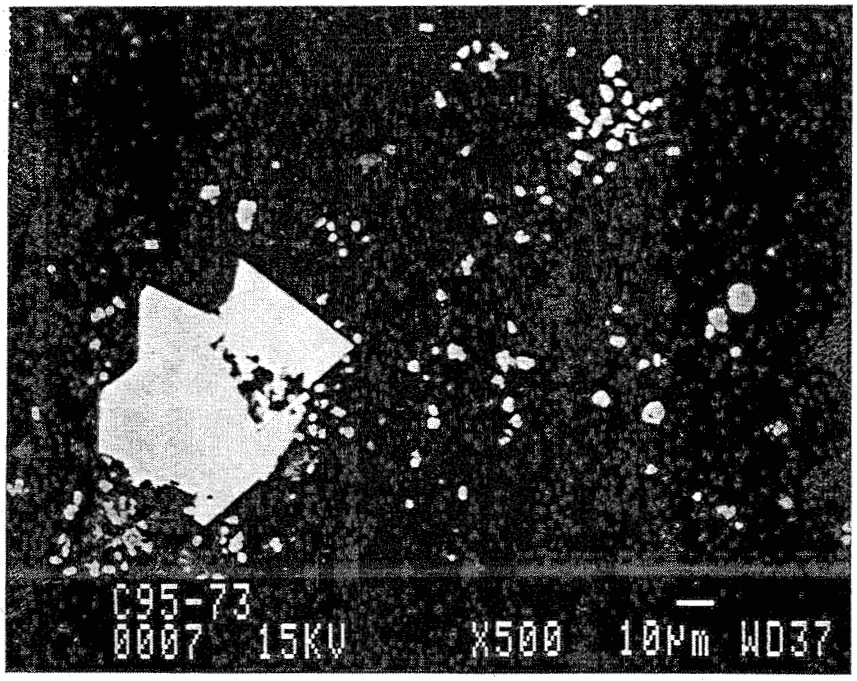

Figure 21. Backscattered SEM image of spheroidal U-P silicate (gray) with tiny cinnabar crystals (bright) in quartz (black), sample C95-72, White King mine.

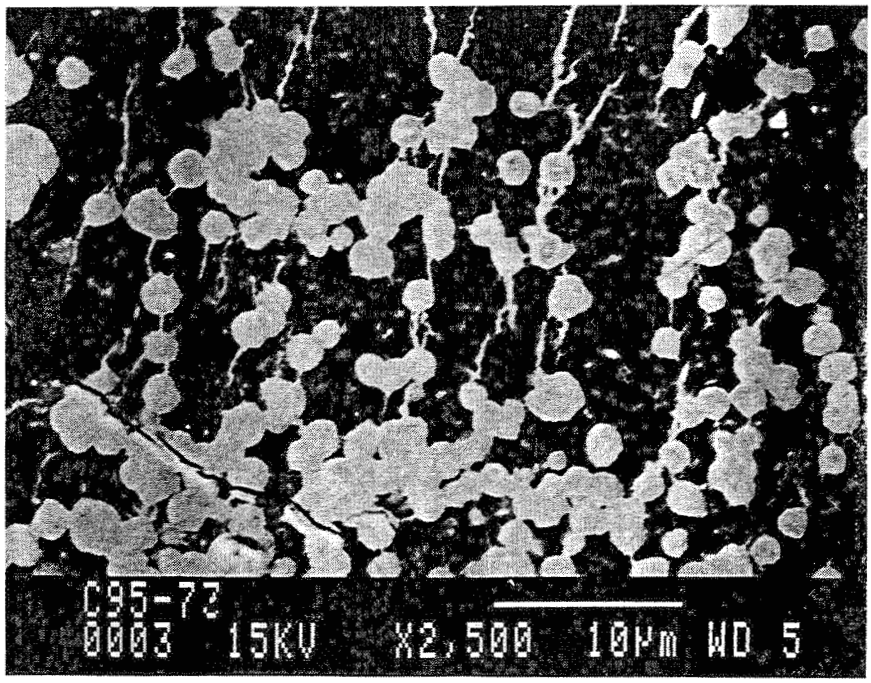

most radioactive sample collected during this study (C95-80) was found to contain saleeite (Mg-U phosphate) during SEM/EDX analysis.

Autunite was reported to occur at both uranium occurrences in ash-flow tuff (Castor and others, 1982a), and uranospinite was reported at one (Cohenour, 1960). Secondary potassium feldspar and limonite are associated with uranium at these occurrences (Castor and Berry, 1981).

Hydrologic setting

Open-pit mine workings at the White King and Lucky Lass mines are largely filled with water (Figs. 18,19). In addition, the water table is near or at the surface in meadow areas adjacent to the mines. When the mines were examined for this study in May 1995, water from both pits was draining into the surface waters of Augur Creek. On the basis of data collected in 1989 from wells drilled to provide information needed for environmental rehabilitation, water table depth ranged from a high of 30 m in hills adjacent to the mine sites to zero in the pits (Fremont National Forest, 1991). On the basis of this information, mineralized rock at the White King and Lucky Lass mines is assumed to be entirely below the water table except for uraniferous rock in the waste dumps.

In water from wells drilled in hills immediately south of the White King mine, which are mainly composed of basalt, pH is near neutral (6.3-8.1), alkalinity is much higher than acidity, bicarbonate appears to be the predominant anion (100-200 mg/L), and sulfate is low (<2 mg/L) (Fremont National Forest, 1991). This water has normal trace metal contents. By contrast, water from the lake in the White King pit and from wells adjacent to the waste dumps generally has low pH and high sulfate content (Fremont National Forest, 1991), presumably due to the break-down of sulfide. In addition, this water generally has relatively high U and As contents, and locally high Pb (Fremont National Forest, 1991).

STEENS MOUNTAIN, OREGON

Uranium occurs in breccia along faults cutting flow-banded low-silica rhyolite in the canyons of Pike Creek and Little Alvord Creek on the east slope of Steens Mountain about 80 km northwest of the McDermitt caldera (Fig. 1). Although some samples contain up to 0.5 % U_3O_8, amounts of radioactive rock at these occurrences are too small to be considered economic (Dayvault, 1983). There is no record of uranium production from the Steens Mountain occurrences.

All of the Steens Mountain uranium occurrences are in a wilderness study area, and roads to the occurrences have been closed. The Pike Creek occurrence (Fig. 22) is accessible by walking approximately 1.5 km up the old access road. An occurrence in Little Alvord Creek is more remote and was not visited during this study.

Geology

In Pike Creek Canyon, the main uranium occurrence was developed by an adit along a 30-cm-wide silicified and hematized breccia zone along a planar, N10° W, 72°E fault that cuts flow-banded aphyric rhyolite. The breccia, which has radioactivity as high as 90 x background, is overlain by a 3-m-thick zone of stockwork silica-iron oxide veins cutting bleached rhyolite. The footwall of the fault is a 2-m-thick zone of friable, purple limonitized rock that Dayvault (1983) identified as diabase, but this rock is flow-banded and resembles nearby rhyolite and is considered here to be altered rhyolite.

About 100 m east of the main Pike Creek uranium occurrence is another occurrence of radioactive silicified breccia along a steeply-dipping N35° W fault. Here the breccia is thinner and has maximum radioactivity at about 10 x background (sample site C95-88).

The Little Alvord Creek uranium occurrence was described by Dayvault (1983) as mineralization along a N35° E, 85° fault that cuts glassy to devitrified spherulitic volcanic rock. The host rock is argillized and iron

stained adjacent to the fault, and a mafic dike was reported to be about 3 m west of, and parallel to, the fault.

Rock chemistry

According to Dayvault (1983), samples from the Pike Creek uranium occurrence contain as much as 0.53% U_3O_8, whereas highly radioactive rock from the Little Alvord Creek contains about 0.03% U_3O_8. Maximum uranium content in samples collected during this study from the Pike Creek occurrence is 0.22%. Uraniferous samples have slightly elevated Mo, W, As, Sb, and Hg, but enrichment of these elements is not as pronounced in uraniferous rocks as in other areas (Table 2, Fig. 5). Dayvault (1983) reported moderately high As, Ba, Hg, and Mo in uraniferous samples from the Steens Mountain area.

Mineral assemblages

According to Dayvault (1983), uranium minerals identified in Steens Mountain occurrences are secondary phosphates and uranophane. The phosphate minerals include autunite and a sabugalite (hydrated Al-U phosphate) - meta-ankoleite (hydrated K-U phosphate) mixture (Dayvault, 1983). SEM/EDX examination of the most uraniferous sample in our collection (C95-85) revealed the presence of U-Ti oxide in tiny disseminated grains (up to 2 μ in diameter) that may be of primary origin, and larger books of autunite (?) along fractures (Fig. 23). An SEM/EDX spectrum of the former mineral contains minor Al and Si peaks, but this may be due to contamination of the spectrum for these small grains by surrounding minerals, which include quartz and feldspar. An SEM/EDX spectrum of the autunite (?) includes minor Si and Mg peaks, possibly due to minor substitution in the mineral (Frondel, 1958, notes minor Mg substitution for Ca in autunite). No sulfide minerals were found in the radioactive breccia from the Pike Creek occurrence, but hematite and limonite are abundant.

Although Dayvault (1983) noted carbonate cement in uraniferous breccia at the Pike Creek occurrence, we found none. In addition to finely granular quartz, which occurs in breccia fragments, the breccia also contains potassium feldspar and cristobalite on the basis of XRD analysis. Thin section examination indicates that the matrix is mainly composed of cristobalite and iron oxide. It is not clear if the quartz and potassium feldspar were deposited during formation of the breccia, or if they were formed earlier, during devitrification of the host rhyolite.

Hydrologic setting

No hydrologic data were collected for the Steens Mountain area. During examination for this study, Pike Creek was flowing and it is shown on the USGS Alvord Hot Springs, Oregon 7.5-minute quadrangle as a perennial stream. The Pike Creek uranium occurrence is about 20 m above the stream (Fig. 22). On the basis of this information, the water table is probably shallow and the unsaturated zone at the uranium occurrence thin.

BOTTLE CREEK, NEVADA

Mines in the Bottle Creek district produced about 4,600 flasks of mercury from deposits in pre-Tertiary rock and Tertiary volcanic rock (Willden, 1964). Uranium mineralization occurs in volcanic rock on Buff Peak about 3 km west of the Bottle Creek district and about 50 km southwest of the McDermitt caldera (Fig. 1). Recent precious-metal exploration centered on veins in Tertiary volcanic and pre-Tertiary rock about 2 km southwest of the uranium occurrences.

Geology

The top of Buff Peak is underlain by flow-banded, devitrified, pink rhyolite with small sparse feldspar and black quartz phenocrysts. This rock is underlain by gray, massive devitrified rhyolite and greenish gray rhyolite vitrophyre with similar, but slightly more abundant, phenocrysts. According to Castor and others (1982b), these are peralkaline high-silica rhyolites. They were deposited on Permian intermediate to mafic volcanic rocks and Permian or Triassic sedimentary rocks.

Figure 22. Pike Creek Canyon U occurrence, Steens Mountain. Small adit (arrow) about 20 m above canyon floor developed uraniferous rock along a fault zone in relatively resistant rhyolite.

Figure 23. Backscattered SEM image of autunite in fracture at Pike Creek Canyon (sample C95-85).

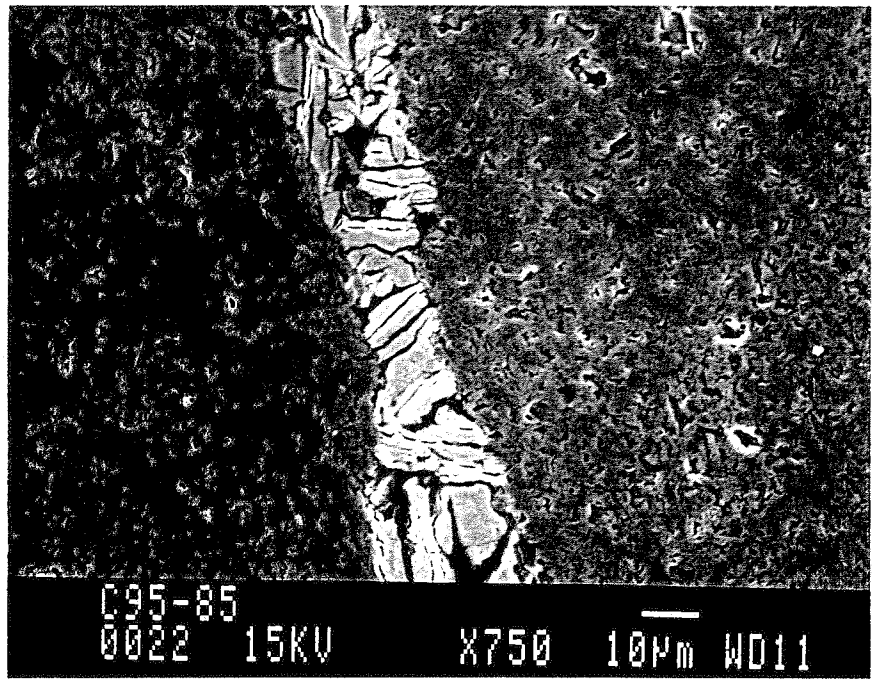

Radioactive rock on Buff Peak is exposed over an area of about 5 x 15 m, and was developed by a few bulldozer trenches cut in altered Tertiary rhyolite just above the contact with pre-Tertiary rocks (Castor and others, 1982b). The most radioactive rock is dark gray, silicified, brecciated, flow-banded rhyolite that occurs as a small seam in argillized volcanic rock. The highest radioactivity measured was about 9 x background.

Rock chemistry

The peralkaline rhyolite on Buff Peak contains as much as 22 ppm U_3O_8 and 49 ppm Th (Castor and others, 1982b), the highest U and Th contents of any unaltered rhyolite in the area of Figure 1. By contrast, unaltered rhyolite and ash-flow samples from Virgin Valley and the McDermitt caldera contain up to 14 ppm U_3O_8 and 30 ppm Th (Castor and others, 1982b; Table 2, this report). The high U content in Buff Peak rhyolite has been verified by samples of rhyolite collected for this study that contain as much as 20 ppm U and 42.5 ppm Th (see sample C95-147, Table 2).

Radioactive rock at the Buff Peak occurrence contains up to 0.17 % U_3O_8, but averages only about 0.01 % U_3O_8 (Castor and others, 1982b). The most radioactive sample collected from Buff Peak during this study contains about 0.11% U, very high Mo (at 744 ppm), and elevated As, Bi, Pb, Sb, Tl, and W (sample C95-150, Table 2).

Mineral assemblages

Only secondary uranium minerals have been positively identified in radioactive rock from the Buff Peak. Castor and others (1982b) report secondary uranyl phosphate and silicate minerals, along with possible brannerite. On the basis of SEM/EDX work, sample C95-150 of this study contains U and Zr(?) silicate with minor Fe and Ca, along with a sparse U-Ti oxide mineral (brannerite?). In addition, this sample contains pyrite and molybdenite. Oxidized portions of the sample contain abundant limonite and trace amounts of sphalerite.

Silica in the radioactive breccia at Buff Peak is chalcedonic to finely granular. Argillized rhyolite adjacent to the breccia contains both montmorillonite and kaolinite.

Hydrologic setting

Only one analysis from one site is available for the Bottle Creek area in the STORET database, and this sample was collected September 1990 from Bottle Creek about 7 km southeast of the uranium occurrence that was sampled during this study. The pH of the sample is 8.14, and the temperature of collection was 14.5°C. No HCO_3 or alkalinity data are available for the site located near the Bottle Creek area. Hence, water type and total dissolved solids are unknown in the area. However, given the values of Ca = 43, Mg = 15, Na = 23, Cl = 15 and SO_4 = 28 mg/L, the water at this site is likely to be a very dilute Ca-Na-HCO_3-SO_4 water. Considerable trace element chemistry for this area was found in the NURE database (Tables 7-9); the data show that spring waters from the Bottle Creek area have lower U contents than in the Virgin Valley area, but higher contents than in the McDermitt area.

The NURE database contains 114 entries for water analyses, yet none of the analyses contain sufficient information on major cations and anions from which to determine water types (i.e., no HCO_3 or SO_4 analyses). In additional, although chemical data from numerous wells are included in the data for Bottle Creek, none of the records contained water level data. All well, spring, and creek data have specific conductance reported, and this ranges from 65 to 1900 mmhos/cm (or in terms of TDS, 42 to 1,216 mg/L, where TDS = 0.64 x SC). The NURE data indicate that pH of the various waters ranges between 6.4 and 10.1, and temperatures range from 7 to 90°C.

PAINTED HILLS AREA, NEVADA

Uranium mines in the Painted Hills, about 40 km north of Reno (Fig. 1), had total production of about 4,000 pounds of U_3O_8 from ore containing 0.23-0.53% U_3O_8 during the 1950s (Hurley and others, 1982).

Mines and prospects in this area were reported to have exposed uranium mineralization containing as much as 15% U_3O_8 (Garside, 1973). The Homestake Mining Company was reported to have explored portions of the Painted Hills in the 1950s, but was said to have failed to locate large tonnages of U ore (Bonham and Papke, 1969).

Geology

Uranium mineralization in the Painted Hills is in a sequence of Miocene and Oligocene felsic volcanic rocks dominated by ash-flow tuff that was originally mapped as the Hartford Hill Rhyolite (Bonham, 1969), a unit named by Gianella (1936) in the Virginia City area. However, this formation name has since been abandoned and parts of the sequence have been assigned to several formal and informal units (Wallace, 1975; Bingler, 1978; Deino, 1985). The uranium occurs in the 23-Ma tuff of Chimney Spring (Garside and others, 1981) and in mafic dikes that cut the tuff (Fig. 24). In the vicinity of the Painted Hills uranium occurrences, the tuff of Chimney Spring is a buff or light gray to pink, spheroidally weathering, welded, crystal-rich rhyolite ash-flow tuff. It generally contains about 25% phenocrysts, mainly of sanidine and smoky quartz with minor plagioclase and biotite, but locally contains as much as 70% phenocrysts. This unit is underlain by a thin sequence of probable tuffaceous debris-flow deposits that contain basalt fragments and petrified wood. The debris deposits are underlain by the Nine Hill Tuff, 23-25 Ma densely welded vitric rhyolite ash-flow tuff with black flattened pumice fragments and relatively sparse phenocrysts. The Nine Hill Tuff is underlain by rhyodacitic to andesitic ash-flow units (Cupp and others, 1977a) that may be correlative with the tuff of Coyote Spring, which is about 28 Ma (Garside and others, 1981). The tuff of Chimney Spring is overlain by rhyolite to andesite ash-flow tuff and additional debris deposits with mafic clasts (Cupp and others, 1977a).

The middle Tertiary tuff sequence described above is cut by mafic dikes that are composed of pyroxene andesite with fine-grained intergranular texture. A single mafic dike that is 2- to 10-m wide, strikes north to northeast, and dips 60° NW to vertical, is the site of much of the uranium mineralization at the Delongchamps mine, Red Bluff adit, and the Garrett prospect (Fig. 24). At the Delongchamps mine, the dike dips about 70° NW. Radioactive rock mainly occurs in the Tuff of Chimney Spring along the footwall contact of this dike in association with limonite, clay, and local opalization. According to Brooks (1956), high-grade uranium ore in the Delongchamps mine occurred in lenticular masses up to 4 m long and 1.5 m wide along this contact.

In general, the mafic dikes themselves are not mineralized, however Cupp and others (1977a) reported the presence of altered dike rock containing as much as 183 ppm U_3O_8. A sample of mafic dike collected for this study contains slightly elevated U at 28 ppm (sample C95-128, Table 2).

In addition to occurrences along the mafic dikes, uranium mineralization also occurs along NE- and NW-striking faults in the Painted Hills. At the Maue-McCray mine (Fig. 24), uranium mineralization occurs in and adjacent to a N10° -20° E fault zone for about 60 m in a zone about 3 m wide (Garside, 1973). This occurrence was not examined during this study.

Geologic mapping by Cupp and others (1977a) shows several WNW-striking faults in the area of U occurrences in the Painted Hills (Fig. 24). On the basis of displacement of the shallowly southeastward dipping Miocene volcanic units, these faults have south side-down vertical displacement or right-lateral displacement (Fig. 24). They are shown displacing the mafic dikes slightly, but this relationship is unclear.

The timing of dike intrusion, faulting, and tilting relative to uranium mineralization at the Painted Hills is unknown and bears on the possible origin of mineralization. The dike may be a feeder related to the Pyramid sequence of mafic lavas, which crop out to the north. These lavas, and therefore the dike, are about 15 Ma. The dike is perpendicular to bedding in the tilted tuffaceous rocks, which suggests that the dike was emplaced before tilting. Regional stratigraphic-structural studies suggest that faulting and tilting may have occurred between 25 and 20 Ma, and between 15 and 7 Ma (L. J. Garside, personal communication, 1996). If the dike is indeed 15 Ma, then tilting of the tuffaceous rocks may have occurred during the younger episode.

Figure 24. Geologic map of the Painted Hills uranium district modified from mapping in Cupp and others (1977).

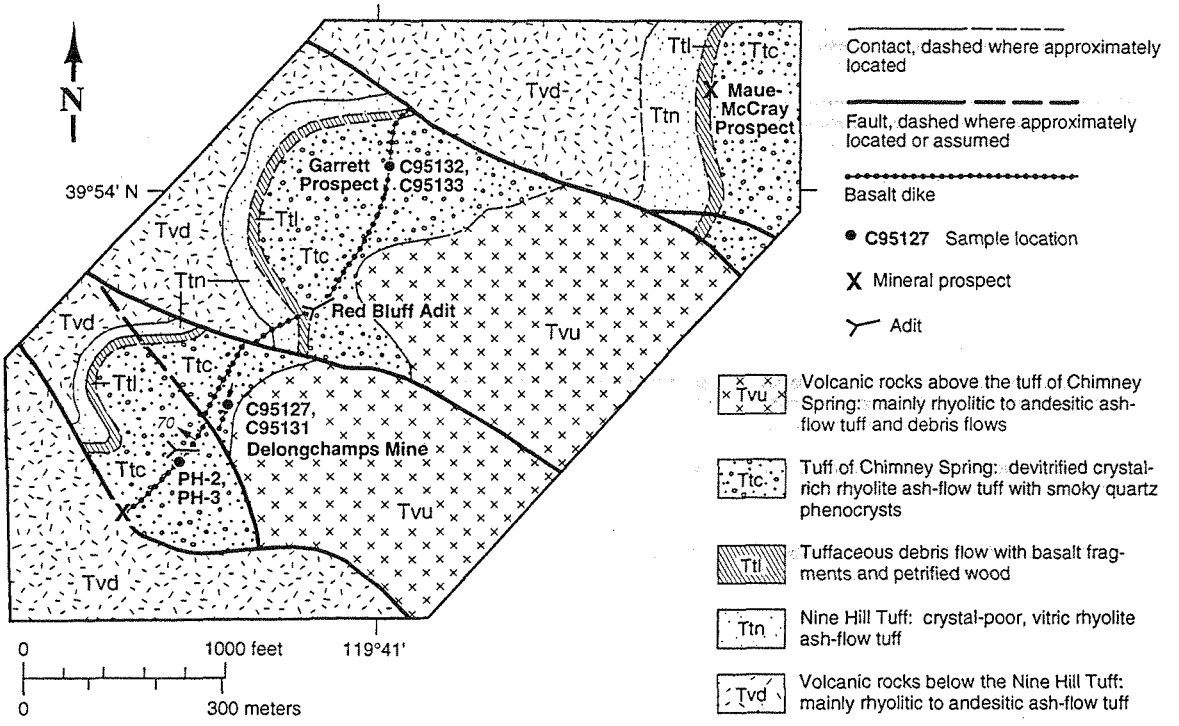

As pointed out by Wallace (1975), high altitude photographs show a circular feature about 40 km in diameter that lies west of the Painted Hills. Cupp and others (1977a) proposed that this feature was a caldera produced during eruption of rhyolite ash-flow tuff sheets that include the Nine Hill Tuff and the Tuff of Chimney Spring. They also speculated that late stage hydrothermal activity related to this caldera produced mineralization such as that in the Pyramid mining district, which includes the Painted Hills uranium occurrences; however, they do not propose a hydrothermal origin for the uranium.

Rock chemistry

Brooks (1956) reported U_3O_8 concentrations as high as 15% in hematite concentrations at the Delongchamps mine, and Hurley and others (1982) reported U concentrations as high as 1.9% from this property. Samples taken for this study include argillized rhyolite from a pit in the Delongchamps mine area that contains 0.42% U (sample PH-3, Table2), and similar rock from the Garrett prospect with 1.28% and 0.83% U (samples C-95-132 and C-95-133, Table 2). Samples of the tuff of Chimney Spring taken outside mineralized areas contain 6-9 ppm U and 17.5-30.1 ppm Th, suggesting little or no U loss. Uranium-rich samples from the Painted Hills contain slightly elevated As, Sb, Pb, Tl, and W contents (Table 2, Fig. 5). In addition, these samples also have high Fe and Ca compared with uraniferous samples from other areas sampled during this study.

Mineral assemblages

Brooks (1956) identified autunite and sabugalite (hydrated aluminum uranyl phosphate) in rock from the Delongchamps mine area, and also tentatively identified phosphuranylite and cleveite (a variety of uraninite). On the basis of XRD and SEM/EDX analyses of sample C95-132 from the Garrett prospect, meta-autunite occurs abundantly as distinctive scaly aggregates that fill fractures and cavities (Fig. 25). In addition, a yellow uranyl silicate mineral, possibly weeksite, is present. SEM/EDX analysis indicates that this phase has relatively low potash content, at about 3 wt% (assuming anhydrous stoichiometry) for weeksite which should contain about 10 wt% potash (calculated with anhydrous stoichiometry). However, EDX peak overlap between U and K may be responsible for this discrepancy.

Alteration products associated with uranium mineralization in the Painted Hills consist mainly of clay minerals (both kaolinite and montmorillonite have been identified), limonite, and silica. Most of the silica is amorphous, but some chalcedonic quartz is also present. Brooks (1956) reported both opal and chalcedony in the Delongchamps mine ore, and states that the opal is fluorescent and contains a yellowish microcrystalline substance that he speculated to be a uranium compound.

Alteration of the ash flow tuff in the footwall of a mafic dike is well displayed in a small prospect pit southwest of the Delongchamps adit (sample sites C95-126-130, Fig. 24). Tuff in a 50-cm-wide zone adjacent to the dike contact is limonitic and resistant due to partial opaline silicification (Fig. 26) and is moderately radioactive, containing about 0.03% U. On the basis of XRD analysis and thin section examination, this rock contains abundant cristobalite, both as pervasive replacement and as crustiform open-space filling. It also contains minor amounts of chalcedonic silica that was deposited in cavities following cristobalite deposition. Tiny lenses of Ba-Mn oxide (possibly hollandite) occur between the crustiform cristobalite and chalcedony. No sulfide or uranium phases were identified. A 1-m-wide zone of non-silicified but somewhat resistant tuff containing minor montmorillonite occurs in the footwall of the silicified zone; this rock contains slightly elevated U at 19 ppm (C95-127, Table 2). Friable, montmorillonite-rich tuff at least 3 m thick that contains U at background levels (C95-130, Table 2) is present further into the footwall.

Hydrologic setting

Nine major element chemical records were retrieved from the Painted Hills area from the STORET database, of which eight were duplicate analyses from the same location collected on different dates. None of the nine analyses contained sufficient information from which to determine the water type at this site. No trace element data were reported in the STORET database. One of the analyses is from Pyramid Lake, and the other is from Hardscrabble Creek. Field data such as specific conductance and pH were not recorded for these sites.

DOGSKIN MOUNTAIN, NEVADA

Seven uranium occurrences have been described on Dogskin Mountain (Cupp and others, 1977a; Garside, 1973) about 50 km north of Reno (Fig. 1). Most are in Tertiary rhyolite ash-flow tuff, and one of these, the Tick Canyon mine, may have produced a small amount of uranium ore (Garside, 1973).

Figure 25. Photomicrograph of autunite (bright) in fracture in limonitized tuff, Garrett prospect, Painted Hills (sample C95-132). Fracture is about 100 μ wide.

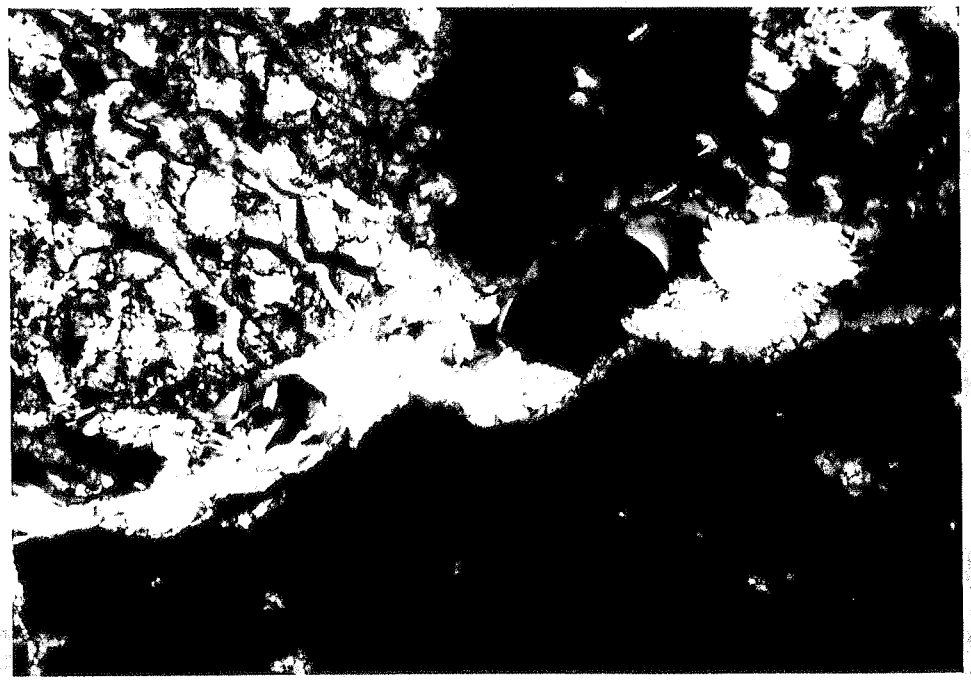

Figure 26. Radioactive rock along the footwall of a mafic dike in a prospect (sample sites C95-126-130), Painted Hills district. Dark resistant rock to left of hammer is limonitic, silicified tuff that contains about 0.03% U. Mafic dike is to the left of this. Hammer rests on slightly argillized tuff.

Geology

Of the seven uranium occurrences on Dogskin Mountain, five are in faults and fractures in Tertiary rhyolite ash-flow tuff that was originally assigned to the Hartford Hill Rhyolite and two are in mixtures of argillized tuff, granitic boulders, and carbonaceous material that lie between Tertiary rhyolite and underlying Mesozoic granitic rocks. Four of the occurrences in Tertiary rhyolite are in a narrow 3-km-long NNW-trending zone on the west flank of Dogskin Mountain; three of these were examined during this study and two, the Tick Canyon mine and the Sunnyside occurrence, were sampled.

The Tick Canyon mine consists of two inclined adits, a short vertical shaft, and several bulldozer scrapes and small prospect pits. According to Cupp and others (1977a), any uranium ore mined at this site came from a 2-m-wide, NW-striking fault in ash-flow tuff that they correlated with a unit that was subsequently named the tuff of Chimney Spring (Deino, 1985). However, Hutton (1978) mapped the host unit as the tuff of Dogskin Mountain, which is considered equivalent to the 28-Ma tuff of Coyote Spring (Garside and Bonham, 1995).

Cupp and others (1977a) reported that uranium minerals were confined to fault gouge at the Tick Canyon mine, and although carbonaceous debris is present, it is not mineralized. However, according to Hurley and others (1982), the host rock is water-laid ash-fall tuff with fossil wood, and uranium also occurs in sandstone and conglomerate containing uraniferous carbonized wood that is stratigraphically within the tuff of Dogskin Mountain.

On the basis of examinations during this study, the most significant uranium mineralization at the Tick Canyon mine is exposed at the adit portals along a fault that strikes about N50° W and dips 40° SW in altered welded ash-flow tuff. The most radioactive rock (represented by sample C95-139 from the northern adit), about 60 x background, consists of bleached, hematitic rock from the shear zone. Altered ash-flow tuff extends more than 2 m into the footwall of the fault and contains hematite-filled fractures and sheeted, gray to nearly black silicified veins up to 1 cm thick with orientations of N35-55W, 70° SW (samples C95-140, 141). A small prospect pit, which is about 50 m northwest of the northern Tick Canyon adit, exposes a zone of similar sheeted silica veins, oriented N40° W, 50° SW, with anomalously high radioactivity (sample site C95-142).

The ash-flow tuff unit that contains the uranium mineralization in Tick Canyon is gray to pink, slightly to moderately welded, and contains about 20% phenocrysts of sanidine, plagioclase, smoky quartz, and minor biotite, along some small lithic and pumice fragments. It is underlain by conglomerate and overlain by light purplish gray, strongly welded ash-flow tuff with about 10% phenocrysts of sanidine, smoky quartz, biotite, and altered plagioclase.

The Sunnyside occurrence, which was developed by a few bulldozed trenches and pits, is in argillized and hematized ash-flow tuff mapped by Hutton (1978) as the tuff of Dogksin Mountain. The most radioactive rock found during this study (30 x background at sample site C95-144) consists of reddish-brown clayey gouge about 3 cm thick along a nearly horizontal fault. The fault cuts altered ash-flow tuff with Fe and Mn oxide along fractures. Samples C95-144 through C95-146 were all collected from the same small pit, which was partially filled with water when visited in mid July 1995. The samples were moist when collected and found to contain green secondary uranium minerals.

Rock chemistry

On the basis of data presented by Hutton (1978), glassy Tertiary ash-flow tuff from Dogskin Mountain contain 4.5-12.6 ppm U_3O_8, whereas devitrified tuff contains as much as 172 ppm U_3O_8 and is clearly enriched. A sample of devitrified ash-flow tuff that was collected for this study from the Tick Canyon area (C95-143) contains 9 ppm U and 21 ppm Th. Whole-rock chemistry reported by Hutton (1978) indicates that the tuff of Dogskin Mountain is a metaluminous low-silica rhyolite, and the Nine Hill Tuff and tuff of Chimney Spring are metaluminous high-silica rhyolite.

Mineralized rock from the Tick Canyon mine contains as much as 0.26% U_3O_8 (Hurley and others, 1982). Samples from anomalously radioactive outcrops in Tick Canyon that were collected for this study contain 175-719 ppm U. They contain a relatively restricted list of elevated trace elements, with only slightly elevated Sb and Pb (Table 2). However, radioactive rock from the Sunnyside occurrence has a different chemical pattern - it contains as much as 0.26% U, along with elevated Ba, Mo, W, As, Zn, Sn, Hg, Tl, and Au (Table 2).

Mineral assemblages

On the basis of XRD and SEM/EDX analyses, uranium-rich rock from both the Tick Canyon mine and the Sunnyside occurrence contains autunite. No other uranium minerals were identified.

XRD analyses of highly radioactive rock from the shear zone at the Tick Canyon mine (sample C95-139) shows that it has been thoroughly altered to montmorillonite. Rock containing sheeted silica veins (C95-142) is locally silicified and biotite phenocrysts are oxidized and partially argillized, but sanidine and plagioclase phenocrysts are unaltered. The silica veins are predominantly composed of chalcedonic quartz with late cavity fillings and crosscutting veinlets of finely granular quartz. Samples from the Sunnyside occurrence contain montmorillonite as the dominant alteration product and no apparent silicification. No sulfide minerals or limonite following sulfide were noted at either occurrence.

Hydrologic setting

No data are available from within the Dogskin Mountain area, but four chemical analyses were selected from the STORET database to be representative of the area given the relatively close proximity of the data sites to the study area (Willow Spring, Fish Springs and Mullen Creek, all near Flanigan, NV). The above mentioned three sites have PO_4, NO_3, and total alkalinity data; but have no HCO_3 values, scarce data for major cations, and no analyses of trace metals. Based on the available analyses, waters in this area appear to be Ca-Na-HCO_3 waters. TDS was calculated using the noted Na, K, Ca, Mg, Cl, SO_4 and alkalinity, and all waters appear to have very low TDS based on the available information (86 to 121 mg/L). Field data such as specific conductance and pH were not recorded for these sites.

PETERSEN MOUNTAIN, NEVADA AND CALIFORNIA

In the Petersen Mountain district, uranium occurs in Tertiary rocks at eight sites (Cupp and others, 1977a; Hurley and others, 1982) in a 10-km-long north-trending zone along the west flank of the north part of Petersen Mountain about 40 km northwest of Reno (Fig. 1). Most of these occurrences are located within 1 km of the California-Nevada border; four are in California and three in Nevada. Total production from the Petersen Mountain district was 2,800 kg of U_3O_8 from approximately 1,000 metric tons of ore, all from two deposits (Cupp and others, 1977a). Only one site, the Buckhorn mine, was examined during this study.

Geology

Uranium mineralization in the Petersen Mountain district occurs in two geologic settings. At six of the occurrences, uranium mineralization is in two units of Tertiary sedimentary rocks. The older unit, which is along the depositional contact between Mesozoic granitic rocks (mainly the Petersen Mountain Granodiorite) and Tertiary volcanic rocks, may be correlative with the Pah Rah Formation (Bonham, 1969). The other overlies the Tertiary ash-flow tuff sequence and was assigned to the Pliocene Truckee Formation (Cupp and others, 1977a). In these sedimentary occurrences, the uranium is mainly in carbonaceous beds of arkosic and tuffaceous sandstone and claystone. The sedimentary rock-hosted occurrences include the Cornelia C deposit, which accounted for most of the U production in the Petersen Mountain district Hurley and others (1982).

At three of the occurrences in the Petersen Mountain district, uranium mineralization is in Tertiary ash-flow tuff (one minor occurrence, the Herbal prospect, has both sedimentary- and volcanic-hosted mineralization). The most significant of these is at the Buckhorn mine, from which about 300 tons of ore

containing 0.24% U_3O_8 were produced. Development at the Buckhorn mine site consists of two adits, two shallow shafts, and some bulldozer trenches.

According to Cupp and others (1977a), uranium mineralization at the Buckhorn Mine is in a thick section of two basal "cooling" units of the Hartford Hill Rhyolite that were deposited in an erosional reentrant in the Petersen Mountain granodiorite. These units probably correspond to the Zamboni Spring and Constantia Station Members of the Seven Lakes Mountain Tuff of Deino (1978) who mapped an area to the north of the Buckhorn mine. Uranium mineralization was found to occur along a zone of 2-12-cm-wide NE-trending fractures that are coated with iron oxide and commonly filled with gouge and breccia (Cupp and others, 1977a). Hurley and others (1982) also report uranium mineralization along fractures and breccia zones, but describe them as being of various orientations and filled with silicified, iron oxide-stained clays. Hetland (1955) described secondary uranium mineral occurrences along iron-stained silicified veinlets.

On the basis of examination of the Buckhorn mine site during this study, rock with radioactivity as high as 45 x background was found in a zone of distinctive yellow altered non-welded ash-flow tuff that may be seen from U.S. Highway 395 about 4 km to the west. Iron oxide-coated fractures were observed within this zone, but were not found to be highly radioactive. The most radioactive rock (sample site C95-135) was reddish brown to light buff, iron oxide-stained tuff from mine waste near the two shafts. An adit in this area was examined, but found to be terminated by caved rock about 10 m from the portal, and not to contain highly radioactive rock. At another caved adit, about 120 m north of the shafts, iron oxide-stained tuff with autunite on the dump had radioactivity as high as 30 x background. Silicified rock was not noted during this examination.

Rock chemistry

On the basis of mineralogy, host rocks at the Buckhorn mine are considered to be metaluminous low-silica rhyolite. Two samples of unaltered vitric ash-flow tuff collected for this study (C95-137, 138) contain 8-9 ppm U and 20-22 ppm Th, which does not indicate U depletion.

The highest U content reported by Cupp and others (1977a) in rock from the Buckhorn mine was 480 ppm U_3O_8 (407 ppm U), but Hurley and others (1982) report amounts as high as 0.36% U_3O_8 (about 0.30% U). During this study, samples containing 0.23% and 0.56% U were collected from the dumps of the southern and northern adits, respectively. Samples with high uranium contents were found to contain weakly elevated As, Ag, and Tl, and moderately elevated Sb and Hg. Sample C95-138, which has the highest U content, has high W, at 116 ppm; with the exception of samples from the Aurora deposit in the McDermitt caldera, this is the highest W in any sample collected during this study.

Mineral assemblages

According to Hetland (1955), silicified veinlets in the Buckhorn mine contain gummite, autunite, and uranophane. During this study, autunite was the only uranium mineral identified.

In addition to limonite and hematite, minerals that appear to be associated with uranium-rich rock at the Buckhorn mine are montmorillonite and possible chlorite. Although silicified veinlets were reported by Hetland, none were noted during this study.

Hydrologic setting

No hydrogeologic data were found for this area.

ORIGIN OF VOLCANIC ROCK-HOSTED URANIUM DEPOSITS, NORTHWESTERN NEVADA AND SOUTHEASTERN OREGON

Volcanic rock-hosted uranium occurrences in northwestern Nevada and southeastern Oregon appear to have been formed by more than one process. Some deposits are clearly epithermal on the basis of

geologic setting, mineralogy, and trace element geochemistry, but others may have been deposited from low-temperature groundwater.

On the basis of geochemical and geological information, it is clear that some of the most important deposits, including that exploited by the White King mine in the Lakeview district, the Moonlight-Horse Creek deposit in the Kings River district, and deposits in the Aurora-Bretz area, were formed by epithermal fluids. These deposits consist of, or are associated with, silicified breccia. In some cases, this silicified breccia contains chalcedonic to finely granular quartz as at Horse Creek and the Bretz mine, or fine granular to drusy comb quartz, as at the Moonlight mine. Silicification at the White King mine seems to be predominantly of opaline cristobalite. Silicified breccia at the Opalite mine, which appears to contain only slightly elevated U, is mainly composed of finely granular quartz. Although it is not known to form an extensive U deposit, chalcedonic U-rich rock from the Buff Peak occurrence is also considered to be of epithermal origin. Chalcedonic to finely granular epithermal quartz indicate epithermal activity, forming at temperatures in excess of 180° C (Fournier, 1985).

Epithermal fluids that formed uranium mineralization at the White King mine were clearly related to rhyolitic intrusion. The high U content of this deposit, along with high contents of other elements, may be due to the lack of effusive activity - the intrusion does not appear to have reached the surface and hydrothermal activity may have been confined under a basalt cap. Other silicified breccia uranium concentrations, such as in the Kings River district, at Steens Mountain, and at Buff Peak, are associated with rhyolite flow rock that was probably vented above shallow intrusive magma chambers.

In addition to the presence of relatively high-temperature silica, the deposits and occurrences mentioned above have associated sulfide minerals that include pyrite ± galena ± cinnabar ± arsenopyrite. The pyrite is generally fine-grained and is framboidal in some cases, as in samples from the Kings River district (Fig. 8) and the Aurora deposit (Roper and Wallace, 1981). Framboidal pyrite is a sulfide textural type that was originally considered to indicate low-temperature, organic origin because of its common occurrence as a diagenetic mineral in carbonaceous sedimentary rock (e.g., Love, 1958), but has since been shown, both experimentally and in geologic occurrence, to form hydrothermally as well (e.g., Sunagawa and others, 1971; Larter and others, 1981).

Because of the boom in exploration for gold deposits in the western U.S., and particularly in Nevada, considerable new information on the trace element chemistry of epithermal deposits is available. Geochemical patterns at the hydrothermal U occurrences examined during this study include high contents of elements that are generally associated with epithermal gold mineralization, such as Ag, As, Bi, Hg, Mo, Sb, Tl, and W.

Uranium-rich rock from both the White King mine and the Kings River district have Ag contents in excess of 10 ppm; in other areas such rock has less than 1 ppm Ag (Fig. 5). Extreme As enrichment is shown by samples from the Kings River district, with up to 1% As, and the White King mine, with more than 1000 ppm As (Fig. 5). Samples from the Bretz mine also have high As (Table 2). Bi, which is typically enriched in hydrothermal deposits that are considered to have a magmatic component, is particularly high (as much as 10 ppm) in samples from the Kings River district and Buff Peak. Hg is typically produced from shallow epithermal deposits associated with volcanic activity. Because the Bretz-Opalite mining district was an important source of Hg, it is not surprising that some of the U-rich samples collected there have high Hg. However, the highest Hg content measured in any sample during this study was in a sample from the White King mine, and many samples from the Kings River district have moderately high Hg at 1 ppm or more (Fig. 5). Tl, also typically high in rocks from epithermal Au deposits, is present in amounts in excess of 10 ppm in samples from White King mine, Kings River area, and Buff Peak. Au is present in slightly elevated amounts in U-rich samples from the White King mine and Opalite mine; it is present in much higher amounts in samples from the Moonlight mine-Horse Creek area. Vein material collected from the Buff Peak area contains high Au but no U and may have formed by hydrothermal activity unrelated to that which produced mineralization at the U occurrence.

Alteration mineral assemblages are also important indicators of hydrothermal activity. The presence of secondary potassium feldspar in rocks in and adjacent to uranium mineralization in the McDermitt caldera and Lakeview district support an epithermal origin, particularly the adularia that occurs in vein samples from, and as replacements of feldspars in altered rock adjacent to, the Moonlight mine. Other alteration minerals, such as clay minerals, that are associated with the epithermal uranium deposits studied may represent hydrothermal alteration. However, the clay minerals identified, kaolinite and montmorillonite, may also be produced by diagenetic or supergene processes.

On the basis of a small amount of chemical data, silicified breccia at the Pike Creek U occurrence on Steens Mountain differs from that in the above areas in having relatively low trace element contents, except for Hg (Table 2, Fig. 5). In addition, silicified rock at this occurrence does not contain sulfide. It is possible that sulfide was originally present in the silicified breccia at Pike Creek, but there is no textural evidence to support this. The associated clay phase is montmorillonite and the silica phase that forms the breccia matrix is cristobalite; neither of these minerals is necessarily of hydrothermal origin. Consequently, the Pike Creek occurrence is of undetermined origin.

The uranium mineralization in the Virgin Valley, Painted Hills, Petersen Mountain, and Dogskin Mountain areas is also of uncertain origin. In addition, the Lucky Lass mine, although located near the hydrothermal system at the White King mine in the Lakeview district, exploited uranium mineralization of undetermined origin. The stratabound mineralization exposed at Cottonwood Creek in the Bretz-Opalite district of the McDermitt caldera, which resembles bedded uraniferous opaline silica at Virgin Valley, is also of unknown origin.

The origin of U mineralization in Virgin Valley is uncertain, but at least three origins are possible. Our favored mechanism is deposition from hydrothermal solutions contemporaneous with igneous activity, and possibly with sedimentation, at the Virgin Valley caldera. Additional possibilities are deposition from much younger hydrothermal solutions (Zielinski, 1982), and mobilization and deposition of uranium by low-temperature diagenetic solutions that altered tuffs of the Virgin Valley Formation (Henry, 1978). It is possible that more than one mechanism was involved, and we suggest below that uranium occurrences along fractures in tuff may reflect secondary mobilization that was much later than primary mineralization.

A primary hydrothermal origin is supported at Virgin Valley by the magmatic or hydrothermal affinity of several associated trace elements, the restriction of U mineralization to a small area, and the obvious potential for hydrothermal activity during caldera-related volcanism. Several elements that are enriched in Virgin Valley U deposits, notably Zn, Cd, Sb, Bi, Te, and Tl, are generally associated with magmatic-related hydrothermal systems. Some other elements, such as As, Mo and Se, are also common in hydrothermal deposits but can also be enriched in low-temperature, sandstone-type U deposits (Harshman, 1974; Spirakis and others, 1981; Spirakis and others, 1984). By comparison with the uraniferous breccia deposits at the White King mine, Lakeview district, and in the Kings River district, McDermitt caldera, U-rich rock from Virgin Valley has generally low contents of most of these elements (Fig. 5). The geographic distribution of trace elements associated with U mineralization in Virgin Valley could reflect zoning away from a source close to deposits in the Canyon Rhyolite.

The small area of U mineralization in Virgin Valley suggests a localized process. Mobilization of U by low-temperature diagenetic solutions, which have affected almost all of the Virgin Valley Formation, should have generated more widespread mineralization.

Hydrothermal activity should be expected during Virgin Valley volcanism. Many ore deposits are associated with calderas, especially with ring-fracture volcanism similar to the Canyon Rhyolite and other rhyolite lavas (Albers and Kleinhampl, 1970; Heald and others, 1987; Lipman, 1992; Henry and others, in press). Hydrothermal circulation would be driven by the underlying intrusion that fed the lavas rather than by the lavas themselves. Hydrothermal activity may be less common with peralkaline igneous systems than with other types, but hydrothermal U mineralization is apparently associated with rhyolitic intrusions of the McDermitt caldera (Rytuba and Glanzman, 1979; this report). As noted above, many of the U deposits

examined by us in northwestern Nevada and southeastern Oregon are associated with rhyolitic intrusions, including some deposits that are clearly of hydrothermal origin.

An alternative of younger hydrothermal activity is based upon the proposal by Zielinski (1982) that uraniferous opal formed from hydrothermal solutions during an episode about 2 Ma ago. This interpretation is based on fluid inclusion homogenization temperatures as high as 250° C and U-Pb isotopic ages of the opal. The analyzed sample for both of these data is apparently from the same area as our samples VV-9 and VV-11 (Fig. 10). Fluid inclusion temperatures ranged from 102° to 250° C, reasonable but highly variable for an epithermal system. However, opal does not form above 180° C (Fournier, 1985), so the higher apparent temperatures are suspect. Possibly for this reason, Zielinski generalized the data to a temperature of 150° C. Regardless of the uncertainties, if the fluid inclusion data are correct they support epithermal conditions of uranium deposition.

The young age of hydrothermal activity is based on U-Pb ages determined on a sample of distinctly zoned, uraniferous opal (Zielinsky, 1982). The zones are indicated by differences in fluorescence intensity, which reflect different uranium concentrations. Four sets of slightly disconcordant $^{206}Pb/^{238}U$ and $^{207}Pb/^{235}U$ ages ranging from 2.5 Ma to 1.9 Ma were obtained on different zones. Zielinski (1982) interpreted these data to indicate that the uraniferous opal formed from hydrothermal fluids that rose along Basin and Range faults in the late Pliocene, contemporaneous with a period of high-angle faulting. Furthermore, Zielinski proposed that uranium in the opal came from leaching of rocks in the hydrothermal conduit and particularly from the host strata. Zielinski cited a high-angle normal fault approximately 1.5 km southwest of the sample area as a possible example of a conduit and noted the presence of a warm spring (~21°C; Cathrall and others, 1984) just south of the mineralized area.

Although these data are interesting, we think they should be interpreted cautiously and we are skeptical of the young age. Circulation of hydrothermal fluids along Basin and Range faults is certainly possible. We mapped a previously unrecognized fault that runs directly through the mineralized area (Fig. 10). Maximum displacement along the fault is only 8 m, but it still could have served as a conduit for hydrothermal fluids. However, similar faults, including some with much greater displacement, are present to the southwest, in the northern part of the caldera, and along the eastern margin of the caldera (Fig. 9), but no uranium mineralization is associated with them. Moreover, these faults show much greater displacement of the 16- to 15-Ma Virgin Valley rocks than of the 9-Ma Mesa Basalt. Therefore, most faulting occurred before 9 Ma. The timing of displacement on the small fault in the uranium area is only known to be post Virgin Valley Formation. Finally, the warm spring near the uranium area and another in the northeastern part of the caldera have low temperatures (maximum 32° C; Cathrall and others, 1984) and low uranium contents (<7 ppb; Castor and others, 1982b). Fluids like these are not similar to the probable mineralizing fluids and likely would not generate uranium deposits.

The possibility that U was released from volcanic glass by low- or moderate-temperature alteration at Virgin Valley is supported by several factors, although we conclude that this origin is unlikely. Unaltered volcanic glass in tuff or rhyolite of Virgin Valley contains 9 to 14 ppm uranium (Tables 2 and 11) and is therefore a major potential source. Volcanic ash is considered to be the source of U in several major mining districts (Dahl and Hagmaier, 1974; Galloway and others, 1979; Hansley and Spirakis, 1992). Mobilization of U by alteration of volcanic glass is suggested by analysis of three diagenetically altered samples of Virgin Valley Formation (Table 3). These samples have been altered to a combination of smectite and clinoptilolite. They have relatively low U contents (3 to 6 ppm) and high Th/U ratios (2.5 to 3.5 vs ~2 for unaltered glass; Table 11), which suggests that alteration removed some U.

A major and seemingly fatal flaw with diagenetic origin is the restriction of U mineralization to a small part of the Virgin Valley basin. Favorable hosts, such as lignite, carbonaceous shale, or carbonaceous wood, are abundant throughout Virgin Valley but are not enriched in U other than in this area. Hosts are notably not enriched in the middle of the basin where diagenetic alteration of tuffaceous sediments has been most intense.

In contrast to our favored middle Miocene, hydrothermal origin of most uranium mineralization, we speculate that uranium minerals that coat fractures in bedded tuff (Fig. 10) and uraniferous opal indicate relatively recent remobilization of uranium. Examples include samples C95-112 and possibly VV-6 and C95-114 (Fig. 10). These samples are distinguished by the occurrence of uranyl minerals as thin coatings along fractures and in cavities, and by the lack of associated epithermal trace elements. We speculate that the uranium was released by erosion and weathering of "primary" deposits, transported by shallow groundwater in the U^{+6} state, and then concentrated by evaporation or some other process. Mobilization of uranium from the "primary" deposits should be occurring, given the fact that they crop out. As one example, dehydration of the water-rich (16 to 23%; Tuchek and others, 1984) and therefore unstable opals of Virgin Valley should release uranium. Coatings of carnotite, autunite, and uranyl silicate on fractures in the uraniferous opal beds reported by Castor and others (1982b) may indicate immediate near-field redeposition of uranium released by this mechanism.

Except for the association of uranium with sulfide in opal and opalized wood, there is no evidence for deposition in the reduced (uranous) state in Virgin Valley. Black unoxidized ores containing U^{+4} minerals are generally considered to be "primary" whereas deposits of U^{+6} minerals are thought of as "secondary." It is possible that initial, or primary, deposition of uranium in Virgin Valley was as uranyl minerals, a scenario advocated for carnotite deposition in some Colorado Plateau deposits, carnotite in Australian calcretes and autunite in Italy (Langmuir, 1978). As noted by Adler (1974) in a paper on sediment-hosted uranium deposits, uranium readily fluctuates between its oxidized and reduced state allowing considerable transformation from one state to the other, and the terms primary and secondary tend to lose meaning. The concept of "primary" or "secondary" mineralization at Virgin Valley may be likewise misleading. Original U deposition in opal at Virgin Valley was probably primary, regardless of the oxidation state of the uranium. It is also probable that the deposition of uranium as carnotite or other uranyl phases along fractures is secondary, having formed as a result of remobilization of earlier primary mineralization. The origin of the occurrences with the highest U content, the weeksite followed by white opal mineralization in breccia in the Canyon Rhyolite, is problematic. It is possible that these occurrences represent hydrothermal vents that supplied U^{+6} and other elements, such as Si, As, Sb, and Tl to the stratiform deposits in tuffaceous sediments nearby. The presence of relatively high Hg and Zn in the most U-rich breccia sample (VV-7) is interesting in this regard, although the sample has low Mo and Bi contents. Alternatively, breccia in the Canyon Rhyolite could have acted as traps for U^{+6} deposition from downward migrating fluids that contained U removed from overlying primary U deposits in tuffaceous sedimentary rocks that have since been removed by erosion.

The origin of uranium occurrences in volcanic rocks in the three districts in southern Washoe County that were studied by us, Painted Hills, Dogskin Mountain, and Petersen Mountain, is also problematic. No primary U minerals were found by us in samples from any of these occurrences, silicification and hydrothermal alteration minerals are sparse, and associated trace elements are generally low but in some cases show slight enrichment. Three mechanisms are possible for the origin of U mineralization in the Painted Hills: concentration by low-temperature ground water along permeability barriers such as mafic dikes in the host volcanic rocks; deposition from thermal fluids related to mafic dike emplacement; and introduction and deposition by hydrothermal activity that occurred after mafic dike emplacement.

Uranium mineralization in the Painted Hills is locally intense, containing as much as 1.3% U in sample C95-132, the highest in any samples collected for this study (Table 2). It occurs in ash-flow tuff mainly along the footwall of mafic dikes, although minor mineralization occurs along fractures in ash-flow tuff. Associated trace element contents, while locally somewhat elevated (e.g., W, As, Sb, Pb, Tl), are not as high as they are in obviously epithermal deposits such as the White King mine (Fig. 5). Uranous minerals have not been identified by us, but uranyl minerals are locally abundant. In addition, associated minerals include clay and limonite along with relatively little silica. Sulfide minerals or limonite that replaced sulfide have not been identified.

Some of the above features support deposition of U from low-temperature ground water in the Painted Hills as proposed by Cupp and others (1977a), who envisioned the controlling mafic dike contacts and

fractures as physical or chemical barriers to fluid migration. In this regard, it is noteworthy that U mineralization occurs on the eastern, or uphill, side of the dikes, which may have intercepted normal downward migration of U-bearing ground water. Cupp and others believed that the U was extracted from the host tuff, which contains relatively high background U contents. This mechanism implies that flow of U-enriched groundwater was similar to probable flow of modern groundwater, that is, from areas of recharge at higher elevations in the present mountain range down and out toward the adjacent valleys. Formation of mineralization after development of the present-day topography is consistent with this mechanism but is not required.

Several features suggest that hydrothermal activity may have been important in the Painted Hills. The U mineralization occurs almost exclusively along the footwalls of the dikes, suggesting that deposition along dike barriers was from ascending fluids. Uranium-bearing fluids may have moved up fractures or other conduits such as permeable layers in the tuff sequence. The tuffaceous lahar exposed near the Red Bluff adit is an example of such a permeable layer. Assuming that eastward rotation of the volcanic units took place prior to U mineralization, the geometry of the geologic setting in the Painted Hills is permissive for such entrapment of ascending fluids; relatively impermeable NW-dipping dikes, or silicified zones along them, could trap fluids moving updip (west) in shallowly eastward-dipping permeable stratigraphic units. The presence of minor amounts of late-stage chalcedony indicates that these fluids were hot (>180° C) during at least part of this process and that the fluids were hydrothermal. Cristobalite deposition may have been in response to dike emplacement, whereas later chalcedonic silica was related to hydrothermal migration.

The presence of as much as 183 ppm U_3O_8 in the mafic dike rock suggests that mineralization took place during or after intrusion of the dikes. Dike-hosted U could be due to secondary remobilization and deposition of primary U that was present prior to dike emplacement, but we think that this is unlikely. Therefore, we believe that production and movement of thermal water in the Painted Hills could have been caused by the mafic dikes themselves or by post-dike hydrothermal activity.

Bonham (1969) stated that the distribution of uranium occurrences in the Painted Hills and elsewhere in southern Washoe County link them to the Tertiary rhyolite and that the chemistry of the uranium mineralization is consistent with leaching from the rhyolite. Bonham further proposed that deposition from groundwater that was heated by a dacite intrusive episode was a possible uranium mineralization mode, and that U would be more readily leached from tuff by thermal groundwater. He cited the presence of peripheral uranium occurrences around centrally located dacite plugs in the Pyramid mining district, which contains base- and precious-metal veins and includes the Painted Hills uranium district. The mafic dikes in the Painted Hills, which have been tentatively correlated with the 14-15-Ma Pyramid sequence (Cupp and others, 1977a), may predate the dacite plugs, which were correlated with the 13-Ma Kate Peak Formation (Bonham, 1969). Therefore, the mafic dikes would have been available as barriers or conduits during hydrothermal activity related to the dacitic intrusion. However, according to K/Ar dates reported by Wallace (1975), dacitic intrusive rocks in the Pyramid mining district are 19-21 Ma, making them too old to have been responsible for U mineralization controlled by the 14-15 Ma dikes.

For the most part, mineralization in ash-flow tuff in the other two uranium districts in southern Washoe County that were examined during this study is similar to that in the Painted Hills, although uranium concentration in these areas is along fault zones and fractures rather than mafic dikes. With some exceptions, samples from both the Petersen Mountain and Dogskin Mountain areas have similar trace element contents to those from the Painted Hills uranium district (Fig. 5). Samples from the Sunnyside occurrence in the Dogskin Mountain area have relatively high Mo, and As, and one sample (C95-144) has high Hg and Au (Fig. 5, Table 2). A sample from the Buckhorn mine has relatively high Hg and W (Fig. 5). The presence of these elements suggests that the U mineralization may have a hydrothermal component.

The only uranium mineral identified in occurrences in the Petersen Mountain and Dogskin Mountain areas is autunite, and as in the Painted Hills, no primary U minerals have been positively identified. In addition, no sulfide was identified during this study. Primary hydrothermal U mineralization is therefore not

indicated. However, the association of chalcedonic silica with elevated U at Tick Canyon indicates deposition during hydrothermal activity. The relatively large area of limonitic staining and argillic alteration at the Buckhorn mine, Petersen Mountain, also suggests hydrothermal activity.

We believe that, on balance, the evidence in the Painted Hills, Petersen Mountain, and Dogskin Mountain uranium districts supports volcanic-rock hosted mineralization related to hydrothermal activity. However, as at Virgin Valley, subsequent remobilization and redeposition of uranyl minerals has probably taken place and may account for rich U mineralization at some sites. Sediment-hosted, organic matter-related U occurrences in the Truckee Formation may also have been deposited by remobilization and redeposition of U from hydrothermal deposits, and some of these occurrences were referred to as "Wyoming" roll-front type deposits by Hurley and others (1982).

The origin of U mineralization in the Virgin Valley and southern Washoe County U districts is uncertain and more detailed work is necessary if these deposits are to be understood. To this end, age constraints on mineralization in both areas are important data, and more thorough work on mineral assemblages coupled with more data on deposit chemistry (particularly major and trace element zoning) are necessary.

COMPARISON OF THE SETTING OF NORTHWESTERN NEVADA AND SOUTHEASTERN OREGON URANIUM DEPOSITS WITH THAT AT YUCCA MOUNTAIN

General geology

The geology in and near the proposed repository site at Yucca Mountain is dominated by the rocks of the southwestern Nevada volcanic field (SWNVF) as defined by Byers and others (1976). Ash-flow tuff and related rocks from at least four major Miocene calderas comprise this volcanic field, which once covered an area of more than 10,000 km^2 (Byers and others, 1989). Volcanic activity of the SWNVF was of middle to late Miocene age, about 15 to 7 Ma, and detailed age data support episodic activity that can be divided into four main stages. The earliest stage includes 15-Ma metaluminous and peralkaline rhyolite ash-flow tuffs (Sawyer and others, 1994). The second stage of volcanic activity, which together with the above mentioned tuffs has been referred to as the "main magmatic stage" by Noble and others (1991) consists of metaluminous rhyolite ash flow sheets and intermediate to rhyolitic lavas that range between about 14 Ma and 12.5 Ma (Sawyer and others, 1990). The second stage includes the Paintbrush Group, a 1300+ km^3 unit consisting of four ash-flow formations and associated bedded tuff units that was erupted between 12.8 and 12.7 Ma (Sawyer and others, 1990) and the underlying Calico Hills Formation, reported by Sawyer and others (1994) to be 12.9 Ma. Following Paintbrush Group eruptions, rhyolitic lavas were extruded between 12.7 and 12.45 Ma at several places in the SWNVF. A 11.7-Ma rhyolite flow was the earliest extrusion in the third, or Timber Mountain, magmatic stage (Fleck and others, 1991). It was followed by eruption of the Timber Mountain Group, the most significant ash-flow sequence in the SWNVF in terms of total volume (2000+ km^3), between 11.6 and 11.45 Ma (Sawyer and others, 1990). Eruption of this unit, which consists of two major formations, produced the Timber Mountain caldera (Byers and others, 1976), a large, well-preserved feature centered about 25 km north of the Yucca Mountain site. Post-collapse volcanic activity in the third magmatic stage, mainly rhyolitic flows, is thought to have continued until about 10.1 Ma (Noble and others, 1991). The fourth stage, or late magmatic stage of Noble and others (1991), includes 9.4- to 7.5-Ma peralkaline to metaluminous ash-flow tuffs and basalt flows as young as 7.0 Ma (Fleck and others, 1991). A hiatus in volcanic activity of about 3 million years followed the late magmatic stage. Pliocene to recent basalt flows and cones from 4 Ma (Carr, 1988) to possibly younger than 15 Ka (Crowe and others, 1988) are distinctly different from the SWNVF volcanism.

Structures affecting the rocks of the SWNVF are mostly considered to have resulted from two interactive tectonic processes that took place about 17-8 Ma: extension of the southern Basin and Range province; and caldera formation. As noted by Sawyer and others (1994), volcanism and extensional tectonism were broadly concurrent in the area, but in detail were episodic in time and not coincident in space. Miocene extension was accommodated by west-dipping normal faults that may bottom in low-angle detachment surfaces and by right-lateral shear along the Walker Lane, a major 100-km-wide northwesterly zone in

western Nevada that includes the SWNVF. Fault patterns related to caldera subsidence and resurgent doming add to the structural complexity.

Steeply westward-dipping normal faults are abundant in the Yucca Mountain area (Scott and Bonk, 1984), and may represent the breakaway zone for detachment faulting that bounds Bare Mountain about 10 km east of Yucca Mountain. According to Hamilton (1988), normal faults at Yucca Mountain were active above an 11 Ma hinge line between more-or-less flat-lying detachment to the east and moderately westward dipping detachment to the west. Hamilton proposed that this detachment surface, which separates Tertiary volcanics from pre-Tertiary rocks, now extends from east of Yucca Mountain to as far west as Death Valley. Carr (1988) proposed that Crater Flat, which lies immediately west of Yucca Mountain, was a caldera formed during the second magmatic stage and that Yucca Mountain normal faulting was caused by reactivation along subsidence-bounding fractures of the same caldera

Outcrops in the area at Yucca Mountain that contains the proposed site for the nuclear repository and related activity, the controlled area, consist mostly of ash-flow tuff of the Paintbrush Group, principally the Tiva Canyon and Topopah Spring Tuffs (Scott and Bonk, 1984). Both units are metaluminous welded ash-flow tuffs with basal high-silica rhyolite compositions and upper low-silica rhyolite (quartz latite) compositions. The proposed repository horizon is in the Topopah Spring Tuff about 80 m above its base.

A bedded tuff sequence between the Tiva Canyon and Topopah Spring Tuffs contains layers of poorly lithified ash-flow tuff, air-fall tuff, water-worked tuff, and possibly some surge deposits. To the north, this bedded tuff unit is interbedded with mappable welded ash-flow tuffs of the Pah Canyon and Yucca Mountain Tuffs.

Volcanic units below the Paintbrush Group are known only from drill hole intersections in the controlled area. They include the Calico Hills Formation, a unit mainly consisting of zeolitized rhyolite nonwelded ash-flow tuff that directly underlies the Topopah Spring Tuff. Below this unit, at progressively deeper levels are ash-flow tuffs of the Crater Flat Group, the Lithic Ridge Tuff, and unnamed older tuffs. Pre-Tertiary rocks were penetrated at a depth of 1244 m by only one drill hole (UE25p#1) in the southern part of the controlled area (Carr and others, 1986).

Rhyolitic flow rocks crop out extensively north of controlled area, and rhyolite to dacite flow rocks have been intersected at depths in excess of 1000 m in drill holes in the north part of the controlled area (Spengler and others, 1981; Maldonado and Koether, 1983).

The Rainier Mesa Tuff of the Timber Mountain Group is exposed in the southern part of the Yucca Mountain controlled area. Minor amounts of a bedded tuff sequence that underlies the Rainier Mesa Tuff also crops out in this area. Canyons and washes in the controlled area contain Quaternary sand and gravel deposits.

Rock chemistry

Ash-flow tuffs in the controlled area at Yucca Mountain are metaluminous high-silica to low-silica rhyolites. Associated bedded tuff units have similar compositions. On the basis of data compiled by Broxton and others (1989), major and trace element contents are essentially normal for such rocks. Trace element data for unaltered rocks, altered rocks, veins, and breccias reported by Castor and others (1990; 1993) indicate that controlled area rocks have low Au and Ag contents, local occurrences of slightly elevated As, Ba, Bi, F, Hg, Mo, Pb, Sb, Te, Tl, and Zn, maximum U at 9.3 ppm, and maximum Th at 26 ppm.

Ash-flow tuff and rhyolite in the McDermitt caldera and Virgin Valley areas are mainly peralkaline high silica rhyolite, however metaluminous rhyolite occurs in both areas. Biotite-bearing rhyolite appears to host U mineralization at the Moonlight mine and may do so elsewhere in the Kings River uranium district, but chemical analyses of unaltered rock from this area are not available. In the Bottle Creek area, the host rhyolite is probably of peralkaline composition. In the Lakeview and Steens Mountain areas, the host rhyolites are metaluminous, high silica varieties. Ash-flow tuff in the Painted Hills, Petersen Mountain, and

Dogskin Mountain areas is chemically similar to ash-flow tuff from Yucca Mountain; it is metaluminous high-silica to low silica rhyolite.

Although trace elements such as As, Bi, F, Hg, Mo, Pb, and Sn are locally high in altered rocks, veins, and breccias in the Yucca Mountain area, enrichment of these elements is minor. In general, elevated amounts of these elements at Yucca Mountain are much lower than in the hydrothermal U deposits in the Lakeview, McDermitt caldera, and Bottle Creek areas, and more closely resemble those in the Virgin Valley, Painted Hills, Petersen Mountain, and Dogskin Mountain area. For the most part, the rocks at Yucca Mountain chemically resemble unmineralized rocks in the uranium areas studied.

Mineral assemblages

As summarized in Broxton and others (1989), the primary mineral assemblages in volcanic rocks at Yucca Mountain are normal for the types of rock in which they occur. Secondary minerals in these rocks are devitrification products and later rock alteration products that include zeolites, clay minerals, and feldspar minerals (Bish and Vaniman ,1985). Zeolites in the Topopah Spring Tuff and the underlying Calico Hills unit are mainly clinoptilolite/heulandite and mordenite, although erionite has been reported (Bish and Vaniman, 1985). Clay minerals in the tuffs at Yucca Mountain near the potential repository horizon are smectite (montmorillonite group). The genesis of alteration minerals at Yucca Mountain is a matter of continuing discussion. For the most part, alteration mineral zonation in Yucca Mountain is vertically zoned in a similar to that in open hydrologic systems (Broxton and others, 1987). However, elevated temperatures as indicated by clay mineralogy (Bish, 1989) suggest that burial diagenesis may have been a factor in Yucca Mountain zeolite formation, and Levy and O'Neil (1989) proposed that the zeolites formed while the host tuffs were cooling. However, on the basis of variations in zeolite mineral chemistry, Livingston (1993) proposed that hydrothermal activity was reponsible for Yucca Mountain zeolite distribution.

Near surface veins and fracture coatings in the Yucca Mountain controlled area contain calcite, opal, and fluorite; deeper veins contain calcite, quartz, analcite, and feldspar minerals along with local barite, fluorite, and Mn and Fe oxide minerals (Caporuscio and others, 1982; Carlos and others, 1991; Castor and others, 1992). Sulfide occurrences, all of pyrite, were proposed mostly to be of ejectal origin in the ash-flow tuff, but minor occurrences of probable in situ hydrothermal origin were noted in drill core from hole G-2 in the north part of the controlled area (Castor and others, 1994).

Primary mineral assemblages (phenocrysts and groundmass minerals) of the host rhyolites in the mineralized areas studied generally resemble those in the Yucca Mountain rocks as they do in most other rhyolites. However, minor mineral components in the peralkaline rocks in some of the uranium areas are somewhat different, particularly mafic phases which are generally present in only minor amounts.

Alteration products, be they diagenetic or hydrothermal, are also similar between Yucca Mountain and the areas of uranium mineralization studied. The clay mineral montmorillonite is common to both Yucca Mountain and the uranium districts. Zeolite minerals, chiefly clinoptilolite/heulandite group minerals, that occur below the potential repository horizon at Yucca Mountain are also common at Virgin Valley and in the McDermitt caldera. Silica alteration and vein minerals – opal, cristobalite, and chalcedony – are also phases shared between Yucca Mountain and the uranium areas. The mineralogical correlation between the U-enriched tuffs and tuffaceous sedimentary rocks at Virgin Valley and the Yucca Mountain tuffs is particularly notable. Both sequences contain locally abundant clinoptilolite and montmorillonite.

Tuffaceous sedimentary rocks of the Virgin Valley Formation in the Virgin Valley caldera have been diagenetically altered to zeolite and clay and appear to show lateral mineralogical zonation with peripheral alteration dominated by clinoptilolite and central deposits in the basin mainly smectite with minor clinoptilolite. Similar diagenetic alteration, typically showing distinctive mineral assemblage zonation, is common in tuffaceous sedimentary sequences and in tuffs at Yucca Mountain (Hoover, 1968; Walton, 1975; Hay and Sheppard, 1977; Surdam, 1977; Broxton and others, 1987). Similar zones may be present in Virgin Valley and could be identified and mapped with additional work.

Pyrite, which is commonly associated with hydrothermal uranium mineralization in some of the areas studied, is present at Yucca Mountain but occurs at depths considerably below the potential repository horizon. Vein, breccia, and fracture-filling minerals at Yucca Mountain are generally present in only minor amounts, but may be important factors in groundwater chemistry. Detailed studies of such features in the U-mineralized areas examined for this report are generally lacking.

Hydrologic setting

Waters in wells at Yucca Mountain range in temperature from 33.8 to 44°C, and are predominantly Na-HCO_3 ±SO_4 waters (Fig. 26). The TDS of the waters varies and ranges from approximately 245 to 530 mg/L. The pH of the waters is near neutral, to slightly basic and ranges from 6.8 to 8.7 (average = 7.66±0.48). Only one analysis of dissolved U is available near Yucca Mountain and this data point is from the Amargosa Hot Spring and not directly on Yucca Mountain. The U value of this water, which may be somewhat representative of the regional carbonate aquifer, is 0.01 mg/L. Water levels in the Yucca Mountain area vary considerably between 28 and 572 m below ground surface, with the greatest depths to water occurring beneath Yucca Mountain itself (346 to 572 m). For instance, a very large water level gradient occurs at Yucca Mountain resulting in very deep groundwater at the site. The southward sloping water table occurs as a decline of 300 m over a distance of less than 2 km, and this abrupt increase in depth to water at the site is attributed to the interaction of deep carbonate and tuff aquifers with a Tertiary basin and range structure beneath Yucca Mountain (Fridrich and others, 1994).

The data sets for the Steens Mountain, Petersen Mountain, Painted Hills, and Dogskin Mountain areas are insufficient for inclusion into a discussion on the comparisons with Yucca Mountain, and these areas are not considered further.

Table 12 lists summary STORET and NURE information used in comparison of the proposed analogue sites with the Yucca Mountain repository. Table 12 shows the main features of the waters at the sites, and as is indicated on this table, there is a distinct lack of available STORET data from the proposed analogue sites. Data from the area surrounding Yucca Mountain, and not only data from wells at the Mountain are included as part of the Table 12 summary. Virtually nothing is known of the hydrology at Petersen Mountain and Painted Hills sites, and only scarce information is available at Dogskin Mountain. Only one analysis is available from Bottle Creek, and this is from the surface in Bottle Creek, and hence is not useful in a discussion of a suitable analogue site. Virgin Valley and the McDermitt area have more complete analytical data from which to base comparisons.

McDermitt, Virgin Valley, and Yucca Mountain waters are all similar in that they have Na or Ca as their dominant cation, and HCO_3 as the dominant anion, with variable amounts of SO_4, and minor concentrations of Cl. All waters listed in Table 12 are near neutral to slightly basic, similar to the Yucca Mountain groundwater. In addition, both the McDermitt and Virgin Valley areas contain both nonthermal and low temperature (>25 to 90°C) thermal waters, similar to the situation at Yucca Mountain, although somewhat higher temperatures are encountered at Virgin Valley than at Yucca Mountain. Waters at all three of these sites are also all relatively dilute. Uranium contents of stream and spring waters in Virgin Valley (6.3 and 7.8 ppb) are slightly higher than those in McDermitt (2.95 and 4.2 ppb), hence, the Virgin Valley waters are more similar to the Yucca Mountain waters (U = 8-10 ppb). The gross hydrogeochemistry at these three sites are similar (compare Figs. 3, 16, and 26) indicating that either the Virgin Valley or McDermitt areas may be suitable as natural analogue sites from the perspective of similarities in water chemistry, with the Virgin Valley site being a slightly better match.

Data on U_3O_8 content of spring, well, drill-hole, and mine waters from the Vya 1° x 2° quadrangle (Castor and others, 1982b) includes some data for both the Virgin Valley and McDermitt areas. Except for a sample with 21 ppb U_3O_8 taken near the Moonlight mine, these waters have relatively normal U contents (2-7 ppb U_3O_8). As pointed out by Castor and others, groundwater samples collected from granitic terrain in the Jackson and Bilk Creek Mountains, which lie between the two uranium areas, have much higher U contents (up to 170 ppb U_3O_8).

Figure 27. Piper diagram showing the general chemical nature of Yucca Mountain groundwater.

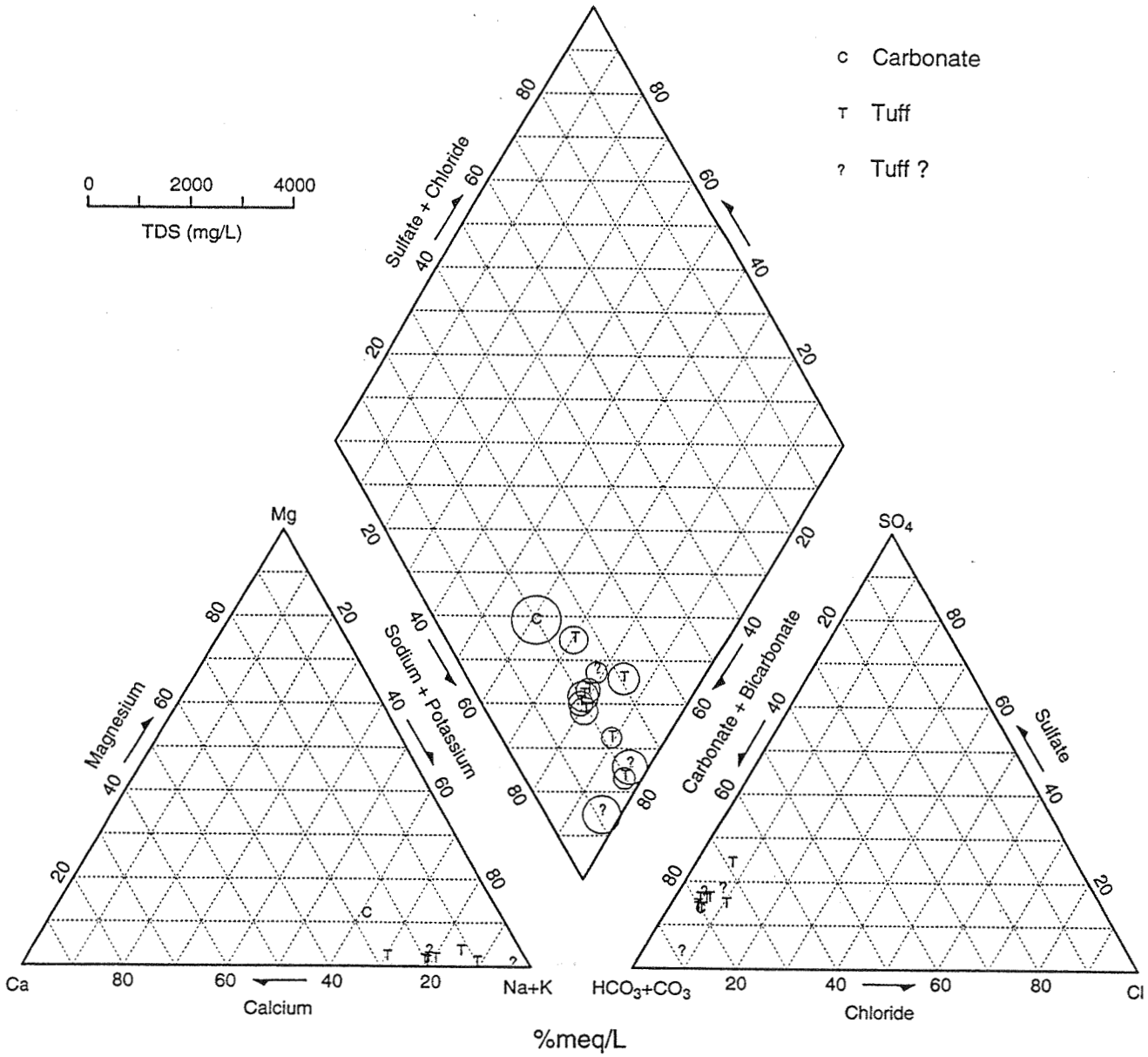

Table 12. Comparison of the main hydrologic features in the study areas.

Study site	Water Type	Temperature (°C)	pH	TDS (mg/L)	Depth to water (m)
McDermitt caldera area	Ca-Na-HCO_3-SO_4	0-28	6.8-9.4	66-724	50
Virgin Valley, nonthermal	Na-HCO_3-SO_4	7-24	6.4-9.7	95-184	<60
Virgin Valley, thermal	Na-SO_4-HCO_3	26.5-92	7.5-9.05	600-630	<60
Lakeview	Ca-Na-HCO_3	7.8	6.3-8.1	?	0
Steens Mountain	?	?	?	?	?
Bottle Creek	Ca-Na-HCO_3-SO_4	7-90	6.4-10.1	42-1216	?
Painted Hills	?	?	?	?	?
Dogskin Mountain	Ca-Na-HCO_3	?	?	86-121	?
Petersen Mountain	?	?	?	?	?
Yucca Mountain	Na-HCO_3-SO_4	33.8-44	6.8-8.7	245-530	28-752*

* Higher values (>300 m) are most representative of the water level depth beneath Yucca Mountain.

The water table is probably much shallower in Virgin Valley and in the McDermitt caldera area than at Yucca Mountain. No published data are available for Virgin Valley, but perennial Virgin Creek may mark the water table along its course. Areas of uranium mineralization are mostly no more than 60 m higher than the creek. Depth to the water table at the Moonlight mine is approximately 50 m, although depths elsewhere in the McDermitt caldera area are greater.

Water levels beneath Yucca Mountain vary from 468 to 752 m below land surface in the southern part of Yucca Mountain based on data reported in Ciesnik (1995). Water level depths are somewhat less in the northern part of the mountain (281 m at one location), and on the flanks (301 to 394 m; Ciesnik, 1995) Nevertheless, all these values are considerably greater than those reported at McDermitt or inferred for Virgin Valley. Hence, any detailed natural analogue study at Virgin Valley or the McDermitt area would have to account for the vast differences in the depths to the water table. One important aspect in selecting the Yucca Mountain site as a repository is the fact that the water table is deep and is not anticipated to inundate the repository for at least 10,000 years. In contrast, the two best analogue sites based on water chemistry currently have water present in the uranium enriched zone. Hence, these sites differ from the Yucca Mountain site but could be useful in studying possible effects to the repository rocks if the water table were to rise. In addition, the higher water temperatures near Virgin Valley and McDermitt might allow for more realistic evaluations of potential water-rock interactions near the repository once filled with radioactive waste.

DISCUSSION OF NATURAL ANALOGUE POTENTIAL AND RECOMMENDATIONS

Our initial characterization of areas of uranium mineralization in tuffaceous rocks of northwestern Nevada and southeastern Oregon has compiled existing data and developed new information to help assess the potential of these areas as natural analogues. The data are summarized in Table 13. Although the level of information varies widely between different sites, several appear to have real potential as analogues whereas others do not. We believe that the most favorable are Virgin Valley and Painted Hills; additionally, the Moonlight Mine-Horse Creek area of the McDermitt caldera warrants further study. The other areas have access problems (Steens Mountain), are very small and(or) have relatively low uranium contents (Bretz mine, Opalite mine, Cottonwood Creek area, Bottle Creek), are nearly completely immersed in water (White King mine, Lucky Lass mine), or are in environments that only remotely resemble that at Yucca Mountain (Aurora deposit). The following discussion considers geologic setting, host rock and uranium mineralogy, evidence for remobilization of uranium, and hydrologic properties and setting.

Table 13. Summary of characteristics of uranium deposits in northwestern Nevada and southeastern Oregon, and comparison with the geologic setting at Yucca Mountain, Nevada

AREA		HOST ROCK							STRUCTURAL & HYDROLOGIC CHARACTER					URANIUM MINERALIZATION							DRILLING		
Subarea or deposit		Lithologies	Mineral Assemblage					Age (Ma)	General	Faulting	Fracture Density	Relative Permeability	Hydrologic Regime	Geometry	U Minerals			Gangue Minerals	Elevated Trace Elements	Age (Ma)	Per-formed	Data Avail.	Spls. Avail.
McDermitt Caldera			Glass	Devit.	Zeolite	Clay	Other								6+	4+	Other						
Kings River district	Moonlight mine - Horse Creek	Granite, rhyolite-intermediate flow rock, intrusive rhyolite (?)	N	P	N	P	Adularia	16.3–16.5	Caldera ring fracture zone, flow complex	Intense	Intense (?)	?	Vadose and saturated, water depth 50 m	Breccia along mod. to steep fault	P	R	U+4 in zircon	Quartz, fluorite, sulfides, adularia	Extreme Ag, As, Au, Mo, Zr; also Ag, Bi, Cu, Hg, Sb, Te, Tl, W	16.3	Yes	Yes	Yes
	Thacker Pass - Rock Creek	Rhyolite flow rock, ash-flow tuff	N	P	P	?	Adularia	ca. 16	Subhoriz. strata, flow complex	Mod.	?	High (?)	?	Stratiform(?) and along faults	P	?	U+4 in zircon		As, Hg, Mo, Sb, W, Tl, Zn, Zr	?	Yes	?	?
	Montana Mountains - Bull Basin	Bedded tuff, volc. sed. rock, ash-flow tuff	N	P	P	P	Carbonate	?	Subhoriz. strata	Mod.	?	?	?	Hot spring, stratiform	?	?	U+4 in zircon	Carbonate	No data for this study	?	Yes	?	?
Bretz Opalite district	Aurora deposit	Trachyandesite, ash-flow tuff, volc. sed. rock	P	P	?	P		ca. 16	Flow complex, subhoriz. strata	Mod.	?	Locally high	Mostly saturated	Stratiform and along steep faults	P	R		Sulfides, Ti oxide	As, Ba, Hg, Mo, Sb, W	?	Yes	Yes	Yes
	Bretz mine	Trachyandesite, ash-flow tuff, volc. sed. rock	P	P	?	?		ca. 16	Caldera ring fracture zone, subhoriz. strata	Intense	Intense (?)	High (?)	Thin vadose zone	Hot Spring and along steep faults	P	?		Sulfides, quartz	As, Hg, Mo, Pb, Sb, W	?	Yes	?	?
	Opalite mine	Bedded tuff, volc. sed. rock	N	P	?	P	Adularia	ca. 16	Subhoriz. strata	?	?	Locally high	Vadose zone	Hot spring	?	?		Sulfides, quartz	Hg, Sb, W	?	Yes	?	?
	Cottonwood Creek	Bedded tuff, volc. sed. rock	N	P	P	?	Opal	ca. 16	Subhoriz. Strata	?	?	?	?	Stratiform	?	?	Organic, opal	Sulfides, quartz, carbonate	As, Bi, Hg, Mo, Sb	?	Yes	?	?
	McDermitt mine	Volc. sed. rock	N	P	P	P		ca. 16	Subhoriz. strata	Mod.	?	?	?	Stratiform, hot spring	?	?	Organic	Sulfides, quartz	No data for this study	15.7	Yes	?	?
Virgin Valley		Bedded tuff, volc. sed. rock, rhyolite flow rock	P	P	P	P	Opal	15.7–16.3	Subhoriz. strata, flow dome complex	Mod.	?	Locally high	Thin vadose zone	Stratiform, along fractures, irreg. breccia masses	P	?	Opal, organic	Opal, Mn oxides, sulfides	As, Cd, Mo, Sb, Se, Zn; local weak Bi, Se, and Tl	16?, 2 to 2.5?	?	?	?
Lakeview district																							
	White King mine	Intrusive rhyolite, bedded tuff, lahars, mafic flow rock	N	P	?	P	Adularia	7–37(?)	Rhy. intrusion in mod. dipping to subhoriz. strata	Mod.	?	?	Saturated	Irregular breccia masses	P	R		Sulfides, cristobalite, quartz	Extreme As, Cs, Hg, Pb, Sb; also Ag, Ba, Cu, Mo, Pb, Tl, Zn	?	Yes	Yes	?
	Lucky Lass mine	Bedded tuff, mafic dike rock	P	P	N (?)	P		15–37(?)	Shallowly dipping strata	?	?	Probably high	Saturated	Along steep fault	?	?			Ag, As, Sb, Tl	?	?	?	?
Steens Mountain		Rhyolite flow rock	N	P	N	?		?	Flow dome	Intense	?	?	?	Breccia veins	?	?		Cristobalite, Fe oxides	Weak As, Hg, Mo, Sb, W	?	?	?	?
Bottle Creek		Rhyolite flow rock	P	P	N	P		?	Subhoriz. flows, flow dome	Mod.	?	?	Vadose zone	Breccia mass	P	?		Quartz, sulfides	As, Bi, Mo, Pb, Sb, Tl, W	?	?	?	?
Southern Washoe County																							
	Painted Hills district	Ash-flow tuff, mafic dike rock, debris deposits	N	P	N (?)	P		15(?)–23	Subhoriz. strata, high-angle dike	Mod.	Mod. (?)	Locally high	Vadose, water depth unknown	Along steep dikes, along fractures	P	?		Quartz, Fe and Mn oxides, cristobalite	Weak As, Pb, Sb, Tl, W	?	Yes	?	?
	Dogskin Mountain	Ash-flow tuff	N	P	?	P			Subhoriz. strata	Intense	?	?	Vadose	Along faults and fractures	P	?		Quartz, Fe oxide	Tick Cyn: weak Sb, Pb; Sunnyside: As, Au, Ba, Hg, Mo, Sn, Tl, W	?	?	?	?
	Petersen Mountain (Buckhorn mine)	Ash-flow tuff	N	P	?	P			Subhoriz. strata	?	Intense (?)	?	Vadose	Along fracture zone (?)	P	?		Fe oxides	Hg, Sb; weak Ag, As, Tl; local W	?	?	?	?
Yucca Mountain		Ash-flow tuff, bedded tuff	P	P	P	P		15–11.5	Subhoriz. strata	Mod.	Mod.	Low to mod.	Vadose, water depth > 300 m								Yes	Yes	Yes

Abbreviations:
Devit. = devitrification products, Spls. = samples, P = present, R = reported, N = not present, ? = no data, Mod. = moderate, Intr. = intrusive, Volc. = volcanogenic, Sed. = sedimentary, Rhy. = rhyolite, Subhoriz. = subhorizontal

Favorable characteristics of Virgin Valley include (1) presence of uranium mineralization, with locally high grades, in subhorizontal, mildly faulted, bedded tuff, tuffaceous sedimentary rock, rhyolitic lava, and lesser air-fall and ash-flow tuff, (2) presence within those rocks of glass, diagenetic minerals (zeolites, smectite, and secondary silica), and minor devitrification minerals similar to those at Yucca Mountain, (3) strong evidence of recent uranium mobilization and retrapping within the tuffaceous rocks, (4) evidence for both intergranular and fracture permeability in the host rocks, and (5) moderately arid setting with exposed uranium mineralization above the water table. Uncertainties remain in the characteristics of primary uranium mineralization; only U^{+6} minerals have been observed, although the presence of pyrite suggests that U^{+4} minerals may have been present and could be preserved in the shallow subsurface. A possible drawback is the relatively shallow (≤60 m) water table.

Although the geologic setting of Virgin Valley is probably the best understood of all the sites investigated, several questions remain that pertain to the mechanisms and history of movement and entrapment of uranium and other elements. Answers to these questions could provide invaluable information regarding the mobility and entrapment of uranium and other elements at the potential nuclear repository at Yucca Mountain. The questions are:

- **How and when did primary uranium mineralization form?** Additional characterization of mineralization is needed to verify our preferred early hydrothermal origin and to determine what is being oxidized or eroded to release uranium. Shallow drilling to intersect unoxidized or less oxidized deposits could help determine the nature of primary mineralization, which would help evaluate the mechanism of formation. Fission-track mapping of existing samples or new samples from shallow drilling is needed to help identify specific uranium sites and association with carbonaceous material, opal, and zeolites or other diagenetic minerals. Redating uraniferous opal by the U-Pb method would be worthwhile to test the interpretation of Zielinski (1982) that mineralization is young.
- **What is the distribution of diagenetic minerals and when did they form relative to uranium mineralization?** The distribution of diagenetic minerals in tuffs in the mineralized area should be mapped to see if a zoning pattern exists and to determine the distribution of potential uranium traps. Did zeolites or other diagenetic minerals play any role in initial uranium deposition? Meaningful ages of zeolite deposition may be obtainable through incremental-heating $^{40}Ar/^{39}Ar$ dating.
- **What is the distribution, age, and source of, and trapping mechanism for, the fracture-controlled uranium mineralization?** It is necessary to determine if it does represent secondary entrapment of remobilized uranium and if it occurs only as fracture coatings or extends into the rock. Uranium-series dating might be used to determine when or if remobilization and secondary entrapment occurred, and aqueous geochemical modeling could evaluate various solubility precipitation mechanisms.
- **What are the physical and chemical hydrologic attributes?** Analysis and characterization of groundwater and surface water is needed to evaluate modern uranium mobility. Available sample sites include Virgin Creek and the hot spring at the south end of the mineralized area. Additional sampling may be possible in existing exploration drill holes or shallow holes drilled specifically for natural analog studies.

Favorable characteristics of the Painted Hills include (1) presence of commonly high-grade (>1% U) uranium mineralization in a moderately faulted and tilted sequence of metaluminous ash-flow tuff units, essentially identical to the setting of Yucca Mountain, (2) existence of mineralization as a relatively simple planar deposit along a dike, (3) presence of devitrification minerals in the ash-flow tuffs and of montmorillonite in bedded tuff, (4) suggestion of present-day uranium mobility from weathering and erosion of the exposed deposit, (5) evidence for both intergranular and fracture permeability in the host rocks, and (6) occurrence in the most arid setting of examined deposits with a probable deep water table. An obvious uncertainty is whether or not zeolites and other diagenetic minerals that occur at Yucca Mountain are present and, as at Virgin Valley, other questions need to be answered:

- **What is the detailed geologic setting?** Additional characterization of the basic geology is needed. The deposit area should be mapped in detail so that mineralization and its geologic controls can be placed in a thorough geologic framework. Mapping would separate different welding zones in the tuffs, as well as distinguish primary pyroclastic from reworked deposits. Detailed study of the ash-flow tuff, bedded tuffs, and mafic dike should include mineralogic analysis, $^{40}Ar/^{39}Ar$ dating, and correlation into a regional stratigraphic sequence.
- **How and when did uranium mineralization form?** The age of mineralization is not known, both in an absolute sense and relative to faulting and tilting of the host tuffs.
- **What is the primary uranium mineralogy and geochemical association?** More data must be collected in order to adequately characterize the mineralization. Underground sampling could be very useful in this regard.
- **What initially trapped uranium and how does this affect subsequent release?** Several mechanisms have been proposed for origin of the mineralization. The mafic dikes and fractures have been proposed as hydrologic barriers, but may also have served as conduits. Characterization of potential stratigraphic zones of permeability is needed. It is particularly interesting that nearby tuffaceous debris flow deposits with carbonaceous material are unmineralized.
- **What is the hydrologic setting and is recent uranium mobility a factor?** Confirmation of modern uranium mobility is needed. Is uranium leaching into ground water and into the ephemeral surface water and/or being trapped nearby? Several springs that occur in nearby canyons and wells in allluvium in the valley floor could be sampled. Sampling and characterization of the fracture controlled mineralization in ash-flow tuff is needed at the Maue-McCray prospect and elsewhere.

Favorable characteristics in the Moonlight mine-Horse Creek area include (1) presence of moderately high-grade uranium mineralization in rhyolitic volcanic rocks, (2) existence of mineralization as a simple planar deposit along a fault at the Moonlight mine, (3) occurrence of uranium as a high-temperature U^{+4} zirconium silicate, (4) moderately arid setting with exposed uranium mineralization above the water table, (5) known age of primary mineralization, and (6) presence of secondary uranium minerals indicating the deposit has been or is being oxidized and eroded. Unlike other areas, considerable core is available for the Moonlight Mine-Horse Creek area. In addition, sampling of groundwater in and around the uranium mineralization can probably be easily done in this area. Groundwater is encountered at a depth of approximately 50 m in the inclined shaft at the Moonlight Mine, several springs occur nearby, it is possible that exploration drill holes that penetrate mineralization at known depths could be sampled, and wells in adjacent valley alluvium can be sampled.

Potential drawbacks for this area include the complex stratigraphic and structural setting of mineralization. Uranium occurs along a fault that is probably part of a caldera ring fracture, and rocks within the caldera are deformed and highly altered. The area was further deformed by Basin and Range faulting along the range front. Host rocks for mineralization and nearby appear to be mostly lavas or domes, although complexly deformed, possibly rheomorphic ash-flow tuff overlies the host rocks. Although devitrification products and possibly minor clay minerals are present, zeolites are absent except in lacustrine beds that are stratigraphically far above the deposit. Modern groundwater flow is probably dominantly fracture controlled.

If the Moonlight mine-Horse Creek area is to be utilized as an analogue site, the following questions should be answered:

- **What is the detailed geologic setting?** Although we assembled a geologic map and cross section of the area from existing 1:62,500 scale mapping and reconnaissance (Fig. 4), more detailed mapping is needed, along with lithologic logging of selected core, to characterize the geology in detail.
- **What is the physical and chemical hydrologic setting?** Analysis and characterization of groundwater and surface water is needed to evaluate modern uranium mobility. Existing exploration holes could be used to measure water depths. Additionally, springs and surface water should be sampled and characterized.

- **Is there evidence for modern uranium mobility along fractures adjacent to the primary mineralization?** Uranyl minerals are known to be present, but have so far only been identified in relatively high-grade ore. Detailed work on near field and far field fracture mineralogy and chemistry would be helpful.

ACKNOWLEDGMENTS

Funding for this project was from the U.S. Department of Energy (US DOE) Yucca Mountain Project Office, Las Vegas, Nevada (contract 1950125-03). Robert Levich (US DOE), Abe van Luik (US DOE), Paul Cloke (SAIC) of the Yucca Mountain Site Characterization Office are thanked for their help in project development. In addition, Eric Smistad (US DOE), Ardyth Simmons (US DOE), and Paul Dixon (Los Alamos National Laboratory) are thanked for providing insight on natural analogue geology.

We are indebted to Frank Dickson and John McCormack of the University of Nevada, Reno, Geology Department for much of the detailed SEM and petrographic information on samples from the U deposits and occurrences. Liang Hsu, NBMG, is thanked for XRD analyses. Mario Desilets, NBMG Analytical Laboratory, supervised sample preparation and submittal to contract laboratories, and monitored analytical quality. Kris Pizarro and Jack Hursh, NBMG, are acknowledged for preparation of maps. Lindsay Christensen, formerly of NBMG, is thanked for compilation of water data.

Janine Cannon, U. S. Forest Service, Lakeview Ranger District, provided information on environmental studies in the Lakeview uranium district. Jim Lebret of Orovada, Nevada, is thanked for providing data on his claims in the Kings River uranium district.

REFERENCES

Adler, H.H., 1974, Concepts of uranium ore formation in reducing environments in sandstones and other sediments, *in* Formation of Uranium Ore Deposits, International Atomic Energy Agency, Vienna, Austria, p. 141-168.

Albers, J. P., and Kleinhampl, F. J., 1970, Spatial relation of mineral deposits to Tertiary volcanic centers in Nevada: U. S. Geological Survey Professional Paper 700-C, p. 1-10.

Alexander, D. H., and Van Luik, A. E., 1991, Natural analogue studies useful in validating regulatory compliance analyses: Proceedings GEOVAL-1990, Symposium on Validation of Geosphere Flow and Transport Models, Swedish Nuclear Power Inspectorate and OECD Nuclear Energy Agency, Stockholm, Sweden, p. 590-597.

Backer, H.A., Williams, G.K., and Bagby, W.C., 1995, Geology, structure, and mineralization of the Kings River uranium deposits, Humboldt County, Nevada in Geology and Ore Deposits of the American Cordillera, Symposium Program with Abstracts, Geologic Society of Nevada, p. A-11.

Bagby, W.C., 1980, Geology, *in* Kings River Summary Report, unpublished Chevron Resources Company report, p. 5.1-5.15.

Berry, M. R., Castor, S. B., and Robins, J. W., 1982, Jordan Valley Quadrangle, Oregon and Idaho: U.S. Dept. of Energy Open-File Report PGJ132.

Bingler, E.C., 1978, Abandonment of the name Hartford Hill Rhyolite Tuff and adoption of new formation names for middle-Tertiary ash-flow tuffs in the Carson City-Silver City area, Nevada: U.S. Geological Survey Bulletin 1457D, 19 p.

Bish, D.L., 1989, Evaluation of past and future alterations in tuff at Yucca Mountain, Nevada, based on clay mineralogy of drill cores USW G-1, G-2, and G-3: Los Alamos National Laboratory Report, LA-10667-MS, 40 p.

Bish, D.L., and Vaniman, D.T., 1985, Mineralogic summary of Yucca Mountain, Nevada: Los Alamos National Laboratory Report, LA–10543–MS, 55 p.

Bonham, H.F., and Papke, K.G., 1969, Geology and mineral deposits of Washoe and Storey Counties, Nevada: Nevada Bureau of Mines and Geology Bulletin 70, 140 p.

Brookins, D. C., 1984, Geochemical aspects of radioactive waste disposal: Springer Verlag, New York, NY, 347 p.

Brooks, H., 1956, Geology of a uranium deposit in the Virginia Mountains, Washoe County, Nevada: M.S. thesis, University of Nevada, Reno, 50 p.

Broxton, D.E., Bish, D.L., and Warren, R.G., 1987, Distribution and chemistry of diagenetic minerals at Yucca Mountain, Nye County, Nevada: Clays and Clay Minerals, v. 35, no. 2, p. 89-110.

Broxton, D.E., Byers, F.M., Jr., and Scott, R.B., 1989, Chemical and mineralogic trends within the Timber Mountain - Oasis Valley caldera complex - evidence for multiple cycles of chemical evolution in a long-lived silicic magma system: Journal of Geophysical Research, v. 94, p. 89-110.

Byers, F.M. Jr., Carr, W.J., Orkild, P.P., 1989, Volcanic centers of southwestern Nevada – evolution of understanding, 1960-1988: Journal of Geophysical Research, v. 94, p. 5908-5924.

Byers, F.M. Jr., Carr, W.J., Orkild, P.P., and Sargent, K.A., 1976, Volcanic suites and cauldrons of Timber Mountain–Oasis Valley Caldera Complex, Southern Nevada: U.S. Geological Survey Professional Paper 919, 70 p.

Caporuscio, F.A., Vaniman, D.T., Bish, D.L., Broxton, D.E., Arney, B., Heiken, G.H., Byers, F.M., Jr., Gooley, R., and Semarge, E., 1982, Petrologic studies of drill cores USW-G2, and UE25b-1H, Yucca Mountain , Nevada: Los Alamos National Laboratory Report LA-9255-MS, 111 p.

Carlos, B., Bish, D., and Chipera, S., 1991, Fracture-lining minerals in the lower Topopah Spring Tuff at Yucca Mountain: Los Alamos National Laboratory Report LA-UR 91-4354, 8 p.

Carr, M. D., Waddell, S. J., Vick, G. S., Stock, J. M., Monsen, S. A., Harris, A. G., Cork, B. W., and Byers, F. M., Jr, 1986, Geology of drill hole UE25p #1: a test hole into pre-Tertiary rocks near Yucca Mountain, southern Nevada: U. S. Geological Survey Open-File Report 86-175, 56 p.

Carr, W. J., 1988, Volcano-tectonic setting of Yucca Mountain and Crater Flat, Southwestern Nevada: U.S. Geological Survey Bulletin 1790, p. 35-49.

Castor, S. B., and Berry, M. R., 1981, Geology of the Lakeview uranium district, Oregon *in* P. C. Goodell and A. C. Waters (editors) Uranium in Volcanic and Volcaniclastic Rocks: AAPG Studies in Geology, no. 13, p. 55-62.

Castor, S. B., Berry, M. R., and Robins, J. W., 1982a, Klamath Falls Quadrangle, Oregon and California: U.S. Dept. of Energy Open-File Report. PGJ061, 29 p.

Castor, S.B., Feldman, S.C., and Tingley, J.V., 1990, Mineral evaluation of the Yucca Mountain Addition, Nye County, Nevada: Nevada Bureau of Mines and Geology Open-File Report 90-4,107 p.

Castor, S. B., Mitchell, T. P., and Quade, J. G., 1982b, Vya Quadrangle, Nevada, California, and Oregon: U.S. Dept. of Energy Open-File Report. PGJ/F135, 25 p.

Castor, S.B., Tingley, J.V., and Bonham, H.F., 1992, Subsurface mineral resource analysis, Yucca Mountain, Nevada - preliminary report 1: lithologic logs: Nevada Bureau of Mines and Geology report to Science Applications International, Las Vegas, NV, 11 p., with appendices.

Castor, S.B., Tingley, J.V., and Bonham, H.F., 1993, Subsurface mineral resource analysis, Yucca Mountain, Nevada - final report of chemical analyses: Nevada Bureau of Mines and Geology report to Science Applications International, Las Vegas, NV, 25 p.

Cathrall, J. B., Siems, D. F., Crenshaw, G. L., and Cooley, E. F., 1984, Geochemical evaluation of the mineral and geothermal resources of the Charles Sheldon Wilderness Study Area, Nevada and Oregon: U. S. Geological Survey Bulletin 1538, p. 51-87.

Cebula, G. T., Kunk, M. J., Mehnert, H. H., Naeser, C. W., Obradovich, J. D., and Sutter, J. F., 1986, The Fish Canyon Tuff, a potential standard for the $^{40}Ar/^{39}Ar$ and fission-track dating methods: Sixth International Conference on Geochronology, Cosmochronology, and Isotope Geology, Terra Cognita, v. 6, p. 139-140.

Chapman, N. A., McKinley, I. G., Shea, M. E., and Smellie, J. A. T., 1992, The Poços de Caldas project: Natural analogues of processes in a radioactive waste repository: Journal of Geochemical Exploration, v. 45, 603 p.

Chevron Resources Company, 1980, Kings River summary report, unpublished company report, 158 p.

Ciesnik, M.S., 1995. Ground-water altitudes and well data, Nye County, Nevada and Inyo County, California: U.S. Geological Survey Open-File Report 93-89, 27 pp.

Cohenour, R.E., 1960, Geology and uranium occurrences near Lakeview, Oregon: U.S. Atomic Energy Commission Open-File Report RME-2070, 31 p.

Conrad, W.K., 1983, Petrology and geochemistry of igneous rocks from the McDermitt caldera complex, Nevada-Oregon, and Adak Island, Alaska – evidence for crustal development: Ph.D. thesis, Cornell University, 325 p.

Conrad, W.K., 1984, The mineralogy and petrology of compositionally zoned ash flow tuffs, and related silicic volcanic rocks, from the McDermitt caldera complex, Nevada-Oregon: Journal of Geophysical Research, v. 89, p. 8639-8664.

Cramer, J. J., 1986, Sandstone-hosted uranium deposits in northern Saskatchewan as natural analogs to nuclear fuel waste disposal vaults: Chemical Geology, v. 55, p. 269-279.

Crowe, B., Harrington, C., McFadden, L., Perry, F., Wells, S., Turrin, B., and Champion, D., 1988, Preliminary geologic map of the Lathrop Wells volcanic center: Los Alamos Report LA-UR-88-4155, 7 p.

Cupp, G. M., Leedom, S. H., Mitchell, T. P., and Allen, D. R., 1977a, Geology, uranium deposits, and uranium favorability of the Hartford Hill Rhyolite and Truckee Formation, southwestern Washoe County, Nevada, and eastern Lassen County, California: Bendix Field Engineering Corp. report for the U.S. Energy Research and Development Administration, GJBX-16(77), 61 p.

Cupp, G. M., Leedom, S. H., Mitchell, T. P., Kiloh, K. D., and Horton, R. C., 1977b, Preliminary study of the favorability for uranium in selected areas in the Basin and Range: U. S. Energy Research and Development Administration GJBX-74(77).

Curtis, D. B., Benjamin, T. M., Gancarz, A. J., Loss, R. D., Rosman, K. J. R., De Laeter, J. R., Delmore, J. E., and Maeck, W. J., 1989, Fission product retention in the Oklo natural fission reactors: Applied Geochemistry, v. 4, p. 49-62.

Dahl, A.R., and Hagmaier, J.L., 1974, Genesis and characteristics of the southern Powder River Basin uranium deposits, Wyoming, USA, *in* Formation of Uranium Ore Deposits, International Atomic Energy Agency, Vienna, Austria, p. 201-218.

Dayvault, R. D., 1983, Data release for parts of the eastern Adel 2° Quadrangle, Oregon: U. S. Dept. of Energy Report. GJBX-38(83), 79 p.

Dayvault, R. D., Castor, S. B., and Berry, M. R., 1985, Uranium associated with volcanic rocks of the McDermitt Caldera, Nevada and Oregon in Uranium deposits in volcanic rocks; proceedings of a technical committee meeting, Panel Proceedings Series International Atomic Energy Agency, STI/PUB/690, p. 379-409.

Deino, A.L., 1985, Miocene/Oligocene ash-flow tuffs of Seven Lakes Mountain, California-Nevada: Part II: Ph.D. dissertation, University of California, Berkeley, p. 314-409.

EarthInfo, Inc., 1993. USGS Quality of Water, EarthInfo CD^2 Reference Manual. EarthInfo, Inc., Boulder, CO.

Fiebelkorn, R.B., Walker, G.W., MacLeod, N.S., McKee, E.H., and Smith, J.S., 1983, Index to K-Ar determinations for the state of Oregon: Isochron/West, no. 37, p. 3-60.

Fisk, E.L., 1968, Cordero mine, Opalite mining district, *in* J.D. Ridge (ed.), Ore deposits of the United States, 1933-1967 (Graton-Sales Volume) v. 2., New York, Am. Inst. Mining, Metall. and Petroleum Engineers, p. 1573-1591.

Fleck, R.J., Lanphere, M.A., Turrin, B.D., and Sawyer, D.A. , 1991, Chronology of late Miocene to Quaternary volcanism and tectonism in the Southwest Nevada volcanic field: Geological Society of America Abstracts with Programs, v. 23, no. 2, p. 25.

Fournier, R. O., 1985, The behavior of silica in hydrothermal systems: Reviews in Economic Geology, v. 2, p. 45-61.

Fremont National Forest, 1991, Remedial investigation/feasibility study for the cleanup and rehabilitation of the White King and Lucky Lass mines: USDA Forest Service Draft Environmental Impact Statement, v. 1 and v. 2, 344 p.

Fridrich, C.J., Dudley, W.W. , and Stuckless, J.S.,1994, Hydrogeologic analysis of the saturated-zone ground-water system, under Yucca Mountain, Nevada: Journal of Hydrology, v. 154, p. 133-168.

Frondel, C., 1958, Systematic mineralogy of uranium and thorium, U.S. Geological Survey Bulletin 1064, 400 p.

Fyock, T. L., 1963, The stratigraphy and structure of the Virgin Valley-Thousand Creek area, northwestern Nevada: Master's thesis, University of Washington, 50 p.

Galloway, W.E., Finley, R.J., and Henry, C.D., 1979, South Texas uranium province; geologic perspective: University of Texas Economic Geology Guidebook, v. 18, 77 p.

Garside, L. J., 1973, Radioactive mineral occurrences in Nevada: Nevada Bureau of Mines and Geology Bulletin 81, 121 p.

Garside, L.J.; Bonham, H.F. Jr.; Ashley, R.P.; Silberman, M.L.; McKee, E.H., 1981, Radiometric ages of volcanic and plutonic rocks and hydrothermal mineralization in Nevada; determinations run under the USGS-NBMG cooperative program: Isochron/West, v. 30, p. 11-19.

Gianella, V.P., 1936, Geology of the Silver City district and the southern portion of the Comstock Lode, Nevada: Nevada Bureau of Mines and Geology Bulletin 29, 105 p.

Glanzman, R.K., and Rytuba, J.J., 1979, Zeolite-clay mineral alteration of volcaniclastic sediments within the McDermitt caldera complex of Nevada and Oregon: U.S. Geological Survey Open-File Report 79-1668, 25 p.

Greene, R.C., 1975, Volcanic rocks of the McDermitt caldera, Nevada-Oregon: U.S. Geological Survey Open-file report 76-753, 80 p.

Greene, R. C., 1984, Geologic appraisal of the Charles Sheldon Wilderness Study Area, Nevada and Oregon: U. S. Geological Survey Bulletin 1538, p. 13-34.

Hamilton, W.B., 1988, Detachment faulting in the Death Valley region, California and Nevada: U.S. Geological Survey Bulletin 1790, p. 51–85.

Hansley, P.L., Spirakis, C.S., 1992, Organic matter diagenesis as the key to a unifying theory for the genesis of tabular uranium-vanadium deposits in the Morrison Formation, Colorado Plateau: Economic Geology, v. 87, p. 352-365.

Hargrove, H. R., 1982, Geology of the southern portion of the Montana Mountains, McDermitt caldera, Nevada, M.S. thesis: Arizona State University, Tempe, 202 p.

Hargrove, H. R., and Sheridan, M F., 1984, Welded tuffs deformed into megarheomorphic folds during collapse of the McDermitt caldera, Nevada-Oregon: Journal of Geophysical Research, v. 89, p. 8629-8638.

Harshman, E.N., 1974, Distribution of some elements in some roll-type uranium deposits, *in* Formation of Uranium Ore Deposits: International Atomic Energy Agency, Vienna, Austria, p. 169-181.

Hay, R. L., and Sheppard, R. A., 1977, Zeolites in open hydrologic systems, *in* F. A. Mumpton, ed., Mineralogy and geology of natural zeolites: Mineralogical Society of America, Short Course Notes, v. 4, p. 93-102.

Heald, P., Foley, N. K., and Hayba, D. O., 1987, Comparative anatomy of volcanic-hosted epithermal deposits: Acid-sulfate and adularia-sericite types: Economic Geology, v. 82, p. 1-26.

Henry, C. D., 1978, Geology and uranium potential, Virgin Valley, Nevada, *in* C. D. Henry and A. N. Walton, eds., Formation of uranium ores by diagenesis of volcanic sediments: Contract Report GJBX-22-79, Bureau of Economic Geology, Univ. of Texas, Austin, p. VIII-1-VIII-52.

Henry, C. D., Castor, S. B., and Elson, H. B., in press, Geology and $^{40}Ar/^{39}Ar$ geochronology of volcanism and mineralization at Round Mountain, Nevada: Geological Society of Nevada Symposium Volume.

Hetland, D.L., 1955, Preliminary report on the Buckhorn claims, Washoe County, Nevada, and Lassen County, California: U.S. Atomic Energy Commission, RME-2039, 13 p.

Hoffman, E.L., 1992, Instrumental neutron activation in geoanalysis: Journal of Geochemical Exploration, v. 44, p. 297-319.

Hoover, D. L., 1968, Genesis of zeolites, Nevada Test Site, *in* Eckel, E.B., ed., Nevada Test Site: Geological Society of America Memoir 110, p. 275–284.

Hurley, B. W., Johnson, C. L., Cupp, G. M., Mayerson, D. L., Dodd, P. A., and Berg, J. C., 1982, Reno Quadrangle, Nevada and California: U.S. Dept. of Energy, PGJ/F037(82), 51 p.

Hutton, R.A., 1978, Geology and uranium content of middle Tertiary ash-flow tuffs in the northern part of Dogskin Mountain, Nevada: M.S. thesis, University of Nevada, Reno,

Krauskopf, K. B., 1988, Radioactive waste disposal and geology: Chapman and Hall, New York, NY, 145 p.

Landsberger, 1989, Update of uranium fission interferences in neutron activation analysis: Chemical Geology, v. 77, p. 65-70.

Langmuir, D., 1978, Uranium solution-mineral equilibria at low temperatures with applications to sedimentary ore deposits: Geochemica et Cosmochemica Acta. V. 42, p. 547-569.

Larter, R.C. Boyce, A.J., and Russel, M.J., 1981, Hydrothermal pyrite chimneys from the Ballynoe baryte deposit, Silvermines, County Tipperary, Ireland: Mineralium Deposita, v.16, p. 309-31.

Levy, S.S., and O'Neil, J.R., 1989, Moderate-temperature zeolitic alteration in a cooling pyroclastic deposit: Chemical Geology, v. 76, p. 321-326.

Livingston, D.D., 1993, The spatial and chemical diversity of zeolitic alteration at Yucca Mountain, Nye County, Nevada: Quarterly Report No. 5 Submitted to the State of Nevada Nuclear Waste Project Office, Technology and Resource Assessment Corp., Boulder Colorado, 84 p.

Lipman, P. W., 1984, The roots of ash flow calderas in western North America: windows into the tops of granitic batholiths: Journal of Geophysical Research, v. 89, p. 8801-8841.

Lipman, P. W., 1992, Ash-flow calderas as structural controls of ore deposits - Recent work and future problems: in Thorman, C. H., ed., Application of structural geology to mineral and energy resources of the central and western United States: U. S. Geological Survey Bulletin 2012, p. L1-L12.

Love, L.G., 1958, Micro-organisms and the presence of syngenetic pyrite: Quarterly Journal of the Geological Society of London, v. 113, p. 429-440.

Mahood, G. A., 1984, Pyroclastic rocks and calderas associated with strongly peralkaline magmatism: Journal of Geophysical Research, v. 89, p. 8540-8552.

Maldonado, F., and Koether, S.L., 1983, Stratigraphy, structure, and some petrographic features of Tertiary volcanic rocks at the USW G-2 drill hole, Yucca Mountain, Nye County, Nevada: U. S. Geological Survey Open-File Rpt. 83-732, 83 p.

Merriam, J. C., 1910, Tertiary mammal beds of Virgin Valley and Thousand Creek in northwestern Nevada; Part 1 Geologic history: University of California Publication Bulletin, v. 6, p. 21-53.

Murphy, W. M., Pearcy, E. C., and Goodell, P. C., 1990, Possible analog research sites for the proposed high-level nuclear waste repository in hydrologically unsaturated tuff at Yucca Mountain, Nevada: Fourth Natural analogue Working Group Meeting, Pitlochry, Scotland, 18-22 June 1990, Final Meeting Report. Brussels: Commission of the European Communities: no. EUR 13014 EN.

Noble, D.C., McCormack, J.K., McKee, E.H., Silberman, M.L., Wallace, A.B., 1988, Time of mineralization in the evolution of the McDermitt caldera complex, Nevada-Oregon, and the relation of middle Miocene mineralization in the northern Great Basin to coeval regional basaltic magmatic activity: Economic Geology, v. 83, p. 859-863.

Noble, D. C., McKee, E. H., Smith, J. G., and Korringa, M. K., 1970, Stratigraphy and geochronology of Miocene volcanic rocks in northwestern Nevada: U. S. Geological Survey Professional Paper 700-D, p. D23-D32.

Noble, D.C., Weiss, S.I., and McKee, E.H., 1991, Magmatic and hydrothermal activity, caldera geology, and regional extension in the western part of the southwestern Nevada volcanic field, in G.L. Raines and others, eds., Geology and Ore Deposits of the Great Basin, Vol, II: Geological Society of Nevada, Reno, Nevada, p. 913-934.

Pearcy, E. C., and Murphy, W. M., 1991, Geochemical natural analogs literature review: Center for Nuclear Waste Regulatory Analyses, Southwestern Research Institute, San Antonio, 128 p.

Peterson, N.V., and McIntyre, J.R., 1970, The reconnaissance geology and mineral resources of eastern Klamath County and western Lake County, Oregon: Oregon Department of Geology and Mineral Industries Bulletin 66, 70 p.

Piper, A.M., 1944. A graphic procedure in the geochemical interpretation of water-analyses: Transactions of the Amercian Geophysical Union, v. 25, p. 914-923.

Plouff, D., 1984, Interpretation of aeromagnetic and gravity data, Charles Sheldon Wilderness Study Area, Nevada and Oregon: U. S. Geological Survey Bulletin 1538, p. 35-49.

Roper, M. W., 1976, Hot spring mercury deposition at McDermitt mine, Humboldt County, Nevada: Society of Mining Engineers, AIME Transactions, v. 260, p.192-195.

Roper, M. W., and Wallace, A. B., 1981, Geology of the Aurora uranium prospect, Malheur County, Oregon, *in* P. C. Goodell and A. C. Waters, eds., Uranium in Volcanic and Volcaniclastic Rocks: AAPG Studies in Geology, no. 13, p.81-88.

Rytuba, J.J., 1995, Evolution of volcanic and tectonic features in caldera settings and their importance in the localization of ore deposits: Economic Geology, v. 89, p. 1687-1696.

Rytuba, J.J., Conrad, W. K., and Glanzman, R. K., 1979, Uranium, thorium, and mercury distribution through the evolution of the McDermitt caldera complex: U.S. Geological Survey Open-File Report 79-541, 12 p.

Rytuba, J.J., and Glanzman, R. K., 1979, Relation of mercury, uranium, and lithium deposits t the McDermitt caldera complex, Nevada-Oregon: Nevada Bureau of Mines and Geology Report 33, p. 109-117.

Rytuba, J. J., and McKee, E. H., 1984, Peralkaline ash flow tuffs and calderas of the McDermitt volcanic field, southeast Oregon and north central Nevada: Journal of Geophysical Research, v. 89, p. 8616-8628.

Samson, S. D., and Alexander, E. C., Jr., 1987, Calibration of the interlaboratory $^{40}Ar/^{39}Ar$ dating standard, MMhb-1: Chemical Geology, v. 66, p. 27-34.

Sawyer, D.A., Fleck, R.J., Lanphere, M.A., Warren, R.G., and Broxton, D.E., 1990, Episodic volcanism in the southwestern Nevada volcanic field: New 40Ar/39Ar geochronologic results: EOS, Transactions of the American Geophysical Union, v. 71, p. 1296.

Sawyer, D.A., Fleck, R.J., Lanphere, M.A., Warren, R.G., Broxton, D.E., and Hudson, M.R., 1994, Episodic caldera volcanism in the Miocene southwestern Nevada volcanic field; revised stratigraphic framework, (40)Ar/(39)Ar geochronology, and implications for magmatism and extension: Geological Society of America Bulletin, v. 106, p. 1304-1318.

Scott, R.B., and Bonk, J., 1984, Preliminary geologic map of Yucca Mountain, Nye County, Nevada, with geologic cross–sections: U. S. Geological Survey Open–File Report 84–484, 10 p., 3 oversize sheets, scale 1:12,000.

Sharp, B. J., 1955, Uranium occurrence at the Moonlight mine, Humboldt County, Nevada: U. S Atomic Energy Commission Report RME-2032(Pt. 1), 14 p.

Smith, R. L., and Bailey, R. A., 1968, Resurgent cauldrons, *in* Coats, R. R., Hay, R., and Anderson, C., eds., Studies in volcanology: Geological Society of American Memoir 116, p. 613-662.

Speer, J.A., 1982, Zircon, *in* Orthosilicates: Reviews in Mineralogy, v. 5, Mineralogical Society of America, Bookcrafters, Chelsea MI, p. 67-112.

Spengler, R.W., Byers, F.M., Jr., and Warner, J.B., 1981, Stratigraphy and structure of volcanic rocks in drill hole USW-G1, Yucca Mountain, Nye County, Nevada: U. S. Geological Survey Open-File Report 81-1349, 50 p.

Spirakis, C.S., Pierson, C.T., and Granger, H.C., 1981, Comparison of the chemical composition of mineralized and unmineralized (barren) samples of Morrison Formation in the Ambrosia Lake uranium area, New Mexico: U.S. Geological Survey Open-file Report 81-0508, 44 p.

Spirakis, C.S., Pierson, C.T., and Santos, E.S., 1984, Chemical characteristics of roll-type uranium deposits in Wyoming and Texas: U.S. Geological Survey Open-file Report 84-0366, 20 p.

Staatz, M. H., and Bauer, H. L., 1951, Virgin Valley opal district, Humboldt County, Nevada: U. S. Geological Survey Circular 142, 7 p.

Sunagawa, I., Endo, Y., and Nakai, N., 1971, Hydrothermal synthesis of framboidal pyrite: Society of Mineralogy and Geology of Japan Special Issue 2, p. 10-14.

Surdam, R. C., 1977, Zeolites in closed hydrologic systems, in F. A. Mumpton, ed., Mineralogy and geology of natural zeolites: Mineralogy Society of America Short Course Notes, v. 4, p. 65-92.

Taylor, A. O., and Powers, J. F., 1955, Uranium occurrences at the Moonlight mine and Granite Point claims, Humboldt County, Nevada: U. S. Geological Survey Report TEM-874A, 16 p.

Tuchek, E. T., Johnson, F. J., and Conyac, M. D., 1984, Economic appraisal of the Charles Sheldon Wilderness Study Area, Nevada and Oregon: U. S. Geological Survey Bulletin 1538, p. 89-139.

U.S. Geological Survey and U.S. Bureau of Mines, 1984, Mineral resources of the Charles Sheldon Wilderness Study Area, Humboldt and Washoe Counties, Nevada, and Lake and Harney Counties, Oregon: U.S. Geological Survey Bulletin 1538, 139 p.

Vera, L. S., 1980, Ore reserve estimates in Kings River Summary Report, unpublished Chevron Resources Company report, p. 12.1-12.2.

Walker, G. W., 1980, Preliminary report on the geology of the Lakeview uranium area, Lake County, Oregon: U. S. Geological Survey Open-File Report 80532, 33 p.

Walker, G.W., 1963, Reconnaissance geologic map of the eastern half of the Klamath Falls (AMS) quadrangle, Lake and Klamath Counties, Oregon: U.S. Geological Survey Mineral Inventory Field Studies Map MF-260, scale 1:250,000.

Walker, G.W., and Repenning, C.A., 1965, Reconnaissance geologic map of the Adel quadrangle, Lake, Harney, and Malheur counties, Oregon: U.S. Geologic Survey Miscellaneous Geologic Investigation Map I-446, scale 1:250,000.

Wallace, A.B., 1975, Geology and mineral deposits of the Pyramid district, southern Washoe County, Nevada: Ph.D. thesis, University of Nevada, Reno, 162 p.

Wallace, A. B., Drexler, J. W., Grant, N. K., and Noble, D. C., 1980, Icelandite and aenigmatite-bearing pantellerite from the McDermitt caldera complex, Nevada-Oregon: Geology, v. 8, p. 380-384.

Wallace, A. B., and Roper, M. W., 1981, Geology and ore deposits along the northeastern margin, McDermitt caldera complex, Oregon in P. C. Goodell and A. C. Waters (editors) Uranium in Volcanic and Volcaniclastic Rocks: AAPG Studies in Geology, no. 13, p.73-80.

Walton, A. W., 1975, Zeolite diagenesis in Oligocene volcanic sediments, Trans-Pecos Texas: Geological Society of America Bulletin, v. 86, p. 615-624.

Welch, A. H., and R. P. Williams, 1987. Data on ground-water quality for the McDermitt 1° x 2° quadrangle, Northern Nevada. U.S. Geol. Surv. Open File Report 85-648-E, Map.

Wendell, W. G., 1970, The structure and stratigraphy of the Virgin Valley-McGee Mountain area, Humboldt County, Nevada: Master's thesis, Oregon State University, 130 p.

Willden, R., 1964, Geology and mineral deposits of Humboldt County, Nevada: Nevada Bureau of Mines and Geology Bulletin 59, 154 p.

Williams, G. K., 1980, Amenability studies in Kings River Summary Report, unpublished Chevron Resources Company report, p. 11.1-11.4.

Zielinski, R. A., 1982, Uraniferous opal, Virgin Valley, Nevada: conditions of formation and implications for uranium exploration: Journal of Geochemical Exploration, v. 16, p. 197-216.